

Michael Scherzer

**Synthesis and Structure Determination of selected  
Metal - Azidopyridine - Complexes**

**MASTER THESIS**

for obtaining the academic degree

Master of Science

at the University of Technology Graz

Ao. Univ.-Prof. Dr. DI Franz A. Mautner

Institute of Physical and Theoretical Chemistry

University of Technology Graz

2012

## Acknowledgements

I am very grateful to the head of the Institute *O. Univ.-Prof. Dr. Georg Gescheidt-Demner* for the provision of equipment and resources to make this work possible.

I would like to give special thanks to *Ao. Univ.-Prof. Dr. Franz A. Mautner* for his intensive and generous support and coordination of my master thesis and for interesting discussions.

I would also like to give great thanks to *Ao. Univ.-Prof. Dr. Karl Gatterer* for his help with all issues regarding spectroscopy.

I would like to thank, *Ao. Univ.-Prof. Dr. Christoph Marschner* and *Ass.-Prof. Dr. Roland Fischer*, for the X-ray measurements and data collection for all single crystals.

Another thank will be given to *BSc. Johannes Hofer* for the UV-VIS-measurements of my complexes and the great collaboration beyond.

Thanks to my laboratory colleague *Christian Berger* for his help during everyday lab life and our great chemical and non-chemical discussions.

I would like to thank *Ing. Helmut Eisenkölbl* for technical- as well as *Mrs. Hilde Freißmuth* for laboratory support.

Last but not least a very special thank I would like to give to my laboratory trainees *Verena Landertshamer, Teresa Alkofer, Barbara Mühlbacher* and *Sabrina Müller* for exhilarating everyday lab life and many memorable hours.

Finally I want to thank Paul Nieman for proof-reading my master thesis .

**dedicated to**  
**Prof. Dr. Viktor Obendrauf (†)**  
**and**  
**my family**

# Table of contents

## 1. Introduction

1.1 <i>General aspects</i>	1
1.2 <i>Technological applications</i>	3
1.3 <i>Organic azides, Inorganic azides – the statement of the problem</i>	4

## 2. Theory

<i>2.1 Fundamentals of crystal structure analysis and x-ray diffraction</i>	
2.1.1 Typical course of a single crystal structure analysis	6
2.1.2 Crystal lattice and the unit cell	7
2.1.3 Crystal systems and the Bravais lattice types	8
2.1.4 Space group and Miller indices	9
2.1.5 Diffraction	11
2.1.6 Bragg's law	11
2.1.7 Atomic scattering factor	12
2.1.8 Structure factor	13
2.1.9 Reciprocal lattice	15
2.1.10 Structure solution	16
2.1.11 Structure refinement	18
2.1.12 Consistency	19
<i>2.2 Chemistry fundamentals of transition metal complexes and their spectroscopy</i>	
2.2.1 Coordination Chemistry	20
2.2.2 Stereochemistry of complexes	20
2.2.3 Hard and soft ligands	22
2.2.4 Low- and high-Field ligands	23
2.2.5 Crystal field theory	24
2.2.6 Ligand field theory	25
2.2.7 $\pi$ -backbonding	27
2.2.8 Crystal field spectroscopy	27
<i>2.3 Fundamentals of pyridines</i>	
2.3.1 Structure	29
2.3.2 Chemical properties	29
2.3.3 Influence on the reactivity	30

## 3. Experimental

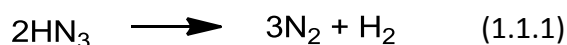
<i>3.1 Preparation</i>	
3.1.1 General procedure	32
3.1.2 Preparation of 4-azidopyridine	32
3.1.3 Preparation of $\text{HN}_3$ saturated water	33
<i>3.2 Used devices</i>	
3.2.1 Single crystal diffraction	34
3.2.2 Powder diffraction	35
3.2.3 FT IR Spectrometry	35
3.2.4 UV-VIS (NIR) Spectroscopy	35
3.2.5 NMR Spectroscopy	35

<b>4. Azidopyridine-azide-complexes</b>	
4.1 [Mn(4-azidopyridine) <sub>2</sub> (N <sub>3</sub> ) <sub>2</sub> ] <sub>n</sub>	36
4.2 [Co(4-azidopyridine) <sub>2</sub> (N <sub>3</sub> ) <sub>2</sub> ] <sub>n</sub>	41
4.3 [Ni(4-azidopyridine) <sub>2</sub> (N <sub>3</sub> ) <sub>2</sub> ] <sub>n</sub>	46
4.4 [Zn(4-azidopyridine) <sub>2</sub> (N <sub>3</sub> ) <sub>2</sub> ] <sub>n</sub>	51
4.5 [Cd(4-Azidopyridine) <sub>2</sub> (N <sub>3</sub> ) <sub>2</sub> ] <sub>n</sub>	56
<b>5. Azidopyridine-thiocyanate-complexes</b>	
5.1 [Ni <sub>2</sub> (4-azidopyridine) <sub>6</sub> (SCN) <sub>4</sub> ]	60
5.2 [Mn(4-azidopyridine) <sub>4</sub> (SCN) <sub>2</sub> ]	65
5.3 [Zn(4-azidopyridine) <sub>4</sub> (SCN) <sub>2</sub> ]	70
5.4 [Co(4-azidopyridine) <sub>4</sub> (SCN) <sub>2</sub> ]	75
<b>6. Azidopyridine-cyanate-complexes</b>	
6.1 [Ni(4-azidopyridine) <sub>4</sub> (OCN) <sub>2</sub> ]	80
6.2 [Co(4-azidopyridine) <sub>2</sub> (OCN) <sub>2</sub> ]	86
6.3 [Zn(4-azidopyridine) <sub>2</sub> (OCN) <sub>2</sub> ]	91
<b>7. Azidopyridine-nitrite-complex</b>	
7.1 [Zn(4-azidopyridine) <sub>2</sub> (NO <sub>2</sub> ) <sub>2</sub> ]	96
<b>8. Azidopyridine-chloro-complex</b>	
8.1 [Zn(4-azidopyridine) <sub>2</sub> (Cl) <sub>2</sub> ]	101
<b>9. Racah parameter and Dq</b>	
	105
<b>10. Discussion</b>	
	108
<b>11. Summary</b>	
	110
<b>12. References</b>	
	111
<b>Attachement</b>	
	114

## 1. Introduction

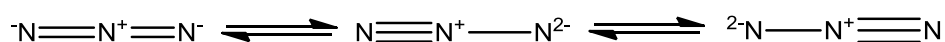
### 1.1. General aspects

Azides are the salts formed by hydroazoic acid (HN<sub>3</sub>). Hydroazoic acid is a weak acid (pK<sub>a</sub> approx. 4.75). Because of its possible thermal (exothermic) decomposition, waterfree HN<sub>3</sub> is highly explosive (eq.1.1.1). Aqueous solutions up to 10 % by weight are considered safe to handle.



Hydroazoic acid and azides are highly toxic! Heavy metal azides are shocksensitive and explosive. They should be handled carefully !

The azid-ion (N<sub>3</sub><sup>-</sup>) is a linear anion and could be described in three possible resonance structures and is known as an example for *pseudohalogenides*:



The most prominent substance used to introduce the azide moiety is NaN<sub>3</sub>. Each year more than 250 tons of azide products are industrially produced (based 2005)<sup>1</sup>.

The azides could be divided into *inorganic* (salt-like ones, e.g. NaN<sub>3</sub>) and *organic* azides (covalent ones, e.g. Tosylazide). Azides were subdivided by Müller<sup>2</sup> in 1972 into following groups, according to their bonding character:

a) *Ionic azides*

formed by alkali and alkaline earth metals (symmetric N<sub>3</sub><sup>-</sup>, ionic bound)

b) *Molecular azides*

formed by semimetals and nonmetals (asymmetric N<sub>3</sub><sup>-</sup>, covalent bound)

c) *Coordinative azides*

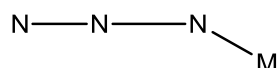
be halfway between ionic and molecular ones. They are found in complexes with heavy metals (like Pb, Cd,...) and act as bridging ligand to form high-molecular chains and networks.

If all three nitrogen atoms have the same distance from each other (same bond length N-N) this azide is said to be *symmetric*, if this is not the case it is *asymmetric*.

Another subdivision was done by Dori and Ziolo<sup>3</sup>. They divided coordinative azides according to their coordination *mode*:

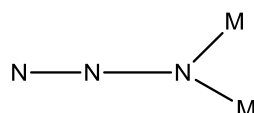
a) *terminal*

A terminal nitrogen from  $\text{N}_3^-$  coordinates to a metal center



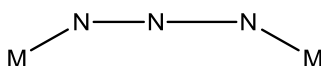
b) *end-on coordination*

One of its terminal nitrogen atoms bridges two metal ions.

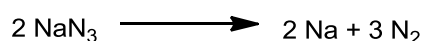


c) *end – end coordination*

Each of its two terminal nitrogen atoms bridges to a metal ion.



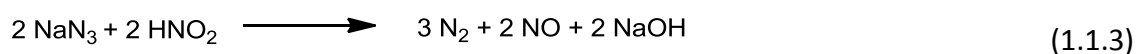
The reaction behavior of organic azides is a bit different from inorganic ones. Inorganic azides tend to decompose violently by *heating* to nitrogen and its metal, like  $\text{NaN}_3$ :



(1.1.2)

The  $\text{N}_3^-$ -ion react with heavy metals (like Ag, Pb or Cd) to shocksensitive and nearly insoluble compounds, like  $\text{AgN}_3$ .

A very useful decomposition reaction of  $\text{N}_3^-$  is the following one. The reaction is sometimes used to destroy residual azides<sup>4</sup>:



In organic reactions the azide anion as well as organic azides itself reacts as nucleophile. The anion undergoes with aromatic systems as well as aliphatic systems, nucleophilic substitution. It easily displaces good leaving groups like  $-\text{Br}$  or  $-\text{Tos}$  (Tosylate).

The loss of  $\text{N}_2$  by using azides is often utilized in organic synthesis (e.g. Curtius rearrangement, Staudinger reaction).

In retrosynthesis the  $\text{R-N}_3$  function serves as  $\text{R-NH}_2$  synthon. Otherwise  $\text{R-N}_3$  could be reduced to  $\text{R-NH}_2$  (e.g. by using  $\text{Pd/H}_2$ ).

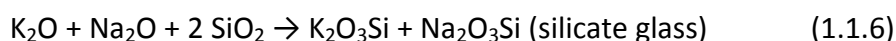
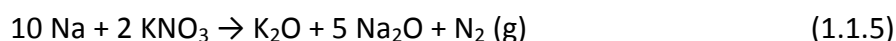
A very well known reaction with organic azides comes from *Click-chemistry*. In this reaction organic azides (as 1,3 dipole) react with alkynes to give 1,2,3 Triazole. This is known as *azide - alkyne – Huisgen – cycloaddition*<sup>5</sup>.

## 1.2 Technological Application

**Explosives :** Heavy metal azides ( $\text{Pb}(\text{N}_3)_2$ ,  $\text{AgN}_3$ ,  $\text{Cd}(\text{N}_3)_2$ ,...) are highly shock- and heatingsensitive. They are used for initial ignition<sup>6</sup>.

**Propellants:** Organic azides, like 2-Dimethylaminoethylazide, are used as rocket propellants<sup>6</sup>.

**Airbags:** The airbag systems of todays cars work based on a decomposition of  $\text{NaN}_3$  which was developed in 1972<sup>8</sup>. Thereby three separate reactions works, in order, as followed. The resulting sodium must be removed because of its high reactivity. Sodium nitrate and silicium oxide oxidize sodium in return to produce additional  $\text{N}_2$ :



**CVD:** (*Chemical Vapor Decomposition*) for the production of semiconductors, organic azides are decomposed under mild conditions to layers of type MeN (metal nitride)<sup>9/10/11</sup>

**Pharmacy:** As example: a very well known Thymidine-derivate with azide is known as Zidovudin. It is a common medicine against HIV-Inifection<sup>12</sup>.

**Lithography:** Bisazides are used to crosslink components during negative and positiv photoresist processes<sup>13/14</sup>.

**Synthesis:** Azides are used widely spread in different reactions in organic chemistry and synthesis. For example to synthesize 1,2,3 triazole (Huisgen-cycloaddition), tetrazole ,...<sup>15</sup>

### 1.3 Organic azides, Inorganic azides – the statement of the problem

The azides and their use in complexes as bridging ligands and in connection with organic azides define the home position for this master thesis. The focus lies at the difference between organic and inorganic azides used next to each other in a complex. The use of inorganic azide, in our case the azide anion ( $N_3^-$ ), as bridging ligand, has its origin in the idea of the design of molecule-based magnets, which is described in the next passage. The decision to try two other ligands,  $NCO^-$  (cyanate) and  $NCS^-$  (thiocyanate – „rhodanide“), is based on the isoelectronicity of  $NCO^-$  to  $N_3^-$  and the possible similar or new coordination modes compared to  $N_3^-$  (also through the presence of the two additional electronegative atoms oxygen and sulphur). The choice of (*para*)-Azidopyridine as ligand and representative of organic azides may offer a variety of new possibilities. It is expected that the organic azide ligand maybe interrupt or promote the ferromagnetic and antiferromagnetic coupling in molecule-based magnets. Another expectation would be the bridging of the  $\alpha$ -N atom (the N-atom next to the C-Atom in  $R-N_3$ ) to an adjacent metal center<sup>16</sup>. The  $\alpha$ -N tend to be more basic than  $\gamma$ -N and therefore this mechanism requires a good  $\pi$ -donor metal center to bridge to  $\alpha$ -N. The azide moiety is also able to activate C – H bonds, so perhaps byproducts or fragments could be obtained<sup>17</sup>. Also the minimal sterical hindrance of the *para*-azido-substitute Pyridine (in contrast to the *ortho*- and *meta*-substitute compound) favours its choice as ligand. At the beginning of this master thesis (May 2012), as far as we know *only two structures* of a metal (both manganese) with 4-Azidopyridine was published (according Cambridge Crystallographic Data Centre, CSD version 5.32 (Update Feb. 2012))<sup>18/19</sup>. Regarding this fact the following metals were examined (in oxidationstate +II) for crystallographic and spectroscopic properties: Cadmium, Cobalt, Manganese, Nickel and Zinc.

In connection to former projects and research treatment of azides, this master thesis focuses also on the very interesting and well developed research field of *molecule-based*

*magnetic materials*. In molecule-based magnets you find so-called „*building blocks*“. This building blocks contain special „discrete“ molecular species, which can be connected through ligands to form the total structure (also superexchange-ligands for polynuclear lattice)<sup>20/21</sup>. The discrete species may be d- or f-block complexes, organic radicals, donor-acceptor complexes or clusters. Lattice forces, covalent bonds and space effects give rise to bridge the building blocks. These structures show spontaneous 3D long-range magnetic order characteristics. The application of azide ( $N_3^-$ ) in the design of molecular magnets based on the discovery, that divalent, *end-to-end* azide bridged paramagnetic metal ion centers show mainly antiferromagnetic coupling. End-on azide bridged metal ions show predominantly ferromagnetic coupling<sup>22/23/24/25</sup>.

## 2. Theory

### 2.1 Fundamentals of crystal structure analysis and x-ray diffraction

#### 2.1.1 Typical course of a single crystal structure analysis

At the beginning of the analytical pathway to determine a crystal structure a *single crystal* is needed. In a single crystal (monocrystalline) the crystal lattice is the same as in the entire substance, that is continuous and without interruption. Grain boundaries and defects associated with these boundaries should be absent. Single crystals are seen as „good“ if they are:

- clear
- have uniform edges and surfaces
- show coherent extinction of polarized light

Single crystals are almost always selected after being viewed under a polarisation-microscope.

Useless crystals are:

- splitted or cracked
- twined
- those showing an incoherent extinction of polarized light.

According to the diameter of an X-ray beam ( $\sim 0,5$  mm), the chosen crystal should be about 0,1 mm (rough-and-ready rule).

This crystal is mounted in an X-ray diffractometer (for single crystals) and the following steps (in this order) are then done for the final structure determination (position of the atoms in the unit cell):

- determination of direction matrix and lattice type
  - Unit cell and formula units (Z) must be identified
- detection of Inversion centre
- determination of Bravais lattice type and space- and point group
- measurement of full diffraction pattern (intensity measurement)

- correction of data (absorption,...)
- structure solution
- structure refinement

The last two tasks are especially costly and must often be modified and repeated in order to achieve the best results for the determined structure. A very good description of crystal structure analysis is given by Massa<sup>26</sup>.

### 2.1.2 Crystal lattice and the unit cell

Crystals are solids, which are built up by atoms, ions or molecules. These solids show a periodic pattern along all three dimensions of space. Crystals are homogenous and display anisotropy. Anisotropy or anisotropic properties are directionally dependent features. The outer regularity of a crystal displays its inner construction. Because of the periodicity you find many points in the crystal with equal surroundings. Therefore a crystal could be seen as a *lattice* (or *crystal lattice*) and its points as *lattice points*. The lattice points, initially, are not identical with the atoms or molecules. The lattice could be positioned in such a way that the lattice points coincide with atom positions, than equivalent atoms will be found throughout the entire crystal. This leads to so-called „*translation symmetry*“.

The smallest repeating unit or mesh in the crystal lattice is called a „*unit cell*“. The unit cell is defined through the vectors  $a$ ,  $b$  and  $c$  and the angles  $\alpha$ ,  $\beta$  and  $\gamma$ . These parameters are known as „*lattice parameters*“. The unit cell illustrates a type of bulk arrangement of atoms, molecules and ions in the crystal.

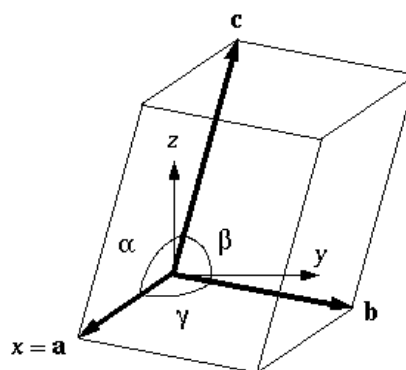


Fig.2.1.1: Unit cell and lattice constants<sup>27</sup>

An important value which is determined by the unit cell is  $Z$  (formula units per unit cell). Another definition associated with the unit cell is “*asymmetric unit*”. The smallest set of atoms which can illustrate the whole content of a unit cell by applying the symmetry operations is known as the asymmetric unit.

### 2.1.3 Crystal systems and the Bravais lattice types

The variation of the lattice parameters  $a, b$  and  $c$  (with  $\alpha, \beta, \gamma$ ) allow the definition of *seven crystal systems*. This classification is also based on the possible symmetry operations of the crystal lattice.

Tab.2.1.1: the seven crystal systems

Crystal system	lattice parameter	angles
1. triclinic	$a \neq b \neq c$	$\alpha \neq \beta \neq \gamma \neq 90^\circ$
2. monoclinic	$a \neq b \neq c$	$\alpha = \gamma = 90^\circ > \beta > 90^\circ$
3. orthorhombic (cuboid)	$a \neq b \neq c$	$\alpha = \beta = \gamma = 90^\circ$
4. tetragonal	$a = b \neq c$	$\alpha = \beta = \gamma = 90^\circ$
5. hexagonal	$a = b \neq c$	$\alpha = \beta = 90^\circ \gamma = 120^\circ$
6. trigonal (rhomdoedric)	$a = b = c$	$\alpha = \beta = \gamma \neq 90^\circ$
7. cubic	$a = b = c$	$\alpha = \beta = \gamma = 90^\circ$

According to the seven crystal systems, M. Bravais<sup>28</sup> defined the 14 so-called *Bravais lattice types*. The unit cell should be small and best display the entire symmetry of the crystal, as per to the idea of M. Bravais. The *primitive* cell is not always the best choice because other forms (*centered cells*) may allow for a better description of the unit cell. *You always choose the crystal system with the highest possible symmetry and the position of the unit cell should coincide with it.* These centered cells could be one-, two-, three- up to four times more primitive than the original one. There are four types of centered cells:

**P** (primitive), **I** (inner centered), **F** (face centered) **A, B, C** (A, B or C-centered)

The 14 Bravais lattice types with the possible centring are illustrated in Fig. 2.1.2.

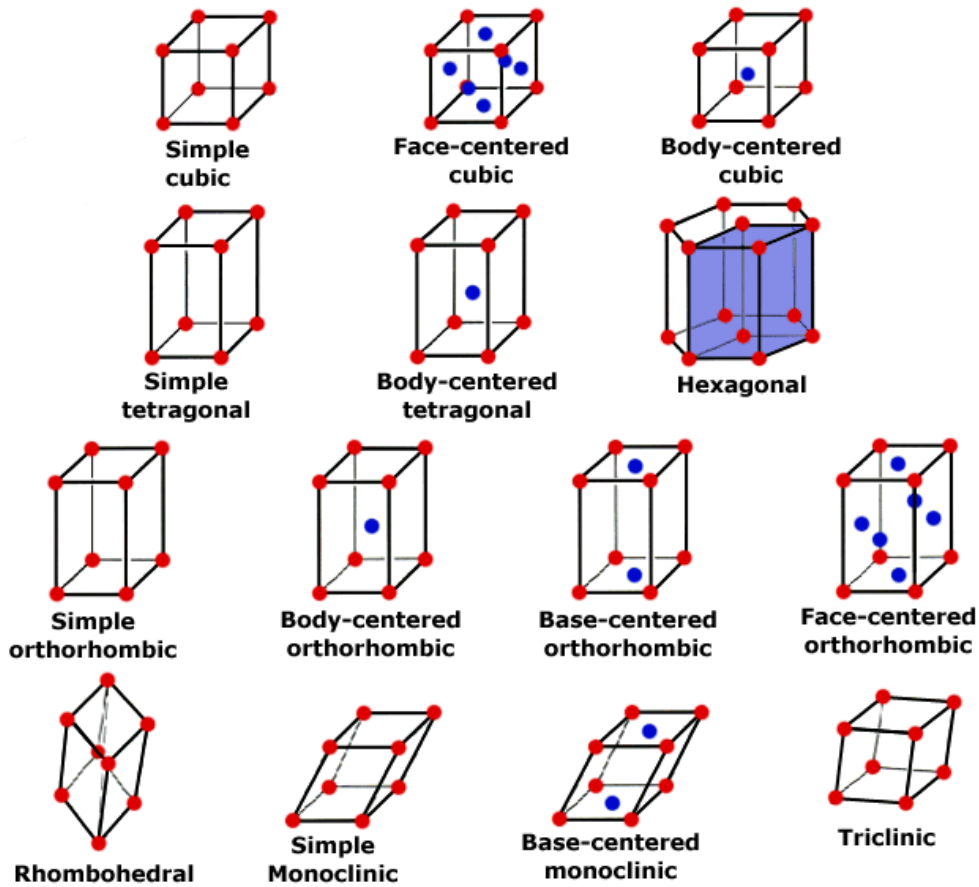


Fig. 2.1.2: the 14 Bravais lattice types<sup>29</sup>

#### 2.1.4 Space group and Miller indices

One of the most essential aspects of crystals are their symmetry operators. The most important symmetry elements are:

- reflection
- rotation
- improper rotation
- glide plane symmetry
- screw axis symmetry
- identity

In combining the 14 Bravais lattice types, the seven crystal systems and the symmetry elements and operations there are 230 possible available *space groups*. This means that 230 different possibilities (space groups) exist for describing all possible crystal symmetries. The descriptions and symbols used to describe the 230 space groups were introduced by Hermann and Mauguin<sup>30</sup>. Another form was also created by Schönflies<sup>31</sup>.

*Miller indices* and *lattice planes* are a facility construction for the description of X-ray diffraction in the three-dimensional case. Diffraction can occur at specific planes in the crystal; called *lattice planes* (the idea of diffraction is described in the next chapter). The position of these lattice planes in the lattice is defined through the Miller indices  $hkl$ . The indices describe the points of intersection of each lattice plane at the unit cell axes. These points are at  $a/h$   $b/k$  and  $c/l$  and define the planes. Each lattice plane contains some points of the crystal lattice. For each plane some equidistant and parallel planes exist such that every lattice point lies on exactly one plane. The indices which intersect the unit cell axes at  $1/h$ ,  $1/k$ ,  $1/l$  are always rational numbers and the reciprocal values are the Miller indices  $hkl$ . They could be zero (for planes parallel to axis) or even negative. The indices could be determined if one were to pick out the plane which is nearest to the origin but does not cross the origin, as is the case at  $1/h$ ,  $1/k$  and  $1/l$ .

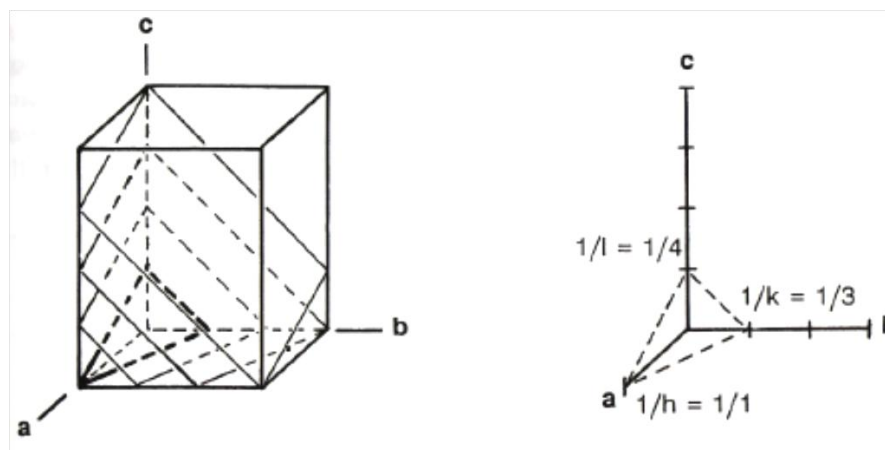


Fig. 2.1.3: Miller indices (right) and examples of lattice planes (left)<sup>32</sup>

### 2.1.5 Diffraction

The easiest way to describe the principle of diffraction is in a *one-dimensional lattice*. In this case monochromatic light, with wavelength  $\lambda$ , is irradiated on a one-dimensional optical grating. The phenomenon called *diffraction* takes place if the wavelength  $\lambda$  is similar to the magnitude of  $d$  (the distance between two adjacent lines). This can be explained through the idea of „*elastic scattering*“ whereby each point of the one-dimensional lattice becomes the source of a spherical wave of the same wave length itself - if these points are then struck by a wave of light. The waves from the individual points interact with each other. Depending on the observation angle  $\Theta$  and the distance between two adjacent points  $d$ , path difference occurs. One would observe constructive or destructive interference, depending on the chosen  $\Theta$ . If  $\Theta$  is chosen such that the path difference is exactly  $n\lambda$  ( $n$  = diffraction order, rational number) it is *constructive interference*- and for  $\lambda/2$  it is *destructive interference*. Between the extremes of  $\Theta$  and arbitrary path differences the extinction of waves does not come from adjacent points but rather from points far off.

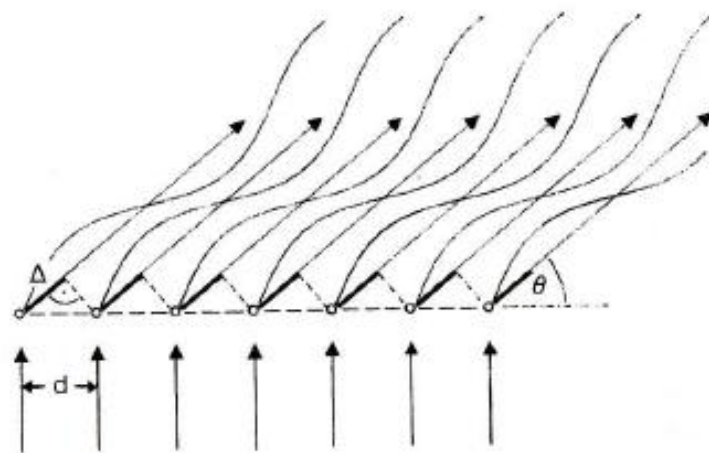
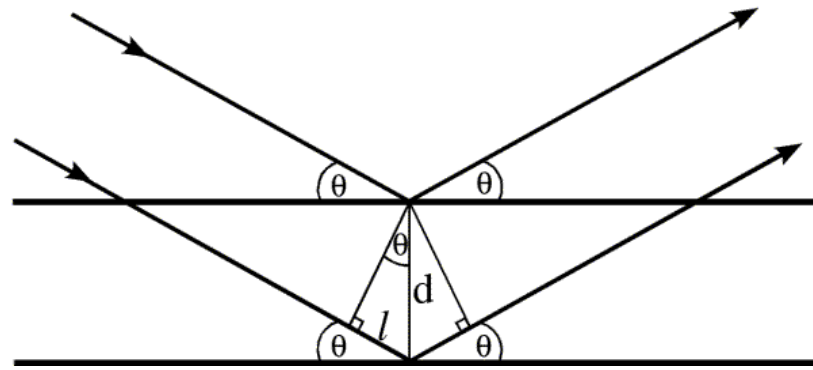


Fig.2.1.4: Diffraction at a one-dimensional lattice<sup>33</sup>

### 2.1.6 Bragg's law

The most important equation in X-ray diffraction is Bragg's law. The *Bragg equation* explains easily how X-rays are diffracted at the lattice planes (reflection) of a crystal. In Fig. 2.1.5 two incident waves are reflected at two adjacent lattice planes with distance  $d$ .

Fig.2.1.5: Derivation of Bragg's law<sup>34</sup>

As can be seen the important fact is the *path difference* between the two reflected waves. Only those angles in which the difference path ( $2d \sin \Theta$ ) is an integer multiple of the wavelength, give a constructive interference. These requirements are related in *Bragg's law*.

$$n\lambda = 2d \sin \Theta \quad (2.1.1)$$

$n$  ... rational number    $\lambda$  ... wavelength    $d$  ... distance between the planes    $\Theta$  ... observation angle

Thus for each set of hkl planes (at a given characteristic distance  $d$  and diffraction order  $n$ ), there exist one *unique angle*  $\Theta$  for observing reflection. In single crystals especially the resulting maximum reflection is quite sharp, because of its three-dimensional periodicity.

### 2.1.7 Atomic scattering factor

The *atomic scattering factor* (or *atomic form factor*  $f$ ) describes interactions between X-rays and electrons, in which the x-rays are scattered. The idea of scattering X-rays was considered up until now to take place on lattice points. The dimension (radial extension) of an electron shell has about the same range as the wavelength of X-rays. Thus scattering at the electron shell could produce a phase difference between X-rays, because the idea of an exact point source does not hold true for electron shells. The resulting phase difference leads to some weakening of the intensities. This weakening depends on the "form" of the shell and  $\Theta$ . As a result, the atomic scattering factor ( $f$ ) is scaled in a way such that the value of the angle to zero is equal to the atomic number.

In general, heavy atoms are better „scatterers“, than light atoms (e.g. especially hydrogen). Another fact is, that  $f$  becomes smaller at increasing  $2\Theta$ .

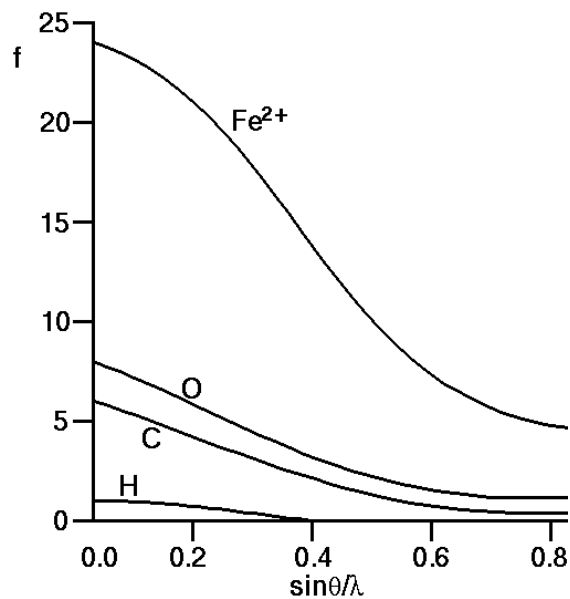


Fig.2.1.6: Atomic scattering factors of different elements<sup>35</sup>

### 2.1.8 Structure factor

The ideas described up until now, have been based on one atom structures (Type A). The influence of a second type of atom (Type B) must now be taken in account. For both types of atoms the translation lattice is the same. If the diffraction angle is perfectly set for the translation lattice of atom Type A. All Type A atoms in this lattice will be in phase. The same is also valid for all Type B atoms in the second translation lattice. Because of the shifting of the second lattice in relation to the first lattice (with interatomic vectors  $x_2, y_2, z_2$ ) and the origin, the second scattering wave becomes *phase shifted*. The phase shift  $\phi_i$  of a scattering wave from atom Type  $i$  must now be determined.

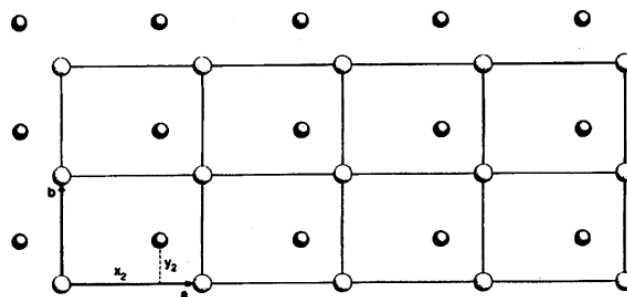


Fig.2.1.7: lattice for two atom structure (A: white B: black)<sup>36</sup>

The phase shift for Type i atoms could be written as:

$$\phi_i = 2\pi (hx_i + ky_i + ly_i) \quad (2.1.2)$$

This information of the phase shift must be added to the atom scattering factor  $f$ . This is done by the multiplication by an *exponential function* (with imaginary argument) as follows:

$$F_{\mathbf{hkl}}(i) = f_i e^{i\phi_i} \quad (2.1.3)$$

The shift between phase A and B is described as  $\phi$ . Applying the Eulerian formula to eq. 2.1.3 results in the following equivalent expression:

$$F_{\mathbf{hkl}}(i) = f_i (\cos\phi_i + i \sin\phi_i) = A_i + iB_i \quad (2.1.4)$$

The calculation of  $\phi_i$  is done using the Miller indices of the lattice plane and the relative coordinates (x,y,z) of an atom i in the unit cell as seen in eq.2.1.2.

The final formula for the *structure factor* ( $F_{\mathbf{hkl}}$ ) results from adding all the diffracted waves together (in regards to their specific phase shifts):

$$F_{\mathbf{hkl}} = \sum_i f_i [\cos 2\pi(hx_i + ky_i + ly_i) + i \sin 2\pi(hx_i + ky_i + ly_i)] \quad (2.1.5)$$

If the structure contains an inversion center, and the origin of the crystal lattice is in that inversion center, the calculation reduces to:

$$F_{\mathbf{hkl}} = \sum_i f_i \cos 2\pi (hx_i + ky_i + ly_i) \quad (2.1.6)$$

*The structure factor  $F_{\mathbf{hkl}}$  describes the connection between the scattered X-rays and the atom positions in a crystal.*

The possibility to invert eq. 2.1.7 to eq. 2.1.8 gives an interesting new view on the structure factor. Now the electron density is a function of  $F_{\mathbf{hkl}}$  (V is the unit cell volume).

$$F_{\mathbf{hkl}} = \sum_i f_i e^{2\pi i(hx_i + ky_i + ly_i)} \quad (2.1.7)$$

$$\rho(XYZ) = \frac{1}{V} \sum_{\mathbf{hkl}} F_{\mathbf{hkl}} e^{-i2\pi(\mathbf{hX} + kY + lZ)} \quad (2.1.8)$$

F is a vectorial item and is therefore described by length and some angle. The phase angle  $\phi_{hkl}$  is not available through the measured intensities. Just  $|F|$  is available. The intensity is proportional to  $|F|^2$ .

There are no simple ways to determine  $\phi_{hkl}$ . This is the major problem in crystal structure analysis and it is called the *phase problem*. Two methods for solving this problem are described in the section “structure solution”.

### 2.1.9 Reciprocal lattice

The reciprocal lattice is an auxiliary mathematical structure for interpreting and describing scattering reflections. Instead of characterizing each lattice plane independently, it is easier to picture the equidistant lattice planes (a couple of planes) through a vector. This vector is perpendicular to the planes and has a length (distance) equal to the adjacent planes. High diffraction angles lead to shorter vectors, because of  $|d| \sim 1/\sin \Theta$ . A new coordinate system can also create some difficulties as the direction of the vector cannot be directly derived from the hkl indices (they are described through  $\mathbf{a}/k$ ,  $\mathbf{b}/k$  and  $\mathbf{c}/l$ ). All axis become *reciprocal*, (eg. axis  $\mathbf{a}$  becomes  $1/a$ , etc). These new axis are named  $\mathbf{a}^*$ ,  $\mathbf{b}^*$  and  $\mathbf{c}^*$ . From the top of each vector these planes are revealed; allowing for the creation of a new lattice - the *reciprocal lattice*. The vector  $d$  for each reciprocal lattice point is defined as:

$$\mathbf{d} = h\mathbf{a}^* + k\mathbf{b}^* + l\mathbf{c}^* \tag{2.1.9}$$

Reciprocal lattices are used to picture reflections graphically and also to control the crystallographic measuring instruments.

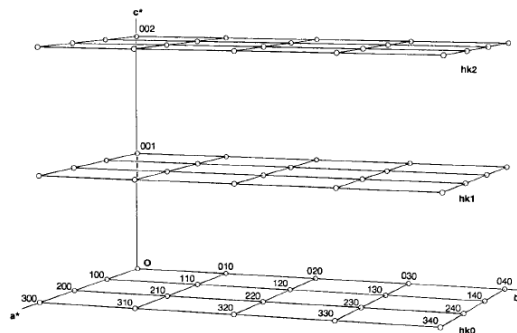


Fig.2.1.8: Reciprocal lattice divided into layers perpendicular to  $c^*$

### 2.1.10 Structure solution

Before the structure solution process can begin the determination of metric, unit cell, space group and the collection of reflection data must be completed. The most important question now is: what is the position of the atoms in the unit cell (more precisely in the asymmetric unit). In regards to the process of finding the correct structure model the phase problem needs to be overcome. The following methods for doing so are those most frequently used. Other processes exist, including modified processes for special applications.

#### Fourier-transformation

The idea behind the strategy of Fourier-transformation has already been described in chapter 2.1.7. Namely that electron density replaces the idea of punctual scatter-centres. This assumption is based on the periodicity of the structure of a crystal. Therefore electron density could be described as periodic changeable magnitude. Due to this fact the electron density can be described through the Fourier sum:

$$\rho(XYZ) = \frac{1}{V} \sum_{\mathbf{hkl}} F_{\mathbf{hkl}} e^{-i2\pi(\mathbf{h}X + \mathbf{k}Y + \mathbf{l}Z)} \quad (2.1.10)$$

The structure factor  $F_{\mathbf{hkl}}$  becomes a Fourier coefficient. If all  $F_0$  (structure factor of each wave) and phases are known, the electron density can be calculated. Thus the crystal structure can be fully determined. The problem in applying this method is, that out if the intensity of  $F_0$  is not available, then only  $|F_0|$  can be returned. There are two ways to overcome the phase problem using this method. The first one is to set up a suited structure model and try to find the best fit ("trial and error"). The other possibility is *Difference-Fourier-synthesis*. The method of *Difference-Fourier-synthesis* takes advantage of the so-called *pseudomaxima* of electron density. This effect comes through the measurement of a limited data set (this means it is not *infinite*). To reduce the obtained effect, the  $F_0$  values (obtained) are then subtracted from the  $F_c$  values (calculated) of the structure model. Applying this, only areas of sharp electron density can be seen at positions where atoms may be absent in the structure model. This method is also used to refine structure models (especially in localizing hydrogen atoms).

## Patterson-Synthesis

The Patterson method<sup>38</sup> works similar to the Fourier-transformation described above. The only disparity lies in the use of  $|F_0|^2$  instead of  $F_0$ . This then gives to the Patterson-function:

$$P_{uvw} = \frac{1}{V^2} \sum_{\mathbf{hkl}} F_{\mathbf{hkl}}^2 \times \cos 2\pi(hu + kv + lw) \quad (2.1.11)$$

The advantage of using  $|F_0|^2$  is that this value provides no information about the phase. So  $\phi_{\mathbf{hkl}}$  need not be known. The only information obtained is that of the interatomic vectors ( $x$ ,  $y$ , and  $z$ ) which are mentioned in chapter 2.1.7. This information describes the phase shift between two different types of atoms within a crystal lattice (Fig. 2.1.7). The calculated values for the Patterson function (in the unit cell) display the maxima of distance vectors between atoms. The vectors could be measured in both directions, therefore the Peterson function is always centro-symmetric. This is illustrated in Fig. 2.1.9. The Patterson space is described using  $u$ ,  $v$  and  $w$  in order to distinguish between this space and the unit cell (crystal space). The product of the atomic numbers of both of the vector's atoms is its intensity. This is the best application of the Patterson method. If there are heavy metals in a structure (like organometallic compounds), their peaks can easily be found as they are the highest ones. The method becomes useless when there are many heavy metal atoms in a structure. The highest peak is located in the origin and mirrors the zero vector between each atom and itself. You can find  $N(N-1)+1$  maxima in an asymmetric unit containing  $N$  atoms.

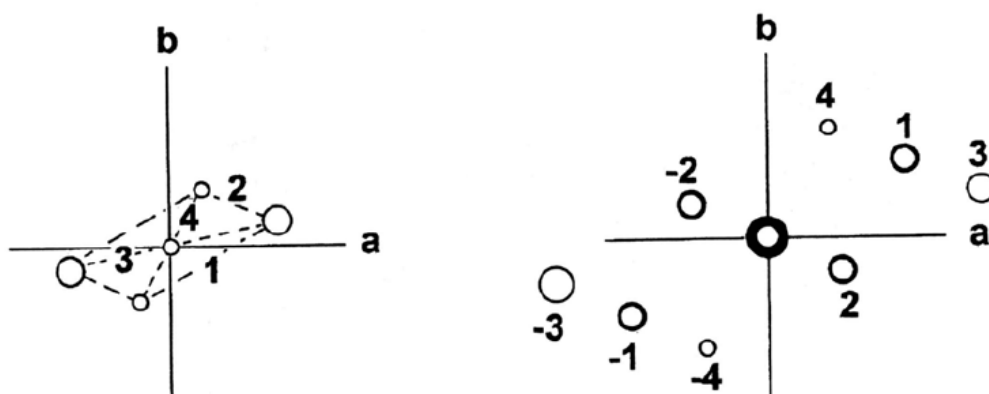


Fig.2.1.9: Crystal space vs. Patterson space<sup>39</sup>

### Direct methods

The following methods try to exploit the direct coherences between *intensities (reflections)* and the structure factor  $F_{hkl}$ .

### Harker-Kasper inequations

The origin of direct methods is found in the work of Harker and Kasper<sup>40</sup>. They established the coherence of symmetry elements and structure amplitudes in a particular pair of reflections using so-called unitary structure amplitudes (U). This amplitude replaces the original  $F_{hkl}$ . U is normalized to the full number of electrons in the unit cell. The unitary structure amplitude gives an overview of how electrons contribute to the structure amplitude of a given reflection.

$$U = \frac{F}{F(000)} \quad (2.1.12)$$

Out of these basic deliberations, so-called *Harker-Kasper inequations* can be deduced and applied.

### Sayre equation

Another important coherence for the application of direct methods, is the *Sayre-equation*<sup>41</sup>. The fundamental proposition of the Sayre equation is that electron density can never become negative and that it is probably concentrated punctual around the atom.

#### 2.1.11 Structure refinement

The refinement will be done once a structure has been solved by either Patterson- or direct methods. The aim of the methods for structure refinement is to optimize the structure model using least squares calculations. Least square refinement tries to optimize the difference between measured and calculated intensities, by modifying the atomic parameter. Another possibility for refining a structure model is to use Difference-Fourier-synthesis. This method is described in the chapter “structure solution” (2.1.9)

### 2.1.12 Consistency

To quantify the consistency of a measured (A MEASURED WHAT?) with a calculated structure solution there are two factors which are in use to evaluate the structure model.

R-Value

The *R-Value* is a measure of the *goodness of a structure model*. There exist more than one definition and alteration for R. The calculated structure factors ( $F_c$ ) are subtracted from the observed ones ( $F_o$ ). For the “regular” R-value:

$$R = \frac{\sum_{hkl} F_o - F_c}{\sum_{hkl} F_o} \quad (2.1.13)$$

Multiplying by 100 gives the percentage of goodness of consistency.

Goodness of fit

The *S-Value* is a parameter for the goodness of refinement in a structure model:

$$S = \sqrt{\frac{\sum_{hkl} w \Delta^2}{m - n}} \quad (2.1.14)$$

w is a weight factor which comes from using the least-square method. It is defined as  $w = 1/\sigma^2$ .  $\sigma$  is the standard deviation from counting statistics at the diffraction measurement. In the m-n term (m= number of reflection, n = number of parameters) the goodness of structural parameters has already been factored in. A perfect goodness value would be 1.0. A correct structure model should have a goodness value of around 1.0.

## 2.2 Chemistry fundamentals of transition metal complexes and their spectroscopy

### 2.2.1 Coordination Chemistry

The coordinative chemistry of transition metals is based on the interaction of d-shell electrons in a metal with suitable ligands. Transition metals often have partially filled d-orbitals and this fact influences the reaction behaviour of the metal centre significantly. In contrast, most main group metals have no d-electrons (e.g. Li) or a filled d-shell (e.g. Si). This leads to a completely different behaviour in reactions compared with transition metals. Transition metal ions (M) can bind various ligands (L) to form a coordination compound. These are called *complexes* ( $ML_n$ ). Complex bonding can be divided roughly into three categories: *n-complexes* (bonding through Lewis acid-base interactions),  *$\sigma$ -complexes* (bonding through  $\sigma$  – electron pairs, leading in some cases to 3 centre – 2 electron bonds) and  *$\pi$ -complexes* (covalent bonds, i.e.  $\pi$ -bonds are participating in the bonding). Reactions with  $\pi$ -acceptors (e.g. CO, Alkynes) or  $\sigma$ -donor ligands (e.g.  $NH_3$ ) are very common but there also exist many other reactions.

The d-electron configuration of transition metals (as complex-centres) is responsible for para- or diamagnetism and for their optical properties. Many transition metal complexes are coloured, this is due to their ability to transfer d-electrons into an excited d-state.

A subfield of coordination chemistry is *organometallic chemistry*. This field works with more covalently bound ligands and metals in a rather reduced oxidation state. Organometallic chemistry is a very important and powerful field when connected with *catalysis*.

### 2.2.2 Stereochemistry of complexes

The configuration of ligands around the metal centre is of high importance in coordinative chemistry. The number of ligands directly bounded to the metal centre is known as the *coordination number*. Sometimes for a given coordination number, more than one possible geometry is available. The stereochemistry of complexes of a given coordination number, depends on the coordination number, d-electron configuration of the metal center, the electronic and steric behaviour of the ligand as well as on the denticity of the ligand. The resulting structure can be explained through VSEPR-theory<sup>42</sup>.

The repulsion between the coordinated ligands, and their bonds, is in an ideal case at a maximum. Lone pairs especially tend in reality to buckle the ideal case of stereochemistry. In Tab.2.2.1 coordination numbers from  $ML_2$  up to  $ML_{12}$  (some different geometries as well) are listed with examples.

Tab.2.2.1: Coordination geometries<sup>43</sup>

type	structure	example
$ML_2$	linear	$HgCl_2, CuCl_2^-$
$ML_3$	trigonal-planar	$Cu(SPM_3)_3^+$
$ML_4$	tetrahedral	$MnCl_4^{2-}$
	quadratic-planar	$AgF_4^-$
$ML_5$	trigonal-bipyramidal	$VCl_5^-, Fe(CO)_5$
	quadratic-pyramidal	$Ni(CN)_5^{2-}$
$ML_6$	octahedral	$Fe(H_2O)_6^{2+}$
	trigonal-prismatic	$Cd(acac)_3^-$
$ML_7$	pentagonal-bipyramidal	$UO_2F_5^{3-}$
	capped octaedric	$MoF_7^-$
	capped trig.-prism.	$Mo(CNBu)_7^{2+}$
$ML_8$	cubic	$U(bipy)_4$
	quadratic-antiprismatic	$Sr(H_2O)_8^{2+}$
	dodecahedral	$Ti(NO_3)_4$
$ML_9$	capped – quadr. - antprism.	$[La(Cl(H_2O)_7)_2]^{4+}$
	threecapped-trig.-prism.	$Pr(H_2O)_9^{3+}$
$ML_{10}$	twocapped-trig.-prism.	$Er(NO_3)_5^{2-}$
$ML_{11}$	octadecahedral	$Th(NO_3)_4(H_2O)_3$
$ML_{12}$	icosahedral	$Ce(NO_3)_6^{3-}$

The most common coordination numbers are:

- $ML_4$  (tetrahedral or quadratic – planar)
- $ML_5$  (trigonal bipyramidal or quadratic pyramidal)
- $ML_6$  (octahedral or trigonal prismatic)

Over the years the bonding characteristics in complexes have been described by different theories. One of the first theories was the *VB(valence bond)-theory*. This theory was introduced by Linus Pauling<sup>44</sup>. This idea of bonding, a simple view of covalent M-L bonds and their polar contributions, is now completely replaced by *crystal field* – and later by the *ligand field theory*. They are presented separately in following chapters.

A very good description and full overview of transition metal chemistry is given by Crabtree<sup>45</sup>.

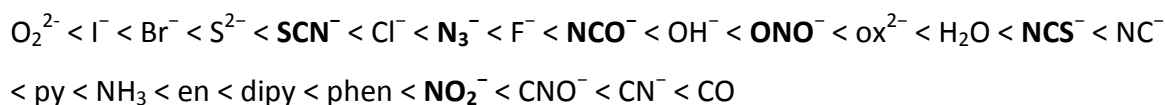
### 2.2.3 Hard and soft ligands

Ligands can be classified in more than one way, according to different aspects. One possibility is to look at ligands based on their ability to be polarized. From this ligands can be classified into two possible groups. *Hard ligands*, like the fluoride anion ( $F^-$ ), form mainly ionic bonds, are difficult to polarize (high electron density) and are small. Their best partner would be a hard metal or cation, e.g.  $H^+$ . *Soft ligands* are big, easy to polarize (small electron density) and form predominantly covalent bonds. An example would be the iodide anion ( $I^-$ ). This concept, of hard and soft interaction, was introduced by Ralph Pearson in 1963<sup>46</sup>. This is also known as *HSAB-concept* (**h**ard and **s**oft **a**cids and **b**ases). So the idea of hard and soft ligands could be extended to a general concept of acid – base interaction. Hard ligands, like  $F^-$ , are Lewis-bases and hence hard bases.  $BH_3$  would be a Lewis-acid, a soft acid and therefore a soft ligand. *Soft acids* (electron acceptors), can also have double or triple bonds. Elements of the second or later row (like  $Hg^{2+}$ ), relatively electropositive elements (e.g. Boron), and metals in low oxidation state ( $Ni^0$ ,  $Re^{+1}$ ) are classified as soft. This concept, and its definition, is widely used in chemistry to explain the stability of compounds and their reaction mechanism, if only in a simple qualitative way. Most interactions in coordination chemistry, as well as organometallic chemistry, are dominated by soft-soft and hard-hard interactions.

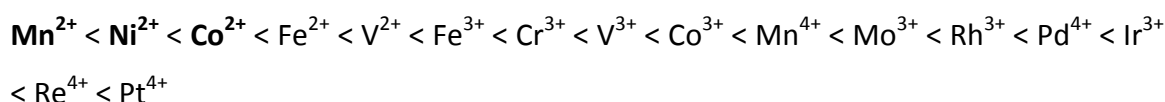
### 2.2.4 Low- and High-Field ligands

Another possibility in the classification of ligands is related to their tendency to increase or decrease the energy splitting of the metal centre d-orbitals into a complex. Transition metal complexes are often coloured. Their colour depends on the ability of the complex to absorb light. This ability is closely related to the complex's d-electron configuration and its participating orbitals. To say it more precisely, the ability corresponds to the splitting of high energy orbitals ( $d_{\sigma}$ ) into low energy orbitals ( $d_{\pi}$ ). This is known as the crystal field splitting parameter  $\Delta$ . The context of the orbital splitting and the corresponding energy difference is described in the next chapter "crystal field theory" (2.2.5). The size of this crystal field splitting corresponds directly to the colours of the complexes. This fact can be used in UV-VIS spectroscopy to determine  $\Delta$  (see chapter 2.2.8 "crystal field spectroscopy"). The ligands and their kind of bonding to the metal centre are the reason for the size of the splitting in complexes. There exist two types: so-called *high-field ligands* (e.g. CO) and *low-field ligands* (e.g. H<sub>2</sub>O). High-field ligands are usually strong  $\sigma$ -donors and  $\pi$ -acceptors. They tend to raise the crystal field splitting. Low-field ligands are weak  $\sigma$ -donors and usually  $\pi$ -donors. They decrease the crystal field splitting.

General trends of ligands depending on their ability to increase or decrease the  $\Delta$  can be seen in the *spectrochemical series of ligands* (from left to right increasing  $\Delta$ ; **fat** ones are used in this master thesis):



The *spectrochemical series* also exists *for metal ions* (from left to right increasing  $\Delta$ ; **fat** ones are used in this master thesis):



An important fact is also that the charge of the metal ion also has an influence on  $\Delta$ . A higher charge (like in Pt<sup>4+</sup>) leads to greater  $\Delta$ . Another trend is that  $\Delta$  increases going down a group (in the periodic table).

## 2.2.5 Crystal field theory

The crystal field theory, developed by H. Bethe and J. H. van Vleck<sup>47</sup> in the 1930s, investigates how the energy levels of transition metal ions are influenced by their environment - the ligands. The simplest case for understanding the theory is the octahedral one. If the octahedral's positively charged metal centre is isolated in space, its five d-orbitals are degenerated (have the same energy). The ligands are considered as negative point charges. For neutral species the lone pair is seen as the location for the negative charge. Now all pieces of the puzzle are brought together. Because the ligands approach the metal centre in order to form the octahedral geometry (directions:  $\pm x$ ,  $\pm y$ ,  $\pm z$ ), the five d-orbitals become differently influenced and as a result are no longer degenerate. Two of the five orbitals point towards the ligands, the  $d_{x^2-y^2}$ - and the  $d_z^2$ -orbital. Due to this fact they are destabilized because of the negative charge of the ligands in this direction. The other three orbitals ( $d_{xy}$ ,  $d_{xz}$ ,  $d_{yz}$ ) are not directly in the direction of the ligands and therefore are less destabilized by its negative charge. The energy difference between these two sets of orbitals, the  $d_\sigma$ -set ( $d_{x^2-y^2}$  and  $d_z^2$ ; short  $e_g$ ) and the  $d_\pi$ -set ( $d_{xy}$ ,  $d_{xz}$  and  $d_{yz}$ ; short  $t_{2g}$ ) is known as *crystal field splitting parameter*  $\Delta$ . A high  $\Delta$ -value means that the metal and its ligands form a strong bond ( $\rightarrow$ high-field ligands).

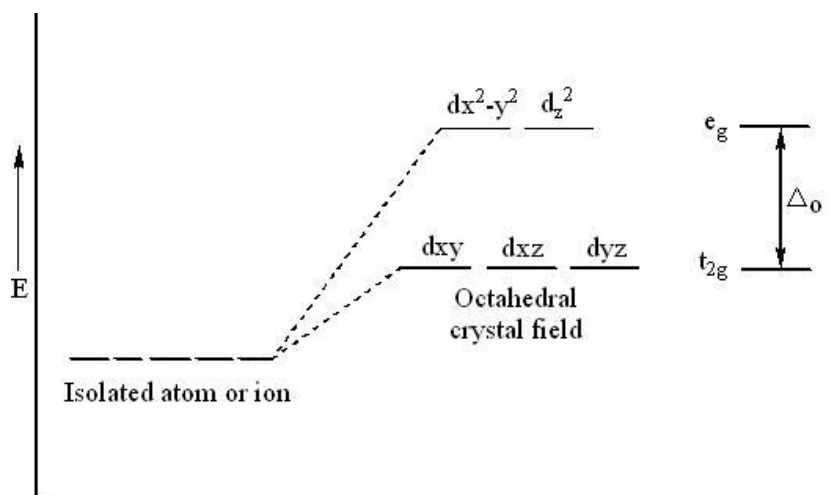


Fig.2.2.1: Crystal field splitting for the octahedral case<sup>48</sup>

Crystal field theory and its crystal field splitting parameter  $\Delta$ , makes two new complex forms (more precisely, two new classifications) possible: *low-spin* and *high-spin* complexes. Low-spin complexes are those which show high crystal field splitting ( $\Delta$ ). In

contrast, high-spin complexes show small  $\Delta$ . For example: a  $d^6$  metal ion in low-spin form would be  $t_{2g}^6 e_g^0$ . All its six electrons are in the three low lying d-orbitals ( $d_{xy}$ ,  $d_{xz}$  and  $d_{yz}$ ) and are paired up. This fact also explains the favoured formation of octahedral geometry in  $d^6$ -metal complexes. If the crystal field splitting is small enough, the electrons could rearrange and form a high-spin complex  $t_{2g}^4 e_g^2$ . Unpaired electrons occupy the two high lying orbitals ( $d_{x^2-y^2}$  and  $d_z^2$ ), due to the Pauli principle and Hund's rule. The driving force behind this phenomenon is the reduced electron-electron repulsion and that the energy cost must be less than the cost of putting another electron into an already singly occupied low-lying orbital. If unpaired spins are found in a complex, that complex is said to be *paramagnetic*. *Diamagnetic* compounds have all spins paired up.

The crystal field theory gives a plausible understanding for the spectra, structure and magnetic properties of transition metal complexes. Crystal field theory could be applied also to all other geometries (eg. the tetrahedral or square-planar case).

### 2.2.6 Ligand field theory

The ligand field theory, in principle, can be seen as extension of the crystal field theory. This theory connects the molecular orbital theory (MO-Theory<sup>49</sup>) with the idea of crystal field splitting. The main point remains the same: how do the ligands influence the d-orbitals of the metal centre. The starting position is nearly identical, just the s- and p-orbitals are additionally considered. This gives nine orbitals for the metal centre (five d-, three p- and one s-orbital). The ligands contribute their lone pairs to the bond ( $\sigma$ -donors). For the sake of comparison, the octahedral case (like in the crystal field theory explanation), will be described. The MO-theory requires forming molecular orbitals from all involved atomic orbitals. Therefore nine atomic orbitals come from the metal centre and six atomic orbitals come from the six ligand lone pairs. This makes fifteen atom orbitals altogether. Thus fifteen molecular orbitals are formed. The orbital-matches between the metal centre and the ligands can be found in the s-orbital, the three p-orbitals and the two  $d_{\sigma}$ -orbitals. These six orbitals form the stable set of *bonding molecular orbitals* - shortened  $\sigma$ -orbitals (*they are the less destabilized ones*). Each bonding orbital generates an identical *antibonding molecular orbital*, shortened  $\sigma^*$ . The

last three remaining orbitals are the  $d_{\pi}$ -orbitals and form the *nonbonding molecular orbitals*. The splitting parameter  $\Delta$  can also be found in ligand field theory. It's between the  $d_{\pi}$ -set and the two lowest lying  $\sigma^*$ -orbitals. If the strength of M-L-bonds increases,  $\Delta$  increases as well. For some  $d^6$ -metal ions in the octahedral case, the  $\sigma$ -MO's and the three  $d_{\pi}$ -MO's are filled with  $18 e^-$  ( $12e^-$  from the six ligands,  $6e^-$  from the  $d^6$ -metal), resulting in a stable configuration. Fig. 2.2.2 shows a typical MO-scheme for octahedral geometry generated through ligand field theory.  $\Delta$  (energy difference between  $e_g^*$  and  $t_{2g}$ ) is shown for both cases. Often there is not just a pure  $\sigma$ -ligand involved; there is a  $\pi$ -acceptor function involved as well. The  $\pi$ -bonding in the octahedral case could be done in two ways. First, one of the three p-orbitals is not used for a  $\sigma$ -bond; second, through a special kind of bonding, called  $\pi$ -backbonding. This second bonding-type is described in the chapter 2.2.7 (" $\pi$ -backbonding"). The symmetry matches in this case are found in the orbitals with  $t_{2g}$ -symmetry. This type of bond requires available  $\pi$  or  $\pi^*$ -orbitals at the ligand.

In a general statement for complex bonding, it could be said, that ligands are nucleophiles (have available electrons in higher orbitals) and metals are electrophiles (have available and empty d orbitals). So the ligands as electron-donors attack the electrophilic metal center and form the bond.

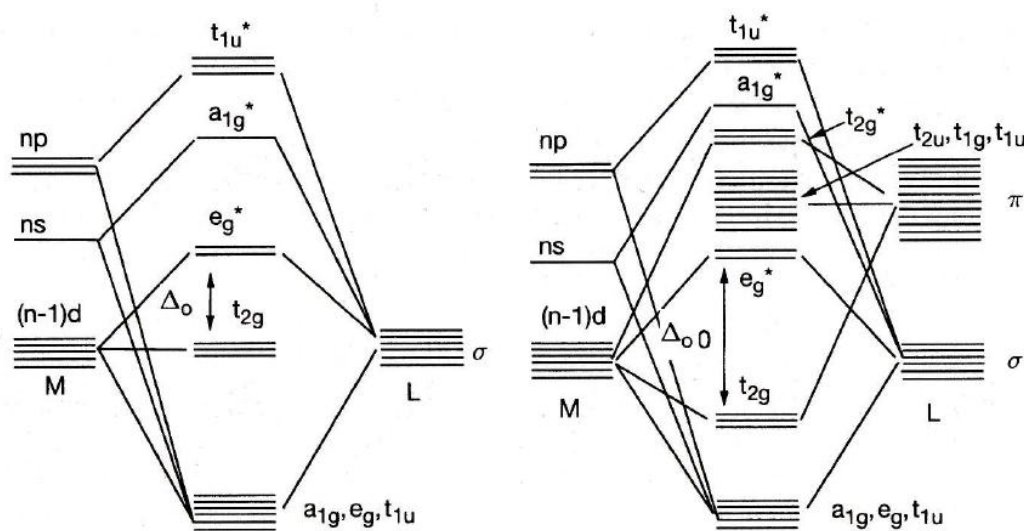


Fig.2.2.2: MO-scheme for octahedral geometry<sup>50</sup> (left:  $\sigma$ - , right:  $\sigma$ - and  $\pi$ -bonds)

### 2.2.7 $\pi$ -backbonding

This particular type of bonding occurs in  $\pi$ -acceptor ligands (e.g. CO or  $\text{NCO}^-$ ) and ligands with multiple bonds. These compounds tend to form strong M-L bonds (therefore they are seen as high field ligands). The mechanism of backbonding is very important and fundamental in transition metal chemistry. The mechanism is easily understood. If the ligand has an empty  $\pi^*$ -orbital (\* indicates anti-bonding orbitals) it would be possible for the metal to lose electron density by pushing electrons into the empty  $\pi^*$ -orbital of the ligand. The symmetry of the two orbitals must be similar, otherwise backbonding isn't possible. Backbonding results in two consequences. First, the splitting parameter  $\Delta$  rises (stronger M-L bond). Second, this allows for low-valent metals to form e.g. CO-complexes. Such metals have high electron density (e.g. W) and through backbonding this is eliminated.

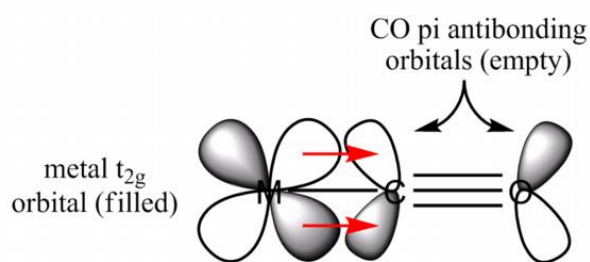


Fig.2.2.3: scheme of  $\pi$ -backbonding in a CO-complex<sup>51</sup>

### 2.2.8 Crystal field spectroscopy

A very interesting feature of transition metal complexes is their ability to absorb light in the UV-VIS range of the spectrum of light. Main group elements absorb light too but mainly in the non-visible UV range. Spectroscopy (especially UV-VIS in the range of 400-700 nm) as tool, offers the possibility to study electronic transitions as well as structural changes in such complexes. Light itself also consists of energy. This energy can<sup>52</sup>:

- raise d-electrons from lower to higher energy levels ("*d-d transition*")
- push electrons between the ligand and metal center back and forth ("*charge-transfer transition*")
- raise ligand-electrons from lower to higher states ("*inner-ligand transition*")

These opportunities allow the important crystal field parameter  $\Delta$  (splitting parameter) to be calculated, as absorption units of the metal centre can be seen in the UV-VIS

spectrum. The calculations are fairly simple for  $d^1$  ions (e.g.  $Ti^{3+}$ ), as no d-electron-electron interactions appear. For systems containing more electrons, possible interactions (also regarding the crystal field interaction) must be taken into account. A full crystal field analysis is very extensive and costly and thus will not be presented within the scope of this master thesis. Only the following two important aspects will be presented in brief: *Sugano-Tanabe diagrams* and the *Racah-parameters*.

*Sugano-Tanabe diagrams*<sup>53</sup> plot the energy difference of each possible excited state of a system against the lowest state of the system (y-axis). On the x-axis the crystal field splitting parameter  $\Delta$  is plotted. Both values are normalized against the Racah-Parameter B. This diagram allows prediction of absorption characteristics for transition metal complexes. All curves which intersect with a vertical line of a given  $\Delta$  show intersection points. These intersection points represent both the number and position of the absorption bands. These data can be compared with obtained experimental values. This is illustrated in Fig.2.2.4.

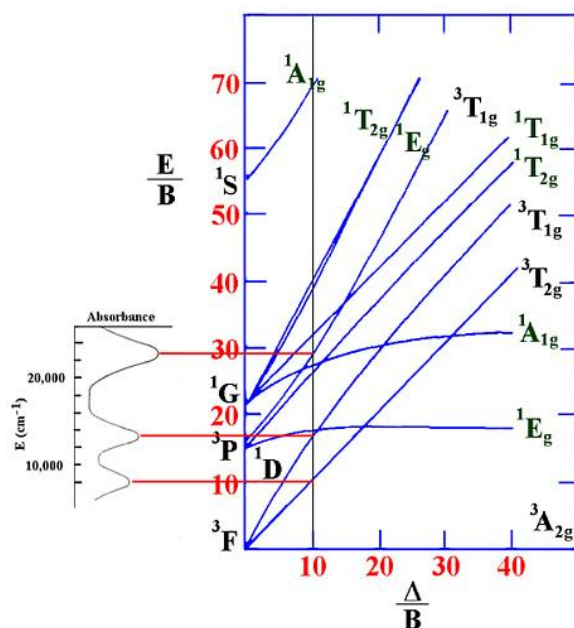


Fig.2.2.4: Sugano-Tanabe-diagram for  $Ni^{2+}$  (in  $O_h$ )<sup>54</sup>

*Racah-parameters*<sup>54</sup> are used to describe electrostatic repulsion of electrons in more-electron-systems. This repulsion depends on the element, spin states and number of electrons and occupied orbitals. The Racah- parameters  $A$ ,  $B$  and  $C$  describe the total repulsion. The values for  $A$ ,  $B$  and  $C$  are empirically determined through spectroscopic methods.

## 2.3 Fundamentals of pyridines

Pyridine chemistry is a vast and well developed field in heterocyclic chemistry. Its principle application is in organic synthetic chemistry. A secondary application field of pyridine chemistry is in coordination chemistry. A short overview of the properties of its chemistry and the influences on these properties will be given in this chapter.

### 2.3.1 Structure

Pyridine has a typical heterocyclic structure and is practically the best known example of a heterocyclus. Fig.2.3.1 illustrates the pyridine structure.

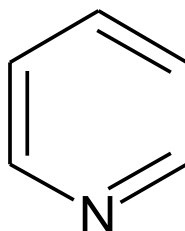


Fig.2.3.1: pyridine structure

Being an aromatic compound its electrons are delocalized over the entire ring ( $\pi$ -electrons). All atoms in pyridine are  $sp^2$  hybridized and their bond lengths are: C-C 139 pm (same as in benzene, it lies between the values of C-C (154 pm) and C=C (134 pm)), C-N 137 pm. The angle between C-N-C is  $117^\circ$  (in benzene C-C-C  $120^\circ$ ). Its lone pair does not contribute to the aromatic system. This fact leads to no positive mesomeric effect by the nitrogen atom. The lone pair influences the chemical properties of pyridine.

### 2.3.2 Chemical properties

Pyridine is weakly basic ( $pK_a$  approx. 5.2). Due to this, the formation of salts (cationic, pyridinium salts; e.g. with HCl) is favoured. Typical reaction behaviour includes, as an amine: acylation, alkylation, protonation and oxidation, and as an aromatic compound: nucleophilic substitution.

The reactions of pyridine could be divided into three groups: with electrophiles, with nucleophiles, and with Lewis-acids.

With electrophiles pyridine undergoes electrophilic substitution. This is a not preferred reaction due to the fact that pyridine is electron deficient (because of the nitrogen atom).

With nucleophiles pyridine undergoes nucleophilic substitution as well as metalation (requires organometallic bases).

With Lewis acids pyridine (as a weak ligand and Lewis base) reacts through the lone pair and will be added. This is a key property for the use of pyridine in complex chemistry.

### 2.3.3 Influence on pyridine's reactivity

Different possibilities can influence the reaction behaviour of pyridine. Reaction conditions always offer a strategy to alter the attitude of a compound. In substances like pyridine the aromatic ring itself offers an opportunity to modify its behaviour. Two effects are of great importance: the *inductive and the mesomeric effect*.

The *mesomeric effect* is based on the ability that an introduced substituent could take part in a possible extension of the mesomeric system of the basic molecule (which already exhibit mesomery). The substituents which show mesomeric effects determine all subsequent reactions and how these reactions proceed. The mesomeric effect is referred to as *M*. According to the ability of the substituent mesomeric effects are classified as either: taking part in extending the mesomeric system (the *+M-effect*) or withdrawing electrons from the mesomeric system (the *-M-effect*). The *+M-effect* activates the molecule and the substituent controls the subsequent substitutions. The *+M-effect* conducts the substituents that follow to substitute in ortho- or para-position. Substituents which show *+M-effect* are for example:  $-\text{NH}_2$ ,  $-\text{OH}$ ,  $-\text{OR}$ ,  $-\text{Phenyl}$ ,  $-\text{F}$ ,  $-\text{Cl}$ ,  $-\text{Br}$ ,  $-\text{I}$ . The *-M-effect* deactivates the molecule and withdraws electrons from the mesomeric system. These substituents have mostly double- or triple bonds. They conduct to a meta-position for the substitutions that follow. Examples would be:  $-\text{COOH}$ ,  $-\text{COOR}$ ,  $-\text{CHO}$  (aldehyde),  $-\text{NO}_2$ . For aromatic systems acidity and basicity could be influenced by substituents with *+M-effect* (basicity sinks) and with *-M-effect* (acidity increases).

The second effect, the *inductive effect*, has its origin in the difference of electronegativity in atoms. The effect is based on electrostatic induction through a molecule with electronegative atoms as substituents. The inductive effect is referred to as *I*. A *-I-effect* means that electrons from an atom with less electronegativity are withdrawn from an atom with higher electronegativity. A *+I-effect* indicates that the substituent pushes electrons to the other atom to increase electron density there. Examples of *+I* are:  $-\text{C}(\text{CH}_3)_3$ , R-Alkyl in general, and of *-I* are:  $-\text{OH}$ ,  $-\text{I}$ ,  $-\text{Br}$ ,  $-\text{NO}_2$ ,  $-\text{NH}_2$ . *+I*-substituents conduct the substitutions that follow to ortho- and para- positions during electrophile aromatic substitution. *-I*-groups tend to conduct to a meta-position. Acidity tends to increase with *-I*-groups (because the proton could be more easily abstracted). *+I*-groups lead to a decreasing acidity. The *I*-effect has a short range (of about three adjacent bonds).

In substitute pyridines, like 4-azidopyriden which is used in this master thesis, both of these two effects are present. In position 4- (or para) the inductive-effect is weak, but leads to increased basicity (*-I*). The mesomeric effect is also *-M* because of the double and triple bonds in the azide moiety. Therefore basicity increases as well.

### 3. Experimental

#### 3.1 Preparation

##### 3.1.1 General procedure

All azide-complexes were prepared with great care and handled carefully! The complexes were synthesized in 100 mL flasks (roughly gas-tight to prevent solvent evaporation) under a fume cupboard. It is recommended to use the *smallest amounts* of azides to minimize each risk. All necessary components were mixed in 100 mL flasks (order and amounts are noted in each compound description). If necessary, heating (in a water bath) or additional solvent is added to achieve a clear solution. If the solution is still not clear, filtration (through a funnel filter and filter circle) is applied. Upon achieving a clear solution it is put into either a compartment dryer (50°), a fridge (4°) or is allowed to stand at room temperature to start crystallizing (exact procedures are noted at each compound description). After crystals were obtained they were filtered through a funnel filter using regular filter circles. The crystals were then put into small closable glasses and stored at the fridge. The mother liquor was also put into the fridge (to allow crystallisation to continue and to be used in case of necessary re-crystallisation).

##### 3.1.2 Preparation of 4-azidopyridine

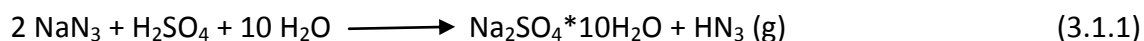
The preparation was performed according to literature<sup>56</sup>. To a solution of 6.0 g (40 mmol) 4-chloropyridine hydrochloride in distilled water (approx. 20-25 mL) NaOH (1 mol/L) was added drop-wise until pH of about 6-6.5 was reached. Then 25 mL methanol was added slowly until the cloudiness disappeared. Now 5.2 g (80 mmol) NaN<sub>3</sub> was added. The solution turned from yellow to red-orange and should remain clear! The resulting clear solution must be on reflux for at least 6.5 h. After the solution cooled down to room temperature extractions with diethylether (small volumes of about 20 mL ether, extracting three to four times) were done. The ether phases were then collected together and dried over MgSO<sub>4</sub>. The solvent was then evaporated in a vacuum. The resulting 4-azidopyridine, an orange-red oily liquid, was produced in about an 80% yield.

The 4-azidopyridine characterisation and reaction control was done by  $^1\text{H-NMR}$ -spectroscopy (in  $\text{D}_2\text{O}$ ):  $\delta$  8,2 (d; pyr) 6,8 (d; pyr) followed by 4,8 (s;  $\text{D}_2\text{O}$ ) and if there was still ether in the product: 3,4 (q;  $\text{Et}_2\text{O}$ ) and 1,0 (t;  $\text{Et}_2\text{O}$ ).

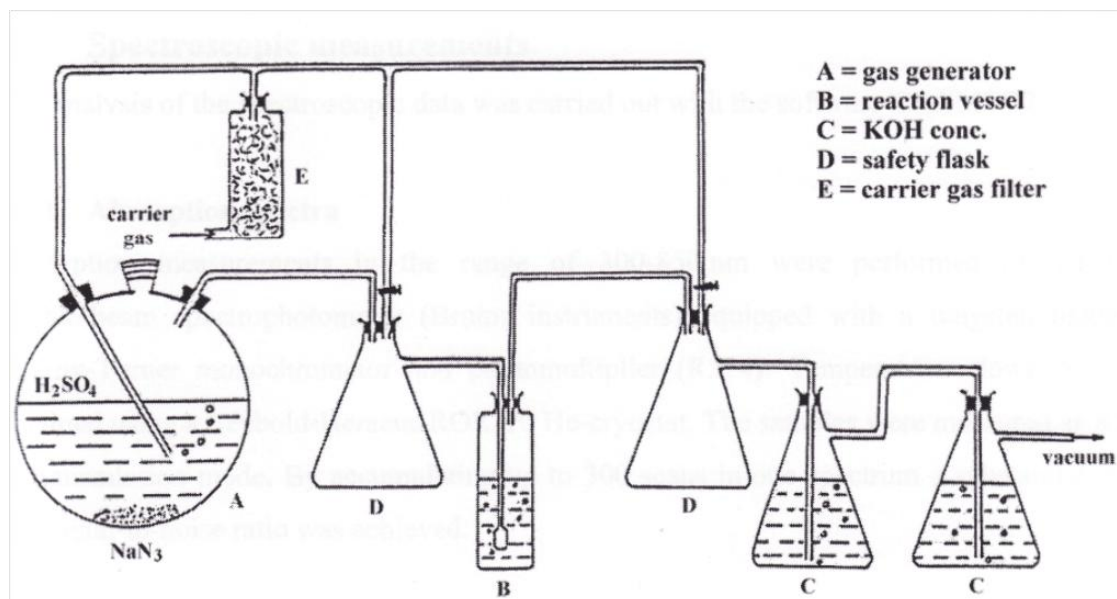
During the experimental work for this master's thesis an interesting discovery was made. It is an absolute *MUST* to use dry and distilled (*FRESH!*) diethylether!!! Commercially available ether *cannot* be used; presumably because of the presence of stabilizers in the ether. These stabilizers probably disturb and/or destroy the product - 4-azidopyridine. In the attachment (p.110) please find two NMR-Spectra pictured, using two different kinds of ether. These spectra show that the use of commercially available diethylether is not useful. By-products arise and the main product exists only in a minor quality. Due to this fact the advice to use fresh ether -though time-costly - for achieving good results is *absolutely necessary!*

### 3.1.3 Preparation of $\text{HN}_3$ saturated water

The  $\text{HN}_3$ -water used was prepared separately in a so-called "azide-generator"<sup>57</sup>. This apparatus is pictured in Fig. 3.1.1. Then dilute  $\text{H}_2\text{SO}_4$  (1:4) is added into E over solid  $\text{NaN}_3$ . About 200mL dist.  $\text{H}_2\text{O}$  were poured into D and the flask is then connected to the generator. The C flasks are needed to absorb dust, flask A is for safety reasons and flask B contains conc. KOH to absorb  $\text{HN}_3$  rests. When the vacuum pump is turned on, the reaction starts. Additional heating could improve  $\text{HN}_3$  formation (especially when the generator was not used for a long time). The gas flow process lasts about 10 minutes. If the pH-paper shows pH 3-4 then the reaction is complete. The reaction follows eq.3.1.1:



The  $\text{HN}_3$  saturated water should always be prepared freshly! Old stocks are often unstable and  $\text{HN}_3$  is evaporated.

Fig.3.1.1: azide-generator<sup>58</sup>

## 3.2 Used devices

### 3.2.1 Single crystal diffraction

X-ray measurements for single crystals are done using two different devices:

First, a Bruker APEX II CCD diffractometer (MoK $\alpha$  radiation  $\lambda = 0,71073 \text{ \AA}$ ) with  $\omega$ -scan mode and graphite-monochromator at 100K. APEX and SAINT<sup>59</sup> software packages were used for data collection and processing. Corrections were applied to all data (for absorption through Laue symmetry requirements)<sup>60</sup>. Structure solution (direct methods) and structure refinement (least-squares) were done by SHELXTL/PC<sup>61</sup> program package. PLATON<sup>62</sup> (a program for automated calculation of derived geometrical data) was used for supporting the structure solution process.

Second, with a Bruker-AXS SMART APEX CCD diffractometer at 100 K with Mo-radiation and graphite monochromator ( $\lambda = 0,7107 \text{ \AA}$ ).

Data collection was done by Ao. Univ.-Prof. Dr. Franz A. Mautner and Ao.Univ.-Prof. Dr. Christoph Marschner.

### 3.2.2 Powder diffraction

Powder diffraction measurements were done with a Bruker AXD Advance D8 diffractometer with  $\text{CuK}\alpha$  radiation ( $\lambda = 1,542 \text{ \AA}$ ). The software used for data collection was XPert<sup>63</sup>.

### 3.2.3 FT IR Spectrometry

For characterizing all synthesized solid compounds (to check existing  $\text{N}_3^-$  or other moieties) a Bruker Alpha P (Platinum-ATR-cap) spectrometer was used. All measurements were done at room temperature. For recording and processing all spectra, OPUS-software<sup>64</sup> was used. The IR-spectrum of each compound can be found in the attachment. The IR-values are described for each compound. The shortcuts are: w (weak), m (medium), s (strong) vs (very strong), sh (shoulder); referring to the intensity of the peak. They are listed from highest to lowest value. All peaks which could be probably allocated were referred to values in "Infrared and Raman spectra of inorganic and coordination compounds" (K. Nakamoto; Wiley; 1986; for  $\text{N}_3^-$ : p. 291 Tab.3; for  $\text{SCN}^-$ : p.284 Tab. 3; for  $\text{OCN}^-$ : p. 290 Tab. 3; for pyridines p.206-213)

### 3.2.4 UV-VIS (NIR) Spectroscopy

Measurements for crystal field analysis of Cobalt- and Nickel-complexes were done by a Perkin-Elmer Lambda-spectrometer (LS950) in the range of  $4000\text{-}45000 \text{ cm}^{-1}$  (pulsed  $\text{D}_2\text{O}$  lamp). The probes were measured in solid state (reflection mode). Data collection and processing was done by UVWinLab software<sup>65</sup>.

### 3.2.5 NMR Spectroscopy

NMR was used for reaction- and product-control of 4-azidopyridine synthesis. After evaporating the rest of the solvent, about 10 mg were placed in a NMR-tube (1cm diameter) and dissolved in a  $\text{D}_2\text{O}$  solvent. Measurements were done on a Bruker AV 3 300 NMR (autorun) spectrometer. Only regular  $^1\text{H}$ -NMR spectra were recorded and used. The spectra were processed and plotted with MestReNova LITE - software<sup>66</sup>.

## 4 Azidopyridine – azide – complexes

### 4.1 [Mn(4-azidopyridine)<sub>2</sub>(N<sub>3</sub>)<sub>2</sub>]<sub>n</sub> (1)

#### Synthesis

Manganese(II)chloride dihydrate (0.161g; 1.0 mmol) and 4-azidopyridine (0.240g; 2.0 mmol) were added to 10 mL of dist. H<sub>2</sub>O. NaN<sub>3</sub> solution (1M; 5 mL) was then slowly added. Some shaking or stirring is recommended in order to homogenize the solution. The solution was then put into a compartment dryer (50°C) for four days. Afterwards the solution was stored at room temperature. Yellowish to white, slightly bleak crystals were obtained (yield approx. 84%).

**C H N –Analytics** found (theor.) in %

C: 31,5 (31,7) H: 2,1 (2,1) N: 50,9 (51,7)

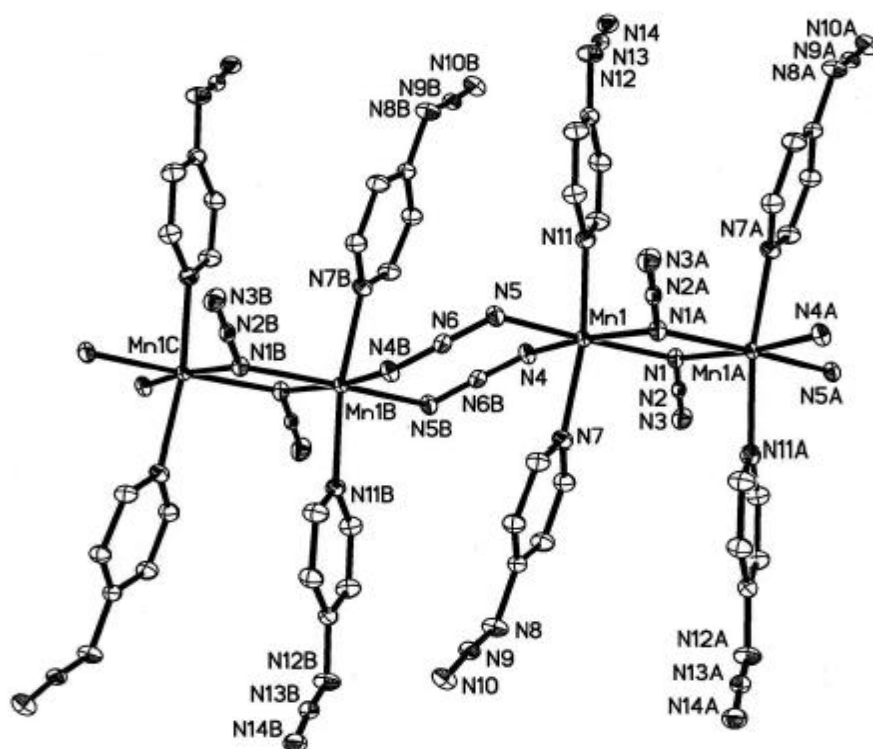
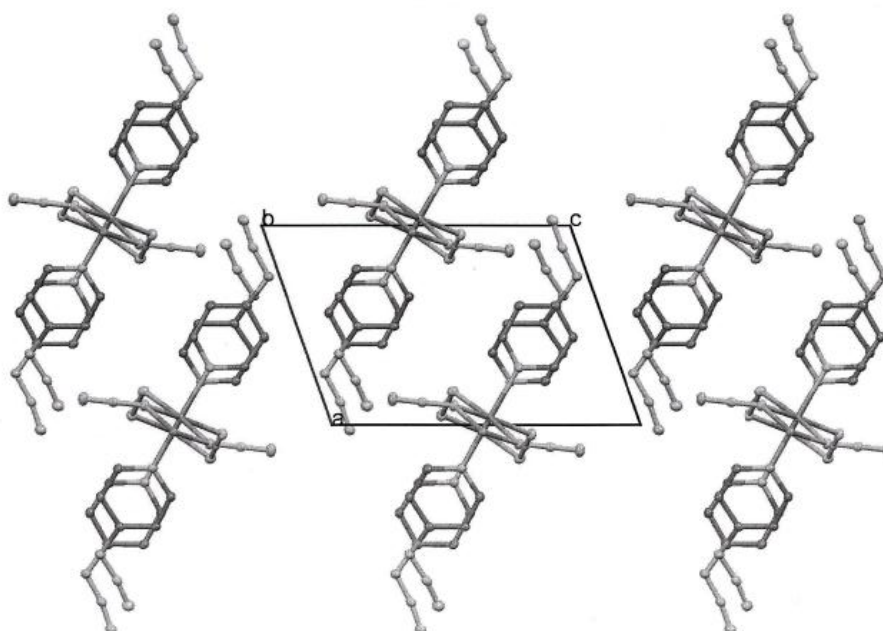
**IR-values** (spectrum on p.111)

$\nu$  (cm<sup>-1</sup>): 2424 w, 2267 w, 2132 sh, 2093 sh, 2054 vs  $\nu_{as}$  (N<sub>3</sub><sup>-</sup>); 1594 vs, 1553 vs, 1498 s, 1417 m, 1133 m, 1009 s, 818 vs (pyridine moiety); 1318 sh, 1285 vs, 1211 s,  $\nu_{sym}$  (N<sub>3</sub>); 535 s, 518 s  $\delta$  N<sub>3</sub><sup>-</sup>

#### Discussion of the structure

[Mn(4-Azidopyridine)<sub>2</sub>(N<sub>3</sub>)<sub>2</sub>]<sub>n</sub> (subsequently abbreviated as **(1)**), crystallizes in triclinic space group P-1. This structure has already been published (in two different modifications)<sup>67/68</sup>. In Table 4.1.1 the crystal data and processing parameter are summarized. Table 4.1.2 shows the relevant bond lengths and angles. Fig.4.1.1 shows the crystal structure of **(1)**. Fig.4.1.2 illustrates the packing arrangement of **(1)**. The asymmetric unit of **(1)** contains one Mn<sup>2+</sup> centre, which is octahedral coordinated. Two coordination sites are occupied by 4-azidopyridine, the other four sites by N<sub>3</sub><sup>-</sup>. The two 4-azidopyridine ligands coordinate in trans position. The azido ligands form double bridges between the metal centres. The formation is alternately EE (end-end) and EO(end-on). The chain is oriented along the b-axis of the unit cell. The arrangement around the metal centre for the Mn<sub>2</sub>( $\mu_{1,3}$ -N<sub>3</sub>)<sub>2</sub> unit is as follows: Mn(1)-N(5) 2.2450(12) Å and Mn(1)-N(4) 2.2400(12) Å. The corresponding bond angles are N(6)-N(5)-Mn(1) 123.85(10)° and N(6)-N(4)-Mn(1B) 119.91(9)°. The ring conformation of Mn<sub>2</sub>( $\mu_{1,3}$ -N<sub>3</sub>)<sub>2</sub> is not planar. The conformation is distorted in a “chair conformation”. This can be evaluated and seen in the  $\delta$

parameter<sup>69</sup> of 34.0°. The Mn(1B)-N(5B)...N(4)-Mn(1) torsion angle equals 50,9°. The other bridge arrangement, the EO configuration (Mn<sub>2</sub>N<sub>2</sub>), is strictly planar. The ring shows the following parameter: N(1A)-Mn(1)-N(1) 81.25(5)°, Mn(1)-N(1A)-Mn(1A) 98.75(5)° and Mn(1)-N(1) 2.2172(11) Å, Mn(1A)-N(1) 2.2156(11) Å. The angle for the plane N(1A)...N(1)-N(2) is 155.1°. The intra-chain distances of Mn ... Mn are asymmetric due to the fact of the alternate EO and EE bridges. In correspondence to the EE ring 5.0309 Å, and the EO ring 3.364 Å. The polymeric chain of **(1)** is slightly corrugated with an Mn(1A)... Mn(1)...Mn(1B) angle of 162.9°. The two axially bound 4-azidopyridine ligands show an angle of N(11)-Mn(1)-N(7) 171.10(4)°. The reason for this deviation from 180° is due to the moving of the axial ligands away from the EO ring. The terminal azido group in para-position (from 4-azidopyridine) is highly asymmetric, with  $\Delta d(\text{N-N})$  (difference of N-N bond lengths within the azide group) 0.1355(18) Å and 0.1222(18) Å. The according bond angle for N(14)-N(13)-N(12) is 170.95(15)° and for N(10)-N(9)-N(8) is 171.14(15)°.

Fig.4.1.1: Structure of [Mn(4-Azidopyridine)<sub>2</sub>(N<sub>3</sub>)<sub>2</sub>]<sub>n</sub>Fig.4.1.2: Packing view of [Mn(4-Azidopyridine)<sub>2</sub>(N<sub>3</sub>)<sub>2</sub>]<sub>n</sub>

Tab. 4.1.1: Crystallographic data and processing parameter

---

Identification-code	RF440
Empirical formula	C <sub>10</sub> H <sub>8</sub> MnN <sub>14</sub>
Formula mass	379.24
System	triclinic
Space group	P-1
a (Å)	8.2450 (3)
b (Å)	8.3050 (3)
c (Å)	11.9444 (5)
α (°)	82.612 (2)
β (°)	69.905 (2)
γ (°)	80.754 (2)
V(Å <sup>3</sup> )	755.74 (5)
Z	1
F (0 0 0)	382
T (K)	100 (2)
μ (MoK <sub>α</sub> )(mm <sup>-1</sup> )	0.904
D <sub>calc</sub> (Mg/m <sup>3</sup> )	1.667
Crystal size	0.38 x 0.22 x 0.17
Θ range (°)	1.82-31.70
Reflections collected	23052
Independent refl./ R <sub>int</sub>	4813/0.0274
Parameters	226
Goodness-of-Fit on F <sup>2</sup>	1.048
R1/wR2 (all data)	0.0291/0.0688
Residual extrema (e/ Å <sup>3</sup> )	0.554/-0.419

---

Tab.4.1.2: Selected bond lengths (Å) and angles (°) for **(1)**

Mn(1')-N(1)	2.2156(11)	Mn(1)-N(1)	2.2172(11)
Mn(1)-N(11)	2.2369(12)	Mn(1)-N(4)	2.2400(12)
Mn(1)-N(5)	2.2450(12)	Mn(1)-N(7)	2.2701(12)
N(1)-N(2)	1.2041(16)	N(2)-N(3)	1.1497(17)
N(5)-N(6)	1.1754(15)	N(6)-N(4'')	1.1794(15)
N(4'')-N(6)	1.1795(15)	N(11)-C(6)	1.3384(18)
N(11)-C(10)	1.3403(18)	N(12)-N(13)	1.2536(17)
N(12)-C(8)	1.4113(18)	N(13)-N(14)	1.1181(17)
N(7)-C(5)	1.3379(18)	N(7)-C(1)	1.3411(17)
N(8)-N(9)	1.2465(17)	N(8)-C(3)	14139.(18)
N(9)-N(10)	1.1243(17)		
N(1')-Mn(1)-N(1)	81.25(5)	N(1')-Mn(1)-N(11)	94.13(4)
N(1)-Mn(1)-N(11)	93.82(4)	N(1')-Mn(1)-N(4)	170.27(4)
N(1)-Mn(1)-N(4)	89.33(4)	N(11)-Mn(1)-N(4)	88.93(4)
N(1')-Mn(1)-N(5)	90.09(4)	N(1)-Mn(1)-N(5)	171.34(4)
N(11)-Mn(1)-N(5)	86.79(4)	N(4)-Mn(1)-N(5)	99.31(4)
N(1')-Mn(1)-N(7)	91.85(4)	N(1)-Mn(1)-N(7)	93.60(4)
N(11)-Mn(1)-N(7)	171.10(4)	N(4)-Mn(1)-N(7)	86.25(4)
N(5)-Mn(1)-N(7)	86.62(4)	N(2)-N(1)-Mn(1')	126.32(9)
N(2)-N(1)-Mn(1)	126.07(9)	Mn(1')-N(1)-Mn(1)	98.75(5)
N(3)-N(2)-N(1)	179.48(14)	N(6)-N(5)-Mn(1)	123.85(10)
N(5)-N(6)-N(4'')	178.74(14)	N(6)-N(4)-Mn(1'')	119.91(9)
C(6)-N(11)-C(10)	116.87(12)	C(6)-N(11)-Mn(1)	120.85(9)
C(10)-N(11)-Mn(1)	122.28(10)	N(13)-N(12)-C(8)	116.50(12)
N(14)-N(13)-N(12)	170.95(15)	N(10)-N(9)-N(8)	171.14(15)
N(9)-N(8)-C(3)-C(4)	(-)-179.67(12)		
N(9)-N(8)-C(3)-C(2)	0.0(2)		
N(13)-N(12)-C(8)-C(7)	(-)-178.72(13)		
N(13)-N(12)-C(8)-C(9)	0.5(2)		

Symmetry codes: (a = ') -x, 1-y, 1-z (b = '') -x, 1-y, 1-z

**4.2 [Co(4-azidopyridine)<sub>2</sub>(N<sub>3</sub>)<sub>2</sub>]<sub>n</sub>****(2)****Synthesis**

Cobalt(II)chloride hexahydrate (0.237g; 1.0 mmol) and 4-azidopyridine (0.240g; 2.0 mmol) were dissolved in 10 mL of dest. H<sub>2</sub>O. The solution was stirred and heated for about 35 min. (approx. 40°C) to dissolve all rests of salt and ligand. After the solution cleared, aqueous NaN<sub>3</sub> solution (1M, 5 mL) was slowly added. The solution turned from slightly pink to deep violet and a grey precipitate formed. The solution is heated to 90° for approximately half an hour and another 10 mL of dist. H<sub>2</sub>O were added to dissolve the precipitate. After the solution cleared it was filtered. The resulting solution was stored in a compartment dryer (50°) for three days. After that, the solution was kept at room temperature, and very small deep violet crystals formed (yield approx. 70 %)

**C H N –Analytics** found(theor.) in %

C: 31,3 (31,3) H: 2,0 (2,1) N: 51,5 (51,2)

**IR-values** (spectrum on p.111)

$\nu$  (cm<sup>-1</sup>): 2421 w, 2264 w, 2129 sh, 2105 sh, 2060 vs  $\nu_{as}$  (N<sub>3</sub><sup>-</sup>); 1598 vs, 1561 vs, 1499 s, 1427 m, 1133 m, 1012 s, 818 vs (pyridine moiety); 1346 sh, 1292 vs, 1211 s,  $\nu_{sym}$  (N<sub>3</sub>); 537 s, 517 s  $\delta$  (N<sub>3</sub><sup>-</sup>)

**Discussion of the structure**

The second azido-bridged complex, [Co(4-Azidopyridine)<sub>2</sub>(N<sub>3</sub>)<sub>2</sub>]<sub>n</sub> (short **(2)**) crystallizes in triclinic space group P-1, as well. Fig.4.2.1 shows its crystal structure. Fig.4.2.2 illustrates the packing view of **(2)**. The asymmetric unit of **(2)** contains one Co<sup>2+</sup> centre which is octahedral coordinated. The coordination sites are occupied by two 4-azidopyridines (axial) and the other four sites are occupied by N<sub>3</sub><sup>-</sup>. The two 4-azidopyridine ligands coordinate in trans position to each other. The double bridges formed between the Cobalt centres are of a different, alternate, style. The azido ligand alternately forms EE (end-end) and EO(end-on) bridges. The chain is oriented along the b-axis of the unit cell. The end-on and end-end formed rings around the Cobalt centre show the following values for the Co<sub>2</sub>( $\mu_{1,3}$ -N<sub>3</sub>)<sub>2</sub> ring: Co(1)-N(6) 2.1682(11) Å and Co(1)-N(4) 2.1651(11) Å. The bond angles for this conformation are: N(5B)-N(6)-Co(1) 123.85(10)° and N(5)-N(4)-Co(1) 120.43(9)°. The Co<sub>2</sub>( $\mu_{1,3}$ -N<sub>3</sub>)<sub>2</sub>-ring is not of planar geometry. A

stable “chair-style” structure is preferred. This conformation can be characterized through the  $\delta$  parameter =  $34.8^\circ$ . The Cobalt-azide chain show a Co(1)-N(6)...N(4B)-Co(1B) torsion angle of  $53.3^\circ$ . The second azide-bridge, the Co<sub>2</sub>N<sub>2</sub> EO-arrangement is entirely planar. The ring is defined by following parameters: N(1A)-Co(1)-N(1)  $80.84(5)^\circ$  and Co(1A)-N(1)-Co(1)  $99.29(7)^\circ$  and the lengths Co(1)-N(1)  $2.1396(11)$  Å and Co(1A)-N(1)  $2.1337(11)$  Å. The angle for the two opposing EO azide-groups N(1A)...N(1)-N(2) is  $156.6^\circ$ . The intra-chain distances of Co ... Co are asymmetric due to alternate EO and EE bridges. For the EE ring it is  $4.979$  Å, and for the EO ring  $3.253$  Å. The angle of  $164.1^\circ$  shows that the chain of **(2)** is not linear but slightly corrugated along Co(1A)... Co(1)...Co(1B). The two axially bounded 4-azidopyridine ligands show an angle of N(11)-Co(1)-N(7)  $172.02(4)^\circ$ , which is similar to the value of **(1)** and is also based on the same reason of repulsion between the EO Azide-group and the azidopyridine as seen in **(1)**. Also the terminal azide moiety of 4-azidopyridine in **(2)** is asymmetric, with  $\Delta d(\text{N-N})$   $0.1321(17)$  Å and  $0.1204(17)$  Å the according bond angle for N(14)-N(13)-N(12) is  $170.55(14)^\circ$  and for N(10)-N(9)-N(8)  $171.28(14)^\circ$ , respectively. In Table 4.2.1 the crystal data and processing parameters of **(2)** can be seen. Table 4.2.2 shows all relevant bond lengths and angles.

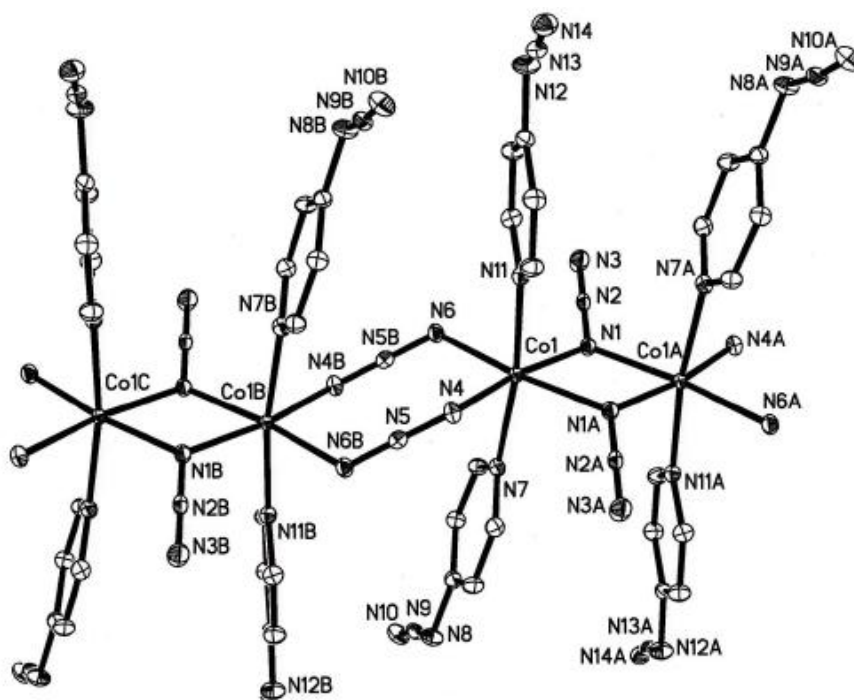


Fig.4.2.1: Structure of [Co(4-Azidopyridine)<sub>2</sub>(N<sub>3</sub>)<sub>2</sub>]<sub>n</sub>

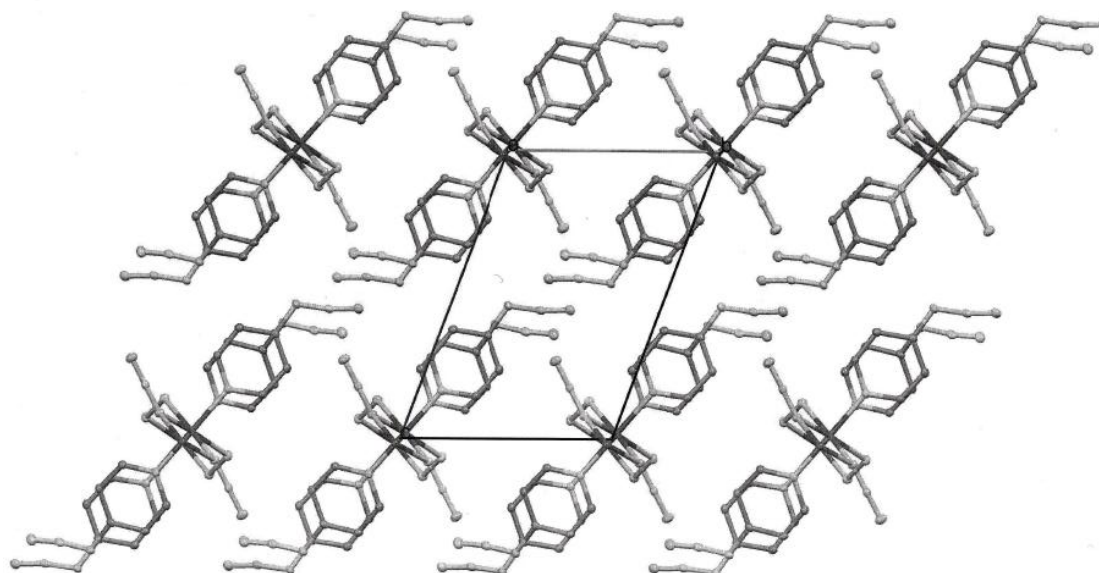


Fig.4.2.2: Packing view of [Co(4-Azidopyridine)<sub>2</sub>(N<sub>3</sub>)<sub>2</sub>]<sub>n</sub>

Tab. 4.2.1: Crystallographic data and processing parameter

---

Identification-code	RF437
Empirical formula	C <sub>10</sub> H <sub>8</sub> CoN <sub>14</sub>
Formula mass	383.23
System	triclinic
Space group	P-1
a (Å)	8.1568 (4)
b (Å)	8.2180 (4)
c (Å)	11.8062 (5)
α (°)	109.973 (2)
β (°)	90.965 (2)
γ (°)	98.611 (2)
V(Å <sup>3</sup> )	733.44 (6)
Z	1
F (0 0 0)	386
T (K)	100 (2)
μ (MoK <sub>α</sub> )(mm <sup>-1</sup> )	1.201
D <sub>calc</sub> (Mg/m <sup>3</sup> )	1.735
Crystal size	0.23 x 0.19 x 0.11
Θ range (°)	1.84-25.50
Reflections collected	15621
Independent refl./ R <sub>int</sub>	2662/0.0341
Parameters	226
Goodness-of-Fit on F <sup>2</sup>	1.102
R1/wR2 (all data)	0.0287/0.0812
Residual extrema (e/ Å <sup>3</sup> )	0.852/-0.574

---

Tab. 4.2.2: Selected bond lengths (Å) and angles (°) for **(2)**

Co(1)-N(11)	2.1309(11)	Co(1')-N(1)	2.1337(11)
Co(1)-N(1)	2.1396(11)	Co(1)-N(7)	2.1510(11)
Co(1)-N(4)	2.1651(11)	Co(1)-N(6)	2.1682(11)
N(1)-N(2)	1.2038(16)	N(2)-N(3)	1.1533(17)
N(4)-N(5)	1.1795(16)	N(5'')-N(6)	1.1773(16)
N(6'')-N(5)	1.1773(16)	N(7)-C(1)	1.3425(18)
N(7)-C(5)	1.3432(17)	N(8)-N(9)	1.2475(17)
N(8)-C(3)	1.4123(17)	N(9)-N(10)	1.1271(17)
N(11)-C(6)	1.3426(17)	N(11)-C(10)	1.3434(17)
N(12)-N(13)	1.2536(17)	N(12)-C(8)	1.4129(18)
N(13)-N(14)	1.1215(17)		
N(11)-Co(1)-N(1')	92.74(4)	N(11)-Co(1)-N(1)	93.70(4)
N(1')-Co(1)-N(1)	80.84(5)	N(11)-Co(1)-N(7)	172.02(4)
N(1)-Co(1)-N(7')	93.81(4)	N(1)-Co(1)-N(7)	91.85(4)
N(11')-Co(1)-N(4)	87.98(4)	N(1')-Co(1)-N(4)	90.60(4)
N(1)-Co(1)-N(4)	171.35(4)	N(7)-Co(1)-N(4)	87.39(4)
N(11)-Co(1)-N(6)	86.72(4)	N(1')-Co(1)-N(6)	171.93(4)
N(1)-Co(1)-N(6)	91.15(4)	N(7)-Co(1)-N(6)	87.43(4)
N(4)-Co(1)-N(6)	97.43(4)	N(2)-N(1)-Co(1')	125.88(9)
N(2)-N(1)-Co(1)	127.16(9)	Co(1')-N(1)-Co(1)	99.16(5)
N(3)-N(2)-N(1)	179.58(15)	N(5)-N(4)-Co(1)	120.43(9)
N(6'')-N(5)-N(4)	178.49(14)	N(5'')-N(6)-Co(1)	123.85(10)
C(1)-N(7)-C(5)	117.02(12)	C(1)-N(7)-Co(1)	121.46(9)
C(5)-N(7)-Co(1)	120.83(9)	N(9)-N(8)-C(3)	116.52(12)
N(10)-N(9)-N(8)	171.28(14)	C(6)-N(11)-C(10)	116.83(12)
C(6)-N(11)-Co(1)	120.87(9)	C(10)-N(11)-Co(1)	122.29(9)
N(13)-N(12)-C(8)	116.99(12)	N(14)-N(13)-N(12)	170.55(14)
N(9)-N(8)-C(3)-C(4)	(-)-0.3(3)		
N(9)-N(8)-C(3)-C(2)	178.79(19)		
N(13)-N(12)-C(8)-C(7)	179.33(19)		
N(13)-N(12)-C(8)-C(9)	(-)-0.2(3)		

Symmetry codes: (a = ') 2-x, -y, -z (b = '') 1-x, -y, -z

**4.3 [Ni(4-azidopyridine)<sub>2</sub>(N<sub>3</sub>)<sub>2</sub>]<sub>n</sub> (3)****Synthesis**

NiCl<sub>2</sub> × 6H<sub>2</sub>O (0.237g; 1.0 mmol) and 4-azidopyridine (0.240g; 2.0 mmol) were dissolved in 7 mL of dist. H<sub>2</sub>O/HN<sub>3</sub>. Greenish to white flakes precipitate in the solution. The solution was stirred and heated to 80°C for half an hour after which 1 mL of dist. H<sub>2</sub>O/HN<sub>3</sub> was added. Then, the solution was filtered. To the resulting emerald-green solution aqueous NaN<sub>3</sub> solution (1M; 5 mL) was added. Once again, a green precipitate was obtained. 10mL dist. H<sub>2</sub>O/HN<sub>3</sub> was then added while heating (90°C for 1h) and stirring until a nearly clear solution was obtained. The solution was again filtered. The solution was placed into a compartment dryer (50°C) for three days. After this period of time, the solution was kept at room temperature. Dark emerald-green, crystals were obtained after one week (yield approx. 61 %). In the event of no crystals forming, the solution could be stored in a fridge (4°C).

**C H N –Analytics** found (theor.) in %

C: 31,3 (31,4) H: 2,1 (2,1) N: 51,0 (51,2)

**IR-values** (spectrum on p.112)

$\nu$  (cm<sup>-1</sup>): 2424 w, 2272 w, 2138 sh, 2109 sh, 2052 vs  $\nu_{as}$  (N<sub>3</sub><sup>-</sup>); 1602 vs, 1562 vs, 1503 s, 1427 m, 1136 m, 1015 s, 814 vs (pyridine moiety); 1357 sh, 1292 vs, 1211 s,  $\nu_{sym}$  (N<sub>3</sub>); 537 s, 521 s  $\delta$  (N<sub>3</sub><sup>-</sup>)

**Discussion of the structure**

The third representative of the 4-azidopyridine-azide class, Ni(4-Azidopyridine)<sub>2</sub>(N<sub>3</sub>)<sub>2</sub>]<sub>n</sub> (abbreviated **(3)**), crystallizes in triclinic space group P-1, like **(1)** and **(2)**. The Tables 4.3.1 and 4.3.2 summarize the crystal data and processing parameter as well as the relevant bond lengths and angles of **(3)**. Fig.4.3.1 displays the crystal structure of **(3)**, and Fig.4.3.2 displays the packing mode of **(3)**. One Ni<sup>2+</sup> centre can be found in the asymmetric unit of **(3)**. The Ni<sup>2+</sup> centre is octahedral coordinated, with two 4-azidopyridine ligands in trans-position and four N<sub>3</sub><sup>-</sup> groups forming double bridges between adjacent metal centres. The bridges are formed alternately in EE (end-end) and EO(end-on) modes. The chain is oriented along the b-axis of the unit cell. The two bridging modes determine the following arrangement around the metal

centre: the  $\text{Ni}_2(\mu_{1,3}\text{-N}_3)_2$  end –end form has the parameter: Ni(1)-N(6) 2.128(4) Å and Ni(1)-N(4) 2.120(4) Å. The corresponding bond angles are N(5B)-N(6)-Ni(1) 123.9(3)° and N(5)-N(4)-Ni(1) 120.3(3)° for this bridging modification. The  $\text{Ni}_2(\mu_{1,3}\text{-N}_3)_2$  does not show planar geometry. The conformation is distorted and tends to form a “chair-like” conformation. This is specified by the  $\delta$  parameter of 35.5°. The Ni(1)-N(6)...N(4B)-Ni(1B) torsion angle of the Ni-chain can be estimated at 54,9°. In contrast to the EE bridges, the EO form ( $\text{Ni}_2\text{N}_2$ ) is indeed planar. The calculated  $\text{Ni}_2\text{N}_2$ -ring parameters are: N(1A)-Ni(1)-N(1) 80.31(16)° and Ni(1A)-N(1)-Ni(1) 99.69(16)° as angles and Ni(1)-N(1) 2.102(4) Å Ni(1A)-N(1) 2.102(4) Å as lengths. The two azide groups in the EO bridges do not indicate a linear plane as they are slightly bent with an angle for N(1A)...N(1)-N(2) of 155,9°. The intra-chain distances of Ni ... Ni are asymmetric, as known from **(1)** and **(2)**. The corresponding values for the EE ring are 4.940 Å and for the EO ring are 3.215 Å. The chain of **(3)** is slightly corrugated along Ni(1A)... Ni(1)...Ni(1B) with an angle of 164.6°. The two 4-azidopyridine ligands, trans coordinated to the  $\text{Ni}^{2+}$  centre, show an angle for N(11)-Ni(1)-N(7) of 173.23(16)°. The terminal azide moiety (at 4-azidopyridine) has asymmetric geometry, with  $\Delta d(\text{N-N})$  values of 0.117(5) Å and 0.151(6) Å and corresponding bond angles for N(14)-N(13)-N(12) of 170.55(14)° and for N(10)-N(9)-N(8) 170.4(5)°, respectively.

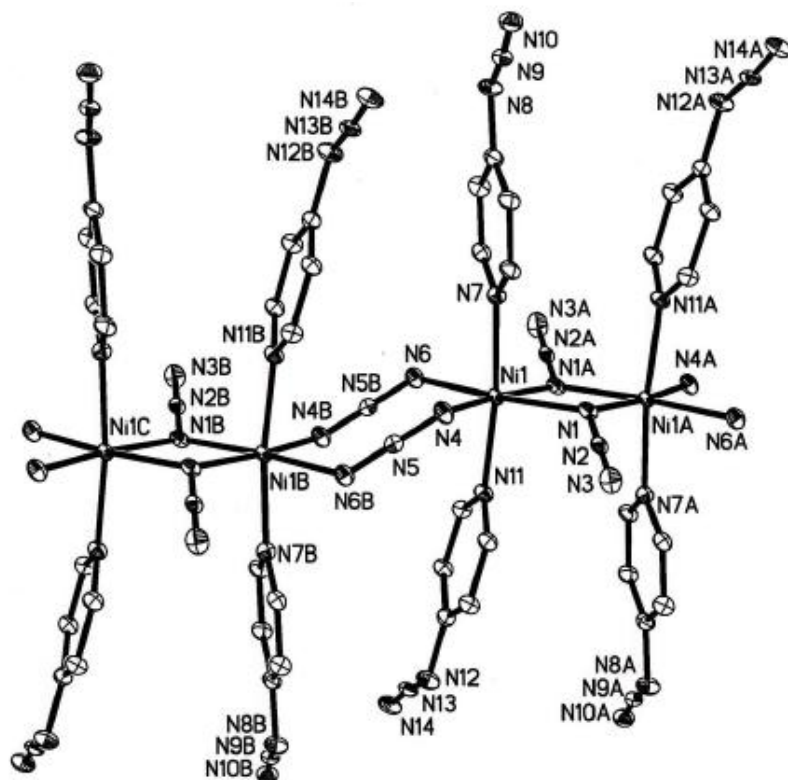


Fig.4.3.1: Structure of  $[\text{Ni}(\text{4-Azidopyridine})_2(\text{N}_3)_2]_n$

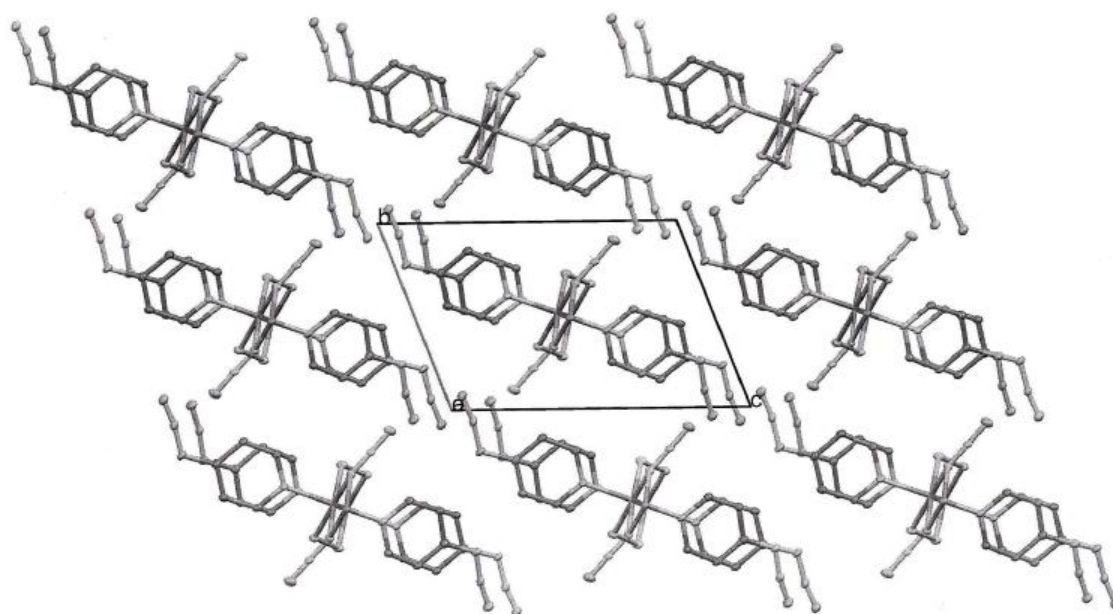


Fig.4.3.2: Packing view of  $[\text{Ni}(\text{4-Azidopyridine})_2(\text{N}_3)_2]_n$

Tab.4.3.1: Crystallographic data and processing parameter

---

Identification-code	AT15
Empirical formula	C <sub>10</sub> H <sub>8</sub> NiN <sub>14</sub>
Formula mass	383.01
System	Triclinic
Space group	P-1
a (Å)	8.0853 (4)
b (Å)	8.2115 (4)
c (Å)	11.7269 (6)
α (°)	109.802 (2)
β (°)	91.023 (3)
γ (°)	98.359 (2)
V(Å <sup>3</sup> )	722.87 (6)
Z	1
F (0 0 0)	388
T (K)	100 (2)
μ (MoK <sub>α</sub> )(mm <sup>-1</sup> )	1.374
D <sub>calc</sub> (Mg/m <sup>3</sup> )	1.760
Crystal size	0.34 x 0.19 x 0.14
Θ range (°)	1.85-30.54
Reflections collected	25788
Independent refl./ R <sub>int</sub>	3946/0.0507
Parameters	221
Goodness-of-Fit on F <sup>2</sup>	1.206
R1/wR2 (all data)	0.0610/0.1682
Residual extrema (e/ Å <sup>3</sup> )	2.135/-0.964

---

Tab. 4.3.2: Selected bond lengths (Å) and angles (°) for (3)

Ni(1)-N(7)	2.086(4)	Ni(1)-N(11)	2.090(4)
Ni(1')-N(1)	2.102(4)	Ni(1)-N(1)	2.105(4)
Ni(1)-N(4)	2.120(4)	Ni(1)-N(6)	2.128(4)
N(1)-N(2)	1.196(5)	N(2)-N(3)	1.154(6)
N(7)-C(1)	1.344(6)	N(7)-C(5)	1.345(6)
N(8)-N(9)	1.259(5)	N(8)-C(3)	1.411(6)
N(9)-N(10)	1.108(6)	N(11)-C(6)	1.348(6)
N(11)-C(10)	1.351(6)	N(12)-N(13)	1.246(5)
N(12)-C(8)	1.401(6)	N(13)-N(14)	1.129(5)
N(4)-N(5)	1.182(5)	N(6'')-N(5)	1.171(5)
N(5'')-N(6)	1.171(5)		
N(7)-Ni(1)-N(11)	173.23(16)	N(7)-Ni(1)-N(1')	93.64(15)
N(11)-Ni(1)-N(1')	90.88(15)	N(7)-Ni(1)-N(1)	91.78(15)
N(11)-Ni(1)-N(1)	93.96(16)	N(1')-Ni(1)-N(1)	80.31(16)
N(7)-Ni(1)-N(4)	87.71(16)	N(11)-Ni(1)-N(4)	88.55(15)
N(1')-Ni(1)-N(4)	171.56(16)	N(1)-Ni(1)-N(4)	91.32(15)
N(7)-Ni(1)-N(6)	86.69(15)	N(11)-Ni(1)-N(6)	88.11(16)
N(1')-Ni(1)-N(6)	92.03(15)	N(1)-Ni(1)-N(6)	172.08(15)
N(4)-Ni(1)-N(6)	96.37(16)	N(2)-N(1)-Ni(1')	126.9(3)
N(2)-N(1)-Ni(1)	125.2(3)	Ni(1')-N(1)-Ni(1)	99.69(16)
N(3)-N(2)-N(1)	179.1(5)	C(1)-N(7)-C(5)	116.5(4)
C(1)-N(7)-Ni(1)	121.3(3)	C(5)-N(7)-Ni(1)	122.1(3)
N(9)-N(8)-C(3)	117.2(4)	N(10)-N(9)-N(8)	170.4(5)
C(6)-N(11)-C(10)	116.0(4)	C(6)-N(11)-Ni(1)	121.9(3)
C(10)-N(11)-Ni(1)	116.6(3)	N(13)-N(12)-C(8)	116.6(4)
N(14)-N(13)-N(12)	171.2(4)	N(5)-N(4)-Ni(1)	120.2(3)
N(5'')-N(6)-Ni(1)	123.9(3)	N(6'')-N(5)-N(4)	178.1(4)
N(9)-N(8)-C(3)-C(4)	(-)0.4(7)		
N(9)-N(8)-C(3)-C(2)	178.5(4)		
N(13)-N(12)-C(8)-C(7)	(-)0.8(8)		
N(13)-N(12)-C(8)-C(9)	179.0(4)		

Symmetry codes: (a = ') 1-x, 1-y, 1-z (b = '') -x, 1-y, 1-z

**4.4 [Zn(4-azidopyridine)<sub>2</sub>(N<sub>3</sub>)<sub>2</sub>]<sub>n</sub> (4)****Synthesis**

Waterfree Zinc(II)chloride (0.136g; 1.0 mmol) and 4-azidopyridine (0.240g; 2.0 mmol) were dissolved in 10 mL of dist. H<sub>2</sub>O. The resulting cloudy solution was then stirred and heated for about 15 min. (at approx. 35° C) in order to dissolve the rest of the salt and ligand. Then NaN<sub>3</sub> solution (1M; 5 mL) was slowly added. The solution remained clear. The resulting solution was stored in a compartment dryer (50°C) for one day. After that, the solution was kept at room temperature. Small white, slightly blear crystals were obtained (yield approx. 80 %).

**C H N –Analytics** found (theor.) in %

C: 30,4 (30,8) H: 2,0 (2,1) N: 50,0 (50,3)

**IR-values** (spectrum on p.112)

$\nu$  (cm<sup>-1</sup>): 2421 w, 2264 w, 2132 sh, 2109 sh, 2064 vs  $\nu_{as}$  (N<sub>3</sub><sup>-</sup>); 1600 vs, 1565 vs, 1502 s, 1426 m, 1132 m, 1014 s, 819 vs (pyridine moiety); 1350 sh, 1295 vs, 1213 s,  $\nu_{sym}$  (N<sub>3</sub>); 538 s, 518 s  $\delta$  (N<sub>3</sub><sup>-</sup>)

**Discussion of the structure**

Again, the crystals of Zn(4-Azidopyridine)<sub>2</sub>(N<sub>3</sub>)<sub>2</sub>]<sub>n</sub>, **(4)**, are from the triclinic space group P-1. The asymmetric unit of this zinc complex contains one octahedral coordinated Zn<sup>2+</sup> centre. Two 4-azidopyridine in trans-position and four N<sub>3</sub><sup>-</sup> ligands can be found. The azido ligands form double bridges between two adjacent metal centres. Two alternate modifications can be observed: EE and EO. The chain is oriented along the a-axis of the unit cell. The arrangement around the metal centre in regards to the two bridging modes for the Zn<sub>2</sub>( $\mu_{1,3}$ -N<sub>3</sub>)<sub>2</sub> (EE) bridge is as follows: Zn(1)-N(6) 2.2077(11) Å and Zn(1)-N(4) 2.2239(11) Å, with corresponding bond angles for N(5B)-N(6)-Zn(1) of 118.64(9)° and for N(5)-N(4)-Zn(1) of 123.12(9)°. The EE ring Zn<sub>2</sub>( $\mu_{1,3}$ -N<sub>3</sub>)<sub>2</sub> is not of planar geometry. The conformation is distorted to form a chair conformation, as it is already known from **(1)**, **(2)** and **(3)**. The determined  $\delta$  parameter is 36.7°. The Zn(1)-N(4)...N(6B)-Zn(1B) torsion angle is 54,7° and displays a not completely linear chain along the metal centres. The other bridge (EO) configuration (Zn<sub>2</sub>N<sub>2</sub>) is completely planar. The EO ring has the following parameter: N(1A)-Zn(1)-N(1) 80.71(4)° and Zn(1A)-N(1)-Zn(1) 99.29(4)° with lengths Zn(1)-N(1) 2.1554(11) Å, and Zn(1A)-N(1) 2.588(11) Å. The

enclosed angle for N(1A)...N(1)-N(2) planes is  $155,5^\circ$  and shows that the two  $N_3^-$  groups of the EO bridge are not totally linear in one plane. The asymmetric distance of Zn ... Zn in the polymeric chain for the EE ring is  $4.986 \text{ \AA}$  and for the EO ring is  $3.288 \text{ \AA}$ . The polymeric chain of **(4)** is slightly corrugated with an Zn(1A)... Zn(1)...Zn(1B) angle of  $163.1^\circ$ . The two 4-azidopyridine ligands show an angle of N(11)-Zn(1)-N(7)  $171.13(4)^\circ$ , which is very similar to the values of the previous complexes. The terminal azido group, in para-position (from 4-azidopyridine), shows strong asymmetric geometry, with  $\Delta d(N-N)$  values of  $0.122(16) \text{ \AA}$  and  $0.132(15) \text{ \AA}$ . The corresponding  $N_3$  bond angle are for N(14)-N(13)-N(12) -  $171.18(13)^\circ$  and for N(10)-N(9)-N(8) -  $170.79(13)^\circ$ , respectively. Crystal data and processing parameters are listed in Table 4.4.1. Tab. 4.4.2 illustrates relevant bond lengths and angles. Fig.4.4.1 displays the crystal structure of **(4)**, Fig.4.4.2 shows the packing arrangement of **(4)**.



Tab. 4.4.1: Crystallographic data and processing parameter

---

Identification-code	RF446
Empirical formula	C <sub>10</sub> H <sub>8</sub> ZnN <sub>14</sub>
Formula mass	389.67
System	Triclinic
Space group	P-1
a (Å)	8.1876 (4)
b (Å)	8.2228 (4)
c (Å)	11.8147 (6)
α (°)	109.876 (2)
β (°)	91.188 (2)
γ (°)	98.745 (2)
V(Å <sup>3</sup> )	737.10 (6)
Z	1
F (0 0 0)	392
T (K)	100 (2)
μ (MoK <sub>α</sub> )(mm <sup>-1</sup> )	1.697
D <sub>calc</sub> (Mg/m <sup>3</sup> )	1.756
Crystal size (mm)	0.17 x 0.14 x 0.11
Θ range (°)	1.84-30.61
Reflections collected	17851
Independent refl./ R <sub>int</sub>	4124/0.0304
Parameters	226
Goodness-of-Fit on F <sup>2</sup>	1.056
R1/wR2 (all data)	0.0226/0.0515
Residual extrema (e/ Å <sup>3</sup> )	0.400/-0.273

---

Tab. 4.4.2: Selected bond lengths (Å) and angles (°) for **(4)**

Zn(1)-N(7)	2.1258(11)	Zn(1)-N(1)	2.1554(11)
Zn(1)-N(11)	2.1575(11)	Zn(1')-N(1)	2.588(11)
Zn(1)-N(6)	2.2077(11)	Zn(1)-N(4)	2.2239(11)
N(1)-N(2)	1.2028(15)	N(2)-N(3)	1.1534(16)
N(4)-N(5)	1.1759(16)	N(5)-N(6)	1.1796(16)
N(6)-N(5)	1.1797(16)	N(7)-C(5)	1.3414(16)
N(7)-C(1)	1.3432(17)	N(8)-N(9)	1.2542(15)
N(8)-C(3)	1.4143(17)	N(9)-N(10)	1.1220(15)
N(11)-C(10)	1.3409(17)	N(11)-C(6)	1.3423(16)
N(12)-N(13)	1.2481(15)	N(12)-C(8)	1.4158(16)
N(13)-N(14)	1.1260(16)		
N(7)-Zn(1)-N(1)	94.82(4)	N(7)-Zn(1)-N(11)	171.13(4)
N(1)-Zn(1)-N(11)	91.17(4)	N(7)-Zn(1)-N(1')	93.20(4)
N(1)-Zn(1)-N(1')	80.71(4)	N(11)-Zn(1)-N(1')	94.21(4)
N(7)-Zn(1)-N(6)	87.62(4)	N(1)-Zn(1)-N(6)	170.72(4)
N(11)-Zn(1)-N(6)	87.48(4)	N(1')-Zn(1)-N(6)	90.23(4)
N(7)-Zn(1)-N(4)	86.08(4)	N(1)-Zn(1)-N(4)	90.70(4)
N(11)-Zn(1)-N(4)	87.32(4)	N(1')-Zn(1)-N(4)	171.29(4)
N(6)-Zn(1)-N(4)	98.41(4)	N(2)-N(1)-Zn(1)	126.57(9)
N(2)-N(1)-Zn(1')	125.61(9)	Zn(1)-N(1)-Zn(1')	99.29(4)
N(3)-N(2)-N(1)	179.57(14)	N(5)-N(4)-Zn(1)	123.12(9)
N(4)-N(5)-N(6'')	178.43(13)	N(5'')-N(6)-Zn(1)	118.64(9)
C(5)-N(7)-C(1)	117.15(11)	C(5)-N(7)-Zn(1)	121.86(9)
C(1)-N(7)-Zn(1)	121.00(8)	N(9)-N(8)-C(3)	116.88(11)
N(10)-N(9)-N(8)	170.79(13)	C(10)-N(11)-C(6)	117.24(11)
C(10)-N(11)-Zn(1)	121.29(8)	C(6)-N(11)-Zn(1)	120.92(8)
N(13)-N(12)-C(8)	116.50(11)	N(14)-N(13)-N(12)	171.18(13)
N(9)-N(8)-C(3)-C(4)	(-)0.3(2)		
N(9)-N(8)-C(3)-C(2)	178.91(12)		
N(13)-N(12)-C(8)-C(7)	(-)0.9(2)		
N(13)-N(12)-C(8)-C(9)	179.05(12)		

Symmetry codes: (a = ') 1-x, -y, 1-z (b = '') -x, -y, 1-z

## 4.5 [Cd(4-azidopyridine)<sub>2</sub>(N<sub>3</sub>)<sub>2</sub>]<sub>n</sub> (5)

### Synthesis

CdCl<sub>2</sub> x H<sub>2</sub>O (0.201g; 1.0 mmol) and 4-azidopyridine (0.203g; 1.5 mmol) were added to 10mL of of dist. H<sub>2</sub>O/HN<sub>3</sub>. A voluminous white precipitate formed in the solution. The solution was stirred and heated to 95°C for one hour. Then the solution is filtered *hot* (otherwise products start to crystallize!). To the resulting clear solution NaN<sub>3</sub> solution (1M; 5 mL) was be added. Again, white flakes start to precipitate in the solution. 8 mL of dist. H<sub>2</sub>O/HN<sub>3</sub> was added while heating (90°C for 2 ½ h) and stirring. The solution was again filtered. After this procedure, the slightly yellow solution was put into a compartment dryer (50°C) for one day. Afterwards the solution was kept at room temperature for two more days. Finally, the clear yellow solution refrigerated (4°C). Long yellow needles, were obtained (yield: estimated 30 %).

### CHN –Analytics found(theor.) in %

Cannot be indicated for less material was available!

### IR-values (spectrum on p.113)

$\nu$  (cm<sup>-1</sup>): 2416 w, 2266 w, 2128 sh, 2102 sh, 2056 vs  $\nu_{as}$  (N<sub>3</sub><sup>-</sup>); 1597 vs, 1563 vs, 1501 s, 1428 m, 1136 m, 1012 s, 820 vs (pyridine moiety); 1351 sh, 1287 vs, 1215 s,  $\nu_{sym}$  (N<sub>3</sub>); 536 s, 514 s  $\delta$  (N<sub>3</sub><sup>-</sup>)

### Discussion of the preliminary structure

The last complex of this class, Cd(4-Azidopyridine)<sub>2</sub>(N<sub>3</sub>)<sub>2</sub>]<sub>n</sub> (abbreviated as **(5)**), was obtained in a very small quantity. Due to this fact only some crystal – parameters are listed here. The processing parameter and crystal data can be found in Tab. 4.5.1. As with all other complexes of this class, **(5)** crystallized in a triclinic space group P-1. In Fig.4.5.1 the crystal structure of **(5)** is pictured. Fig.4.5.2 shows the packing arrangement of **(5)**. The asymmetric unit of **(5)** contain two Cd<sup>2+</sup> centres. Each of these two centres is ligated octahedrally by two 4-azidopyridine ligands and by four N<sub>3</sub><sup>-</sup> groups. The two 4-azidopyridine ligands coordinate in trans position to each other. With an angle of N(1)-Cd(1)-N(5) of 171.13(4)°. The two bridging styles, the EO and EE modes, can be found alternately between two metal centres. Again, the polymeric chain of **(5)** is oriented along the b-axis of its unit cell. The arrangement of the EE mode, the Cd<sub>2</sub>( $\mu_{1,3}$ -N<sub>3</sub>)<sub>2</sub> ring, has no planar geometry. The conformation is distorted to a “chair-style formation”.

This fact can be evaluated and proved by the  $\delta$  parameter of  $43.0^\circ$ . The Cd(1B)-N(23B)...N(21)-Cd(1) torsion angle is  $60.0^\circ$  - this indicates a slightly distorted chain. The other the EO configuration bridge ( $\text{Cd}_2\text{N}_2$ ) is completely of planar geometry. The ring has the following parameter: the angle for N(11A)...N(11)-N(12) is  $150,6^\circ$  and this indicates that the two azido-groups are slightly bent. The intra-chain distances of Cd ... Cd are asymmetric due to the fact of alternate EO and EE bridges. Corresponding to the EE ring  $4.997 \text{ \AA}$ , the EO ring is  $3.516 \text{ \AA}$ . The chain of **(5)** is slightly corrugated with an Cd(1A)... Cd(1)...Cd(1B) angle of  $169.8^\circ$ .

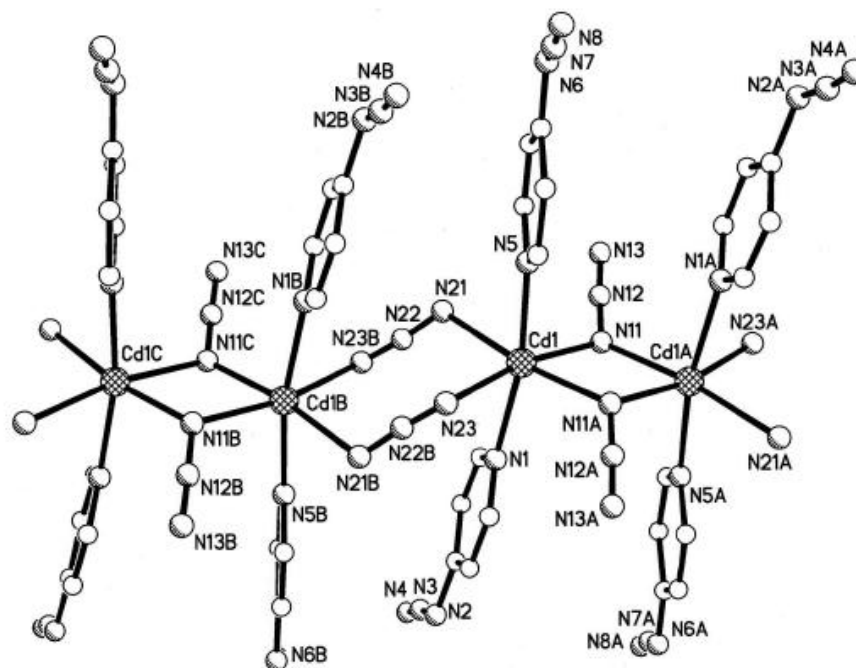


Fig.4.5.1: Structure of  $[Cd(4\text{-Azidopyridine})_2(N_3)_2]_n$

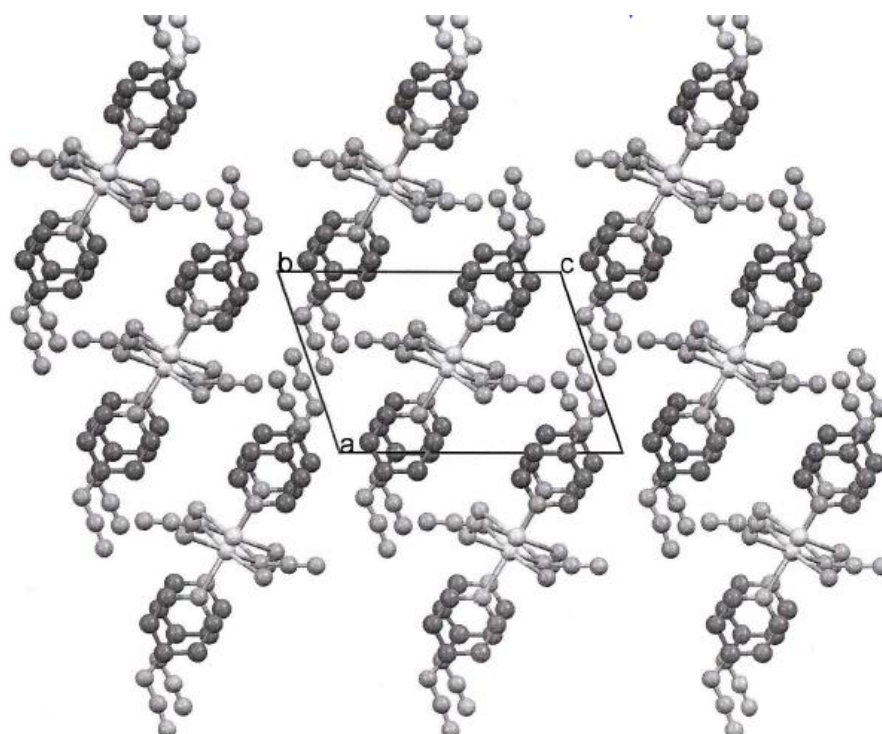


Fig.4.5.2: Packing view of  $[Cd(4\text{-Azidopyridine})_2(N_3)_2]_n$

Tab. 4.5.1: Crystallographic data and processing parameter

---

Identification-code	J929C
Empirical formula	C <sub>10</sub> H <sub>8</sub> CdN <sub>14</sub>
Formula mass	436.71
System	Triclinic
Space group	P-1
a (Å)	8.2152 (12)
b (Å)	8.4075 (13)
c (Å)	12.029 (2)
α (°)	82.26 (2)
β (°)	70.12 (2)
γ (°)	80.17 (2)
V(Å <sup>3</sup> )	767.2 (2)
Z	2
F (0 0 0)	428
T (K)	100 (2)
μ (MoK <sub>α</sub> )(mm <sup>-1</sup> )	1.453
D <sub>calc</sub> (Mg/m <sup>3</sup> )	1.890
Crystal size	0.34 x 0.25 x 0.17
Θ range (°)	1.81-25.27
Reflections collected	4754
Independent refl./ R <sub>int</sub>	2440/0.1335
Parameters	101
Goodness-of-Fit on F <sup>2</sup>	1.271
R1/wR2 (all data)	0.1929/0.6316
Residual extrema (e/ Å <sup>3</sup> )	6.212/-6.645

---

## 5. Azidopyridine-thiocyanate-complexes

### 5.1 $[\text{Ni}_2(4\text{-azidopyridine})_6(\text{SCN})_4]$ (6)

#### Synthesis

Nickel(II)chloride hexahydrate (0.237g; 1.0 mmol) and 4-azidopyridine (0.240g; 2.0 mmol) were dissolved in 10mL of dist.  $\text{H}_2\text{O}$ . A slightly cloudy green solution was formed. The solution was then heated to and stirred at  $85^\circ\text{C}$  for approx. 20 minutes. Then, the solution was filtered. To the resulting clear solution solid KSCN (0,486g; 5 mmol) was added. The solution turned from a greenish to azure-blue color and became cloudy. Heating (at approx.  $85^\circ\text{C}$ ) and stirring were required again for about 20 minutes. The resulting blue-greenish solution was filtered to remove any undissolved residues and then put into the compartment dryer ( $50^\circ\text{C}$ ) over night. The solution was then kept at room temperature while long green needles began to crystallize. The crystals were obtained in about 50 % yield.

**C H N –Analytics:** found(theor.) in %

C: 40,2 (38,2) H: 2,4 (2,3) N: 38,3 (36,6)

**IR-values** (spectrum on p.113)

$\nu$  ( $\text{cm}^{-1}$ ): 2419 w, 2267 w, 2129 sh, 2100 vs, 2072 sh  $\nu_{\text{as}}$  ( $\text{NCS}^-$ ,  $\text{N}_3^-$ ); 1597 s, 1560 s, 1499 s, 1424 m, 1131 m, 1012 s, 813 vs (pyridine moiety); 1352 sh, 1295 vs, 1211 s,  $\nu_{\text{sym}}$  ( $\text{NCS}^-$ ;  $\text{N}_3^-$ ); 520 s  $\delta$  ( $\text{N}_3^-$ ); 2267 w, 2129 sh, 2100 vs, 1632 w, 777 sh (probably SCN moiety, interference with  $\text{N}_3^-$  - moiety)

#### Discussion of the structure

According to the upper synthesis strategy the complex  $[\text{Ni}_2(4\text{-Azidopyridine})_6(\text{SCN})_4]$  (shortened (9)) occurs as dimer. The dimeric structure of (6) crystallizes in the monoclinic space group P21/c. All crystal- and processing parameters are listed in Table 5.1.1. In Table 5.1.2 relevant bond lengths and angles are summarized. The structural arrangement of (6) can be seen in Fig.5.1.1 and shows that the center of inversion is located between the two bridged metal centers. The unit cell of (6) contains 2 formula units. The packing mode of (6) can be seen in Fig.5.1.2. The ligands around the metal center are as follows: three 4-azidopyridine and three thiocyanate groups at each nickel centre. Two thiocyanate ions form a double bridge between

the metal centres. The bridging arrangement characteristics are: N(14)-C(17) 1.1589(15) Å and C(17)-S(1) 1.6441(11) Å. The SCN<sup>-</sup> bridge is nearly linear with an angle for N(14)-C(16)-S(1) of 177.66(4)°. The values for the simply coordinated terminal SCN<sup>-</sup> group are in good agreement with the observed values for  $\mu_{\text{N14-S1}} - \text{SCN}^-$ . These values are: N(13)-C(16) 1.1639(15) Å and C(16)-S(2) 1.6340(11) Å and its angle N(13)-C(16)-S(2) of 179.38(11)°. The parameters of the metal centres are: Ni(1)-N(14) 2.0431(9) Å, Ni(1)-N(5) 2.1037(9) Å, Ni(1)-N(1) 2.0993(9) Å, Ni(1)-N(9) 2.1163(9) Å and Ni(1)-N(13) 2.0369(10) Å. These values indicate a slightly distorted octahedral geometry around the Ni<sup>2+</sup> centres. The corresponding bond angles are: N(9)-Ni(1)-N(5) 176.58(4)°, N(1)-Ni(1)-S(1) 178.29(3)° and N(14)-Ni(1)-S(1) 92.13(3)°. The distance between the two nickel centres is 5.9392(4) Å for Ni(1) – Ni(1A). The azide moiety from 4-azidopyridine is strongly asymmetric, with  $\Delta d(\text{N-N})$  0.127(15) Å, 0.124(16) Å and 0.115(15) Å. The corresponding bond angles are: for N(2)-N(3)-N(4) 171.68(12)°, for N(6)-N(7)-N(8) 172.67(13)° and for N(10)-N(11)-N(12) 172.35(12)°, respectively.

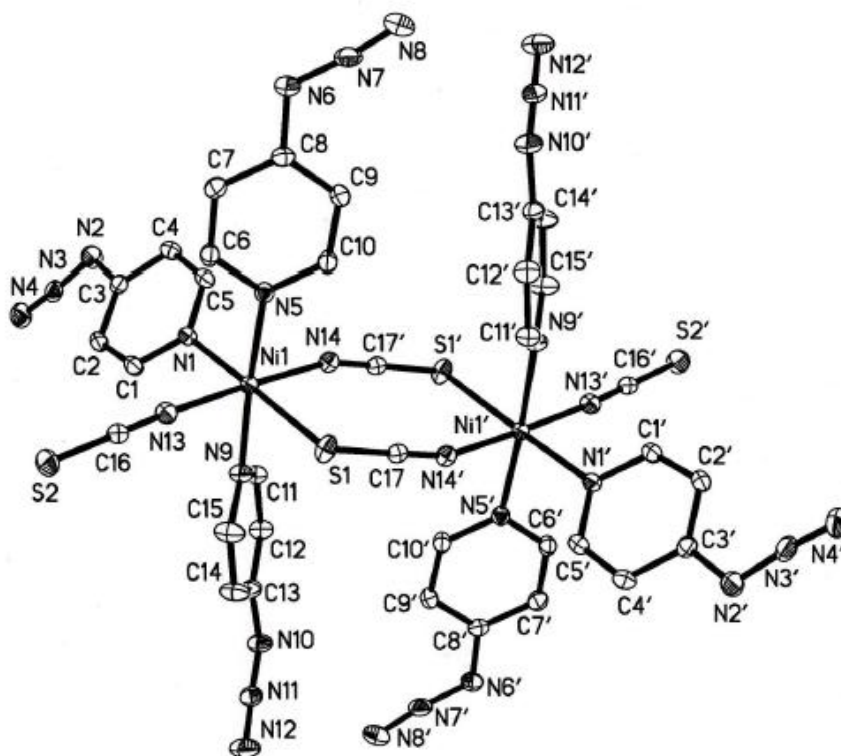


Fig.5.1.1: Structure of  $[\text{Ni}_2(4\text{-Azidopyridine})_6(\text{SCN})_4]$

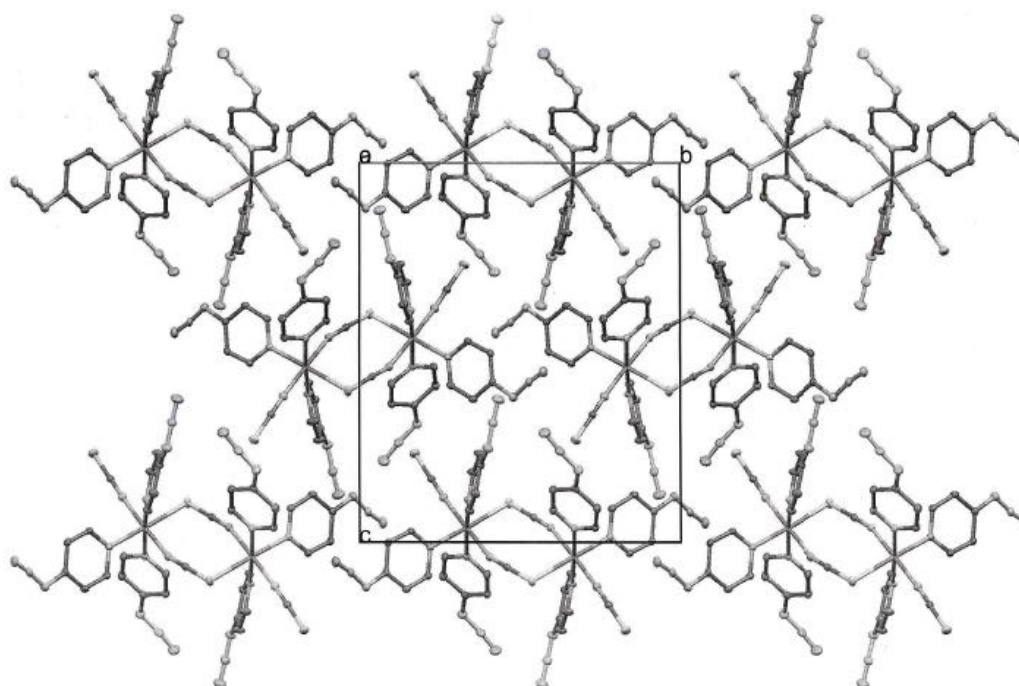


Fig.5.1.1: Packing view of  $[\text{Ni}_2(4\text{-Azidopyridine})_6(\text{SCN})_4]$

Tab.5.1.1: Crystallographic data and processing parameter

---

Identification-code	RF435F2
Empirical formula	C <sub>34</sub> H <sub>24</sub> N <sub>28</sub> Ni <sub>2</sub> S <sub>4</sub>
Formula mass	1070.47
System	Monoclinic
Space group	P 21/c
a (Å)	8.2019 (4)
b (Å)	15.6290 (7)
c (Å)	18.0638 (8)
α (°)	90.00
β (°)	101.487 (2)
γ (°)	90.00
V(Å <sup>3</sup> )	2269.17 (18)
Z	2
F (0 0 0)	1088
T (K)	100 (2)
μ (MoK <sub>α</sub> )(mm <sup>-1</sup> )	1.077
D <sub>calc</sub> (Mg/m <sup>3</sup> )	1.567
Crystal size (mm)	0.22 x 0.16 x 0.09
Θ range (°)	1.74-30.55
Reflections collected	106090
Independent refl./ R <sub>int</sub>	6949/0.0361
Parameters	307
Goodness-of-Fit on F <sup>2</sup>	1.013
R1/wR2 (all data)	0.0236/0.0658
Residual extrema (e/ Å <sup>3</sup> )	0.463/-0.348

---

Tab. 5.1.2: Selected bond lengths (Å) and angles (°) for **(6)**

Ni(1)-N(1)	2.0993(9)	N(1)-Ni(1)-N(5)	90.59(3)
Ni(1)-N(5)	2.1037(9)	N(5)-Ni(1)-N(13)	92.71(4)
Ni(1)-N(9)	2.1163(9)	N(5)-Ni(1)-N(9)	176.58(4)
Ni(1)-N(13)	2.0369(10)	N(9)-Ni(1)-S(1)	88.59(3)
Ni(1)-N(14)	2.0431(9)	N(14)-Ni(1)-S(1)	92.13(3)
Ni(1)-S(1)	2.5481(3)	Ni(1)-S(1)-C(17)	101.29(4)
N(13)-C(16)	1.1639(15)	N(14)-C(17)-S(1)	179.46(19)
C(16)-S(2)	1.6340(11)	N(1)-Ni(1)-S(1)	178.29(3)
N(14)-C(17)	1.1589(15)	N(14)-Ni(1)-N(13)	177.66(4)
C(17)-S(1)	1.6441(11)	Ni(1)-N(13)-C(16)	176.38(9)
C(3)-N(2)	1.4092(14)	N(13)-C(16)-S(2)	179.38(11)
N(2)-N(3)	1.2511(14)	C(3)-N(2)-N(3)	115.82(10)
N(3)-N(4)	1.1237(15)	N(2)-N(3)-N(4)	171.68(12)
C(8)-N(6)	1.4122(14)	C(8)-N(6)-N(7)	115.23(10)
N(6)-N(7)	1.2500(15)	N(6)-N(7)-N(8)	172.67(13)
N(7)-N(8)	1.1255(16)	C(13)-N(10)-N(11)	115.35(10)
C(13)-N(10)	1.4163(14)	N(10)-N(11)-N(12)	172.35(12)
N(10)-N(11)	1.2427(14)		
N(11)-N(12)	1.1273(15)		
		C(4)-C(3)-N(2)-N(3)	170.03(11)
		C(2)-C(3)-N(2)-N(3)	(-) 8.36(17)
		C(7)-C(8)-N(6)-N(7)	(-) 173.68(11)
		C(9)-C(8)-N(6)-N(7)	6.76(17)
		C(12)-C(13)-N(10)-N(11)	179.37(11)
		C(14)-C(13)-N(10)-N(11)	0.64(18)

Symmetry codes: (a = `) 1-x, 2-y, 1-z; (b = ``) -x, y+½, -z+½; (c) -x, -y, -z; (d) x, -y-½, z-½

**5.2 [Mn(4-azidopyridine)<sub>4</sub>(SCN)<sub>2</sub>] (7)****Synthesis**

MnCl<sub>2</sub> x 2H<sub>2</sub>O (0.161g; 1.0 mmol) and 4-azidopyridine (0.240g; 2.0 mmol) were dissolved in 10mL of dist. H<sub>2</sub>O. The slightly skin-coloured solution remained clear. Solid KSCN (0,486g; 5.0 mmol) was then added to the solution while stirring and heating (at about 40°C for 5 min.). The resulting solution was placed in a compartment dryer (50°) for one day. After that, the solution was stored at room temperature. Colourless cloudy crystals were obtained ( and if they were not, the solution can be placed in a fridge in order for crystallization to begin). The yield is about 70 %.

**C H N –Analytics** found(theor.) in %

C: 37,9 (40,5) H: 2,6 (2,5) N: 36,1 (38,7)

**IR-values** (spectrum on p.114)

$\nu$  (cm<sup>-1</sup>): 2431 w, 2277 w, 2129 sh, 2053 sh  $\nu_{as}$  (NCS<sup>-</sup>, N<sub>3</sub><sup>-</sup>); 1594 s, 1558 s, 1498 s, 1424 m, 1131 m, 1004 s, 816 vs (pyridine moiety); 1353 sh, 1284 vs, 1212 s,  $\nu_{sym}$  (NCS<sup>-</sup>, N<sub>3</sub><sup>-</sup>); 532 sh, 517 s  $\delta$  (NCS<sup>-</sup>, N<sub>3</sub><sup>-</sup>) 2277 w, 2100 vs, 1632 w, 727 sh, 678 s (probably SCN moiety, interference with N<sub>3</sub><sup>-</sup> moiety)

**Discussion of the structure**

The second thiocyanate complex, [Mn(4-Azidopyridine)<sub>4</sub>(SCN)<sub>2</sub>] (**7**), crystallizes in the monoclinic space group P21/c as monomers. Each of the two independent polyhedra have four 4-azidopyridine ligands and two axially thiocyanate groups ligated to the manganese centre. The metal centre is also the centre of inversion for the molecule. Four units of (**7**) can be found in the unit cell. The ligands arrange in the following style: Mn(1)-N(1) 2.3071(10) Å and Mn(1)-N(5) 2.3058(11) Å and Mn(1)-N(21) 2.1793(11) Å. The two terminal SCN<sup>-</sup> groups are intrinsically asymmetric with N(21)-C(21) 1.1651(17) Å and C(21)-S(21) 1.6324(13) Å. The group is slightly distorted from 180° to 178.52(12)°. The terminal azido group in para-position (from 4-azidopyridine) is strongly asymmetric, with  $\Delta d(N-N)$  0.131(19) Å and 0.128(16) Å. The corresponding bond angles are: for N(2)-N(3)-N(4) 172.38(19)° and for N(6)-N(7)-N(8) 171.69(15)°, respectively. In Tab. 5.2.1 crystallographic data and processing parameter are

listed. Tab. 5.2.2 summarizes all relevant bond angles and lengths. The structure of **(7)** is shown in Fig.5.2.1. The packing plot is illustrated in Fig.5.2.2. All data for the second polyhedra are close to the values of the first polyhedra and can therefore be taken from Tab. 5.2.2.

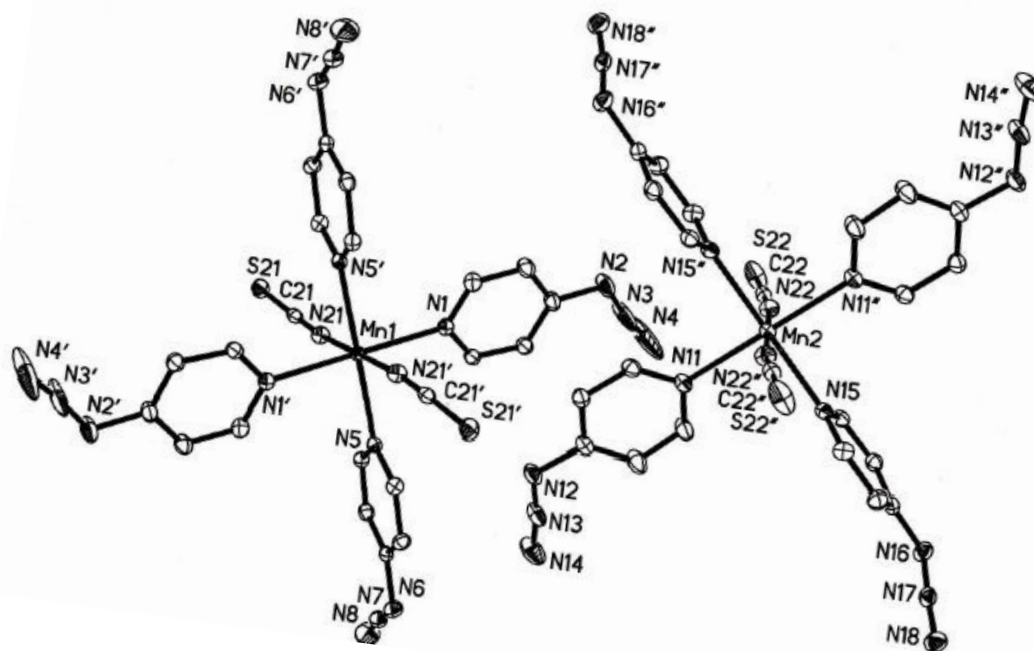


Fig.5.2.1: Structure of  $[\text{Mn}(\text{4-Azidopyridine})_4(\text{SCN})_2]$

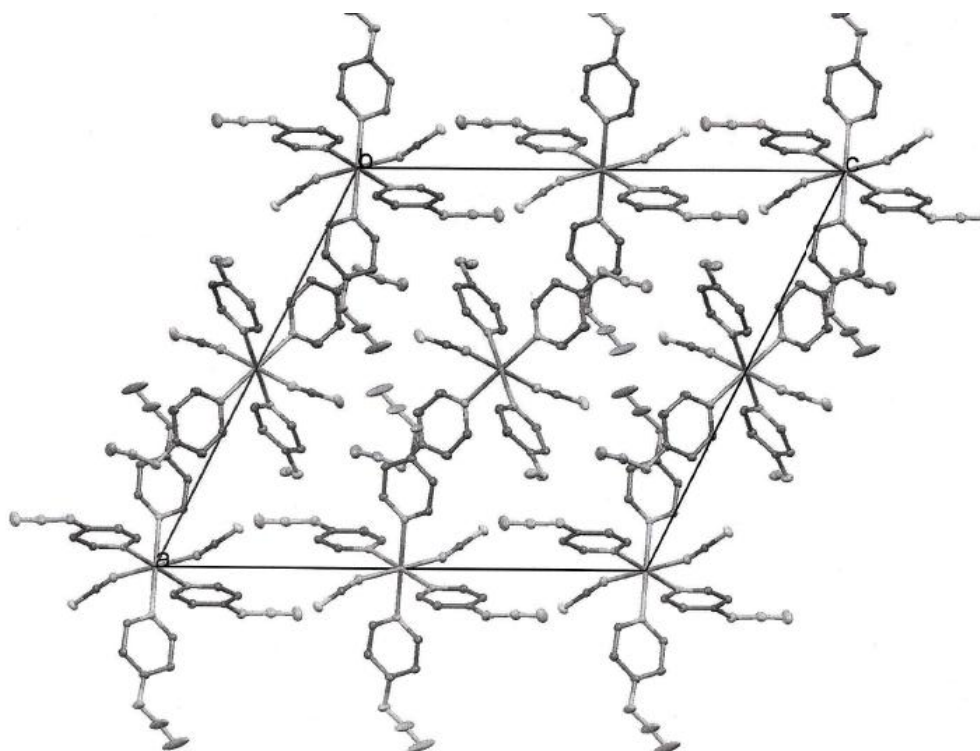


Fig.5.2.2: Packing view of  $[\text{Mn}(\text{4-Azidopyridine})_4(\text{SCN})_2]$

Tab. 5.2.1: Crystallographic data and processing parameter

---

Identification-code	RF449BF2
Empirical formula	C <sub>22</sub> H <sub>16</sub> MnN <sub>18</sub> S <sub>2</sub>
Formula mass	651.59
System	Monoclinic
Space group	P 21/c
a (Å)	19.1886 (7)
b (Å)	7.9392 (3)
c (Å)	20.9193 (8)
α (°)	90.00
β (°)	116.443 (2)
γ (°)	90.00
V(Å <sup>3</sup> )	2852.73 (19)
Z	4
F (0 0 0)	1324
T (K)	100 (2)
μ (MoK <sub>α</sub> )(mm <sup>-1</sup> )	0.659
D <sub>calc</sub> (Mg/m <sup>3</sup> )	1.517
Crystal size (mm)	0.31 x 0.14 x 0.13
Θ range (°)	1.20-29.00
Reflections collected	152865
Independent refl./ R <sub>int</sub>	8011/0.0402
Parameters	391
Goodness-of-Fit on F <sup>2</sup>	1.044
R1/wR2 (all data)	0.0289/0.0744
Residual extrema (e/ Å <sup>3</sup> )	0.476/-0.474

---

Tab. 5.2.2: Selected bond lengths (Å) and angles (°) for (7)

Mn(1)-N(21)	2.1793(11)	Mn(2)-N(22)	2.1690(12)
Mn(1)-N(5)	2.3058(11)	Mn(2)-N(11)	2.3130(11)
Mn(1)-N(1)	2.3071(10)	Mn(2)-N(15)	2.3162(11)
N(21)-C(21)	1.1651(17)	N(22)-C(22)	1.1596(18)
C(21)-S(21)	1.6324(13)	C(22)-S(22)	1.6261(14)
N(2)-N(3)	1.2427(19)	N(13)-N(14)	1.1228(18)
N(3)-N(4)	1.111(2)	N(16)-N(17)	1.2443(17)
N(6)-N(7)	1.2480(16)	N(16)-C(18)	1.416(7)
N(7)-N(8)	1.1200(18)	N(17)-N(18)	1.1230(17)
		N(12)-N(13)	1.2436(17)
N(21)-Mn(1)-N(5)	90.63(4)	N(22)-Mn(2)-N(11)	89.73(4)
N(21)-Mn(1)-N(1)	92.81(4)	N(22)-Mn(2)-N(15)	90.02(4)
N(5)-Mn(1)-N(1)	89.81(4)	N(15)-Mn(2)-N(11)	91.29(4)
C(21)-N(21)-Mn(1)	162.82(10)	C(22)-N(22)-Mn(2)	171.73(11)
N(21)-C(21)-S(21)	178.52(12)	N(22)-C(22)-S(22)	179.07(12)
N(3)-N(2)-C(3)	113.58(12)	N(13)-N(12)-C(13)	116.49(12)
N(4)-N(3)-N(2)	172.38(19)	N(14)-N(13)-N(12)	171.21(15)
N(7)-N(6)-C(8)	116.20(12)	N(17)-N(16)-C(18)	115.70(11)
N(8)-N(7)-N(6)	171.69(15)	N(18)-N(17)-N(16)	171.20(14)
N(3)-N(2)-C(3)-C(4)	(-) 178.81(18)	N(13)-N(12)-C(13)-C(12)	178.95 (13)
N(3)-N(2)-C(3)-C(2)	0.8(3)	N(13)-N(12)-C(13)-C(14)	(-)1.2 (2)
N(7)-N(6)-C(8)-C(7)	(-) 3.24(19)	N(17)-N(16)-C(18)-C(19)	(-)163.13 (12)
N(7)-N(6)-C(8)-C(9)	177.34(12)	N(17)-N(16)-C(18)-C(17)	16.4 (2)

Symmetry codes: (a = `) x, y, z; (b = ``) -x, y+½, -z+½; (c) -x, -y, -z; (d) x, -y-½, z-½

**5.3 [Zn(4-azidopyridine)<sub>4</sub>(SCN)<sub>2</sub>]****(8)****Synthesis**

Zinc(II)chloride (0.136g; 1.0 mmol) and 4-azidopyridine (0.240g; 2.0 mmol) were dissolved in 10mL of dist. H<sub>2</sub>O. A white cloudy solution resulted. Heating and stirring up to 75°C (for approx. 35 minutes was required to achieve a clear solution. Then if necessary, the solution was filtered. To the clear solution solid KSCN (0,486g; 5 mmol) was added while stirring for about 5 minutes. The resulting solution was colourless (if it was not then further heating and stirring for approx 30 min. at 70°C followed) was then placed in a compartment dryer (50°C). After three days long yellowish to white crystals began to crystallize. The crystals were obtained in about a 75 % yield.

**C H N –Analytics** found(theor.) in %

C: 33,9 (39,9) H: 1,9 (2,4) N: 32,4 (38,0)

**IR-values** (spectrum on p.114)

$\nu$  (cm<sup>-1</sup>): 2432w, 2264w, 2135 sh, 2065 sh  $\nu_{as}$  (NCS<sup>-</sup>, N<sub>3</sub><sup>-</sup>); 1599 s, 1580 s, 1498 s, 1424 m, 1131 m, 1007 s, 821 vs (pyridine moiety); 1354 sh, 1299 vs, 1209 s,  $\nu_{sym}$  (NCS<sup>-</sup>, N<sub>3</sub>); 535 sh, 518 s  $\delta$  (NCS<sup>-</sup>, N<sub>3</sub><sup>-</sup>); 2277 w, 2100 vs, 1595 vs, 727 sh, 678 s (probably SCN moiety, interference with N<sub>3</sub><sup>-</sup> - moiety)

**Discussion of the structure**

As it was expected, [Zn(4-Azidopyridine)<sub>4</sub>(SCN)<sub>2</sub>] (abbreviated **(8)**) crystallized in the monoclinic space group P21/c. Again just one polyhedra of the two independent ones will be discussed due to their similarities. The zinc centre indicates a coordination number of six and has therefore four units of 4-azidopyridine and two SCN<sup>-</sup> groups octahedrally ligated around the metal centre. The centre of inversion, an important symmetry operator, is located at the metal centre. The Z value for this complex was estimated at four formula units per unit cell. The following parameters define the surrounding of the Zn<sup>2+</sup> core: Zn(1)-N(1) 2.1969(18) Å and Zn(1)-N(5) 2.2200(18) Å and Zn(1)-N(21) 2.0804(19) Å. The two terminal SCN<sup>-</sup> groups are intrinsically asymmetric: N(21)-C(21) 1.165(3) Å and C(21)-S(21) 1.635(2) Å. The group is slightly distorted from 180° to 177.8(2)°. The  $\Delta d(N-N)$  values are (0.136(3) Å and 0.132(3) Å with

corresponding bond angles: for N(2)-N(3)-N(4)  $172.3(3)^\circ$  and for N(6)-N(7)-N(8)  $171.4(3)^\circ$ , respectively. Crystallographic data as well as processing parameters are summarized in Tab. 5.3.1. Tab. 5.3.2 illustrates the relevant bond angles and lengths. The structure of **(8)** is shown in Fig.5.3.1; the packing plot in Fig.5.3.2.

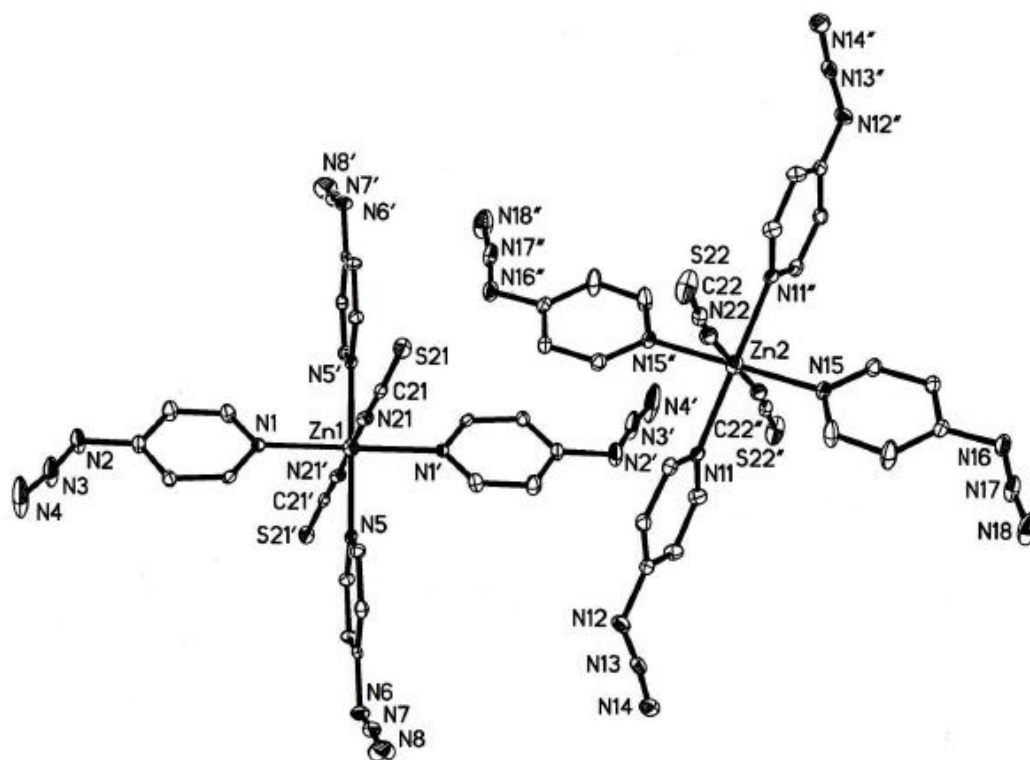


Fig.5.3.1: Structure of  $[\text{Zn}(\text{4-Azidopyridine})_4(\text{SCN})_2]$

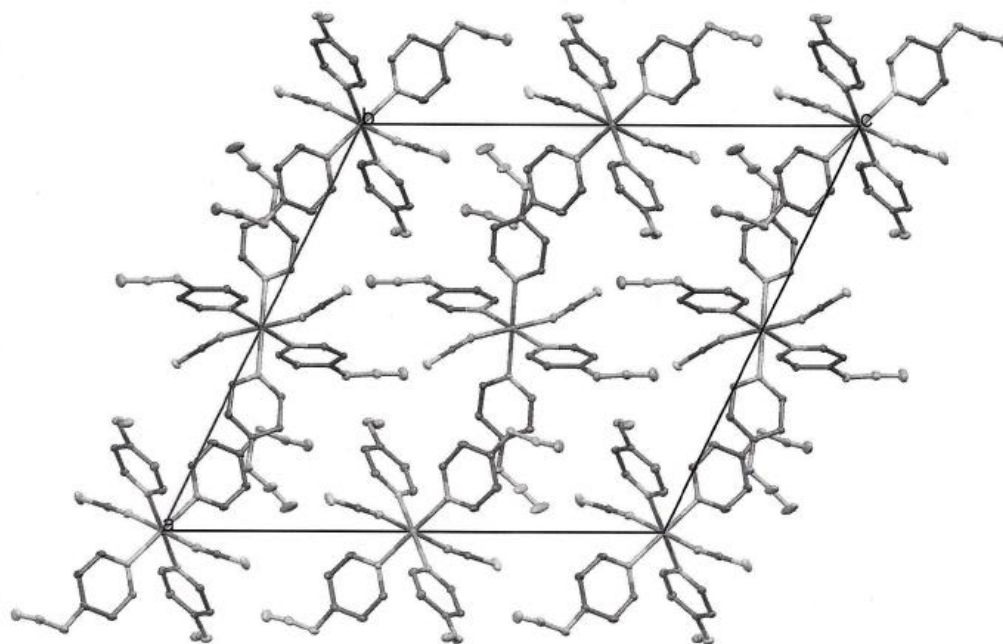


Fig.5.3.2: Packing view of  $[\text{Zn}(\text{4-Azidopyridine})_4(\text{SCN})_2]$

Tab. 5.3.1: Crystallographic data and processing parameter

---

Identification-code	RF447BF2
Empirical formula	C <sub>22</sub> H <sub>16</sub> ZnN <sub>18</sub> S <sub>2</sub>
Formula mass	662.06
System	Monoclinic
Space group	P 21/c
a (Å)	19.0082 (5)
b (Å)	7.8756 (2)
c (Å)	20.9499 (6)
α (°)	90.00
β (°)	115.9160 (10)
γ (°)	90.00
V(Å <sup>3</sup> )	2820.83 (13)
Z	4
F(0 0 0)	1344
T (K)	100 (2)
μ (MoK <sub>α</sub> )(mm <sup>-1</sup> )	1.069
D <sub>calc</sub> (Mg/m <sup>3</sup> )	1.559
Crystal size	0.27 x 0.21 x 0.12
Θ range (°)	1.20-34.00
Reflections collected	67252
Independent refl./ R <sub>int</sub>	11183/0.0981
Parameters	391
Goodness-of-Fit on F <sup>2</sup>	0.997
R1/wR2 (all data)	0.0556/0.1626
Residual extrema (e/ Å <sup>3</sup> )	0.809/-2.127

---

Tab. 5.3.2: Selected bond lengths (Å) and angles (°) for **(8)**

Zn(1)-N(21)	2.0804(19)	Zn(2)-N(22)	2.071(2)
Zn(1)-N(1)	2.1969(18)	Zn(2)-N(15)	2.1917(18)
Zn(1)-N(5)	2.2200(18)	Zn(2)-N(11)	2.2337(19)
N(21)-C(21)	1.165(3)	N(22)-C(22)	1.167(3)
C(21)-S(21)	1.635(2)	C(22)-S(22)	1.625(2)
N(2)-N(3)	1.253(3)	N(13)-N(14)	1.129(3)
N(3)-N(4)	1.117(3)	N(16)-N(17)	1.249(3)
N(6)-N(7)	1.250(3)	N(16)-C(18)	1.416(3)
N(7)-N(8)	1.118(3)	N(17)-N(18)	1.116(3)
		N(12)-N(13)	1.241(3)
N(21)-Zn(1)-N(1)	92.65(7)	N(22)-Zn(2)-N(15)	89.96(7)
N(21)-Zn(1)-N(5)	91.05(7)	N(22)-Zn(2)-N(11)	89.67(7)
N(1)-Zn(1)-N(5)	90.57(7)	N(15)-Zn(2)-N(11)	91.21(7)
C(21)-N(21)-Zn(1)	163.86(17)	C(22)-N(22)-Zn(2)	172.92(18)
N(21)-C(21)-S(21)	177.8(2)	N(22)-C(22)-S(22)	179.2(2)
N(3)-N(2)-C(3)	113.4(2)	N(13)-N(12)-C(13)	115.4(2)
N(4)-N(3)-N(2)	172.3(3)	N(14)-N(13)-N(12)	171.1(2)
N(7)-N(6)-C(8)	116.2(2)	N(17)-N(16)-C(18)	116.5(2)
N(8)-N(7)-N(6)	171.4(3)	N(18)-N(17)-N(16)	171.3(3)
N(3)-N(2)-C(3)-C(2)	1.7(4)	N(13)-N(12)-C(13)-C(14)	(-) 160.9 (2)
N(3)-N(2)-C(3)-C(4)	(-) 178.2 (3)	N(13)-N(12)-C(13)-C(12)	19.3(3)
N(7)-N(6)-C(8)-C(7)	(-) 5.0(3)	N(17)-N(16)-C(18)-C(19)	(-) 178.1(2)
N(7)-N(6)-C(8)-C(9)	175.5(2)	N(17)-N(16)-C(18)-C(17)	1.7 (4)

Symmetry codes: (a = `) x, y, z; (b = ``) -x, y+½, -z+½; (c) -x, -y, -z; (d) x, -y-½, z-½

**5.4 [Co(4-azidopyridine)<sub>4</sub>(SCN)<sub>2</sub>]****(9)****Synthesis**

CoCl<sub>2</sub> × 6H<sub>2</sub>O (0.236g; 1.0 mmol) and 4-azidopyridine (0.240g; 2.0 mmol) were added to 10mL of dist. H<sub>2</sub>O. A beautiful pink solution (with greyish precipitate) was obtained. Then it was heated up to 60°C for 10 minutes in order to dissolve the rest of the salt and ligand. Next, solid KSCN (0,486g; 5.0 mmol) was added. The solution turned to purple. After adding KSCN, the solution was stirred and heated (80°C) for about 45 minutes. Meanwhile 5 mL of H<sub>2</sub>O (dist.) was added to make the solution clear. The complex-solution was then placed in a compartment dryer (50°C) over night. Following two days at room temperature dark purple crystals began to grow. Yield: approx. 65%

**C H N –Analytics** found(theor.) in %

C: 40,0 (40,3) H: 2,4 (2,4) N: 38,2 (38,4)

**IR-values** (spectrum on p.115)

$\nu$  (cm<sup>-1</sup>): 2433w, 2262w, 2135 sh, 2062 sh  $\nu_{as}$  (NCS<sup>-</sup>, N<sub>3</sub><sup>-</sup>); 1600 s, 1560 s, 1497 s, 1424 m, 1133 m, 1009 s, 816 vs (pyridine moiety); 1354 sh, 1285 vs, 1209 s,  $\nu_{sym}$  (NCS<sup>-</sup>, N<sub>3</sub>); 533 sh, 514 s  $\delta$  (NCS<sup>-</sup>; N<sub>3</sub><sup>-</sup>); 2277 w, 2102 vs, 1600 vs, 727 sh, 675 s (probably SCN moiety, interference with N<sub>3</sub><sup>-</sup> - moiety)

**Discussion of the structure**

The last representative of the rhodanide complexes [Co(4-Azidopyridine)<sub>4</sub>(SCN)<sub>2</sub>] **(9)** rystallized in the monoclinic space group P21/c as well. Owing to the two independent polyhedra showing very similar values, only one of them will be discussed. The ligand arrangement is exactly the same as in **(8)** and **(7)** - two SCN<sup>-</sup> and four 4-azidopyridines. The metal centre is also the centre of inversion for the molecule. Four formula units are found in the unit cell of **(9)**. According to the former complexes, the ligands reveal the following parameters: Co(1)-N(1) 2.199(4) Å and Co(1)-N(5) 2.221(4) Å and Co(1)-N(21) 2.079(5) Å. Due to the fact that the centre of inversion is located at the metal centre, the angles around the Co<sup>2+</sup> centre are exactly 180.0°. The two terminal SCN<sup>-</sup> groups are, as known, intrinsically asymmetric N(21)-C(21) 1.168(7) Å and C(21)-S(21) 1.639(6) Å. The group is slightly distorted

from 180° to 178.1(5)°. The  $\Delta d(\text{N-N})$  values for **(9)** are 0.111(8) Å and 0.130(8) Å. The corresponding bond angles are: for N(2)-N(3)-N(4) 172.4(7)° and for N(6)-N(7)-N(8) 171.7(6)°, respectively. The summarized crystal- and processing parameters are in Tab. 5.4.1. Tab 5.4.2 contains the relevant bond angles and lengths. The structure of **(9)** can be seen in Fig. 5.4.1; the packing plot in Fig.5.4.2.

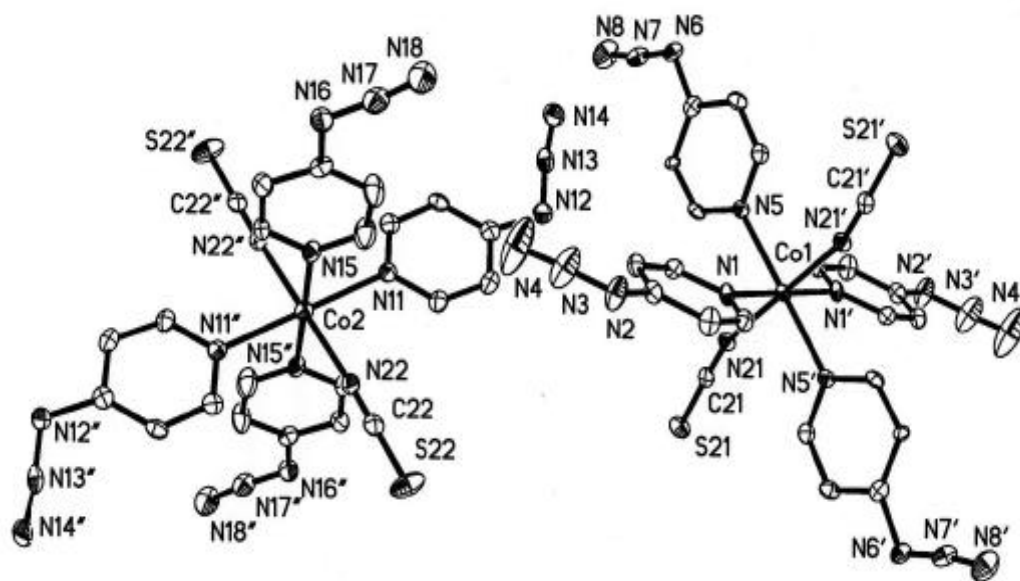


Fig.5.4.1: Structure of  $[\text{Co}(\text{4-Azidopyridine})_4(\text{SCN})_2]$

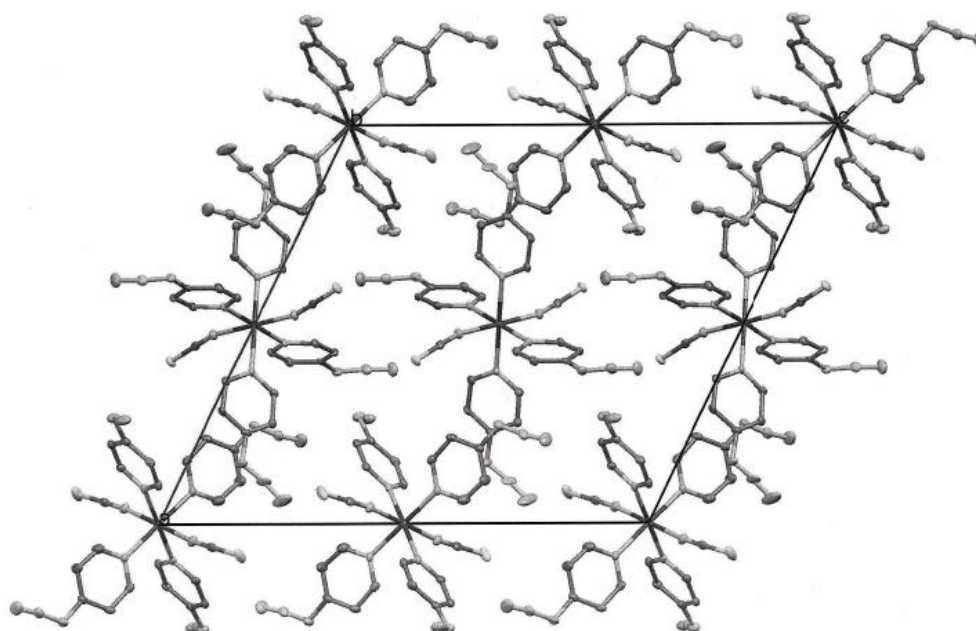


Fig.5.4.2: Packing view of  $[\text{Co}(\text{4-Azidopyridine})_4(\text{SCN})_2]$

Tab. 5.4.1: Crystallographic data and processing parameter

---

Identification-code	J923BF2
Empirical formula	C <sub>22</sub> H <sub>16</sub> CoN <sub>16</sub> S <sub>2</sub>
Formula mass	655.60
System	Monoclinic
Space group	P 21/c
a (Å)	19.0396(17)
b (Å)	7.8896(6)
c (Å)	20.9844(18)
α (°)	90.00
β (°)	115.904(14)
γ (°)	90.00
V(Å <sup>3</sup> )	2835.5(5)
Z	4
F (0 0 0)	1332
T (K)	100(2)
μ (MoK <sub>α</sub> )(mm <sup>-1</sup> )	0.803
D <sub>calc</sub> (Mg/m <sup>3</sup> )	1.536
Crystal size (mm)	0.45 x 0.12 x 0.08
Θ range (°)	1.20-25.00
Reflections collected	20514
Independent refl./ R <sub>int</sub>	5269/0.0772
Parameters	391
Goodness-of-Fit on F <sup>2</sup>	1.297
R1/wR2 (all data)	0.0932/0.1805
Residual extrema (e/ Å <sup>3</sup> )	0.956/-1.007

---

Tab. 5.3.2: Selected bond lengths (Å) and angles (°) for **(9)**

Co(1)-N(21)	2.079(5)	Co(2)-N(22)	2.071(5)
Co(1)-N(1)	2.199(4)	Co(2)-N(15)	2.200(5)
Co(1)-N(5)	2.221(4)	Co(2)-N(11)	2.233(5)
N(21)-C(21)	1.168(7)	N(22)-C(22)	1.158(7)
C(21)-S(21)	1.639(6)	C(22)-S(22)	1.639(6)
N(2)-N(3)	1.241(8)	N(13)-N(14)	1.120(7)
N(3)-N(4)	1.131(8)	N(16)-N(17)	1.249(7)
N(6)-N(7)	1.258(7)	N(16)-C(18)	1.416(7)
N(7)-N(8)	1.128(7)	N(17)-N(18)	1.119(7)
		N(12)-N(13)	1.245(7)
N(21)-Co(1)-N(1)	92.52(17)	N(22)-Co(2)-N(15)	90.26(18)
N(21)-Co(1)-N(5)	91.02(17)	N(22)-Co(2)-N(11)	90.43(18)
N(1)-Co(1)-N(5)	90.59(17)	N(15)-Co(2)-N(11)	90.91(17)
C(21)-N(21)-Co(1)	164.1(4)	C(22)-N(22)-Co(2)	173.0(5)
N(21)-C(21)-S(21)	178.1(5)	N(22)-C(22)-S(22)	179.6(4)
N(3)-N(2)-C(3)	113.5(5)	N(13)-N(12)-C(13)	115.9(5)
N(4)-N(3)-N(2)	172.4(7)	N(14)-N(13)-N(12)	172.1(6)
N(7)-N(6)-C(8)	115.2(5)	N(17)-N(16)-C(18)	116.6(5)
N(8)-N(7)-N(6)	171.7(6)	N(18)-N(17)-N(16)	172.0(6)
N(3)-N(2)-C(3)-C(2)	1.2(9)	C(11)-C(12)-C(13)-N(12)	(-) 177.1 (5)
N(3)-N(2)-C(3)-C(4)	(-) 178.3 (6)	N(13)-N(12)-C(13)-C(12)	17.6(8)
N(7)-N(6)-C(8)-C(7)	(-) 4.9(8)	N(17)-N(16)-C(18)-C(19)	(-) 177.7(5)
N(7)-N(6)-C(8)-C(9)	174.5(5)	N(17)-N(16)-C(18)-C(17)	0.0 (9)

Symmetry codes: (a = `) x, y, z; (b = ``) -x, y+½, -z+½; (c) -x, -y, -z; (d) x, -y-½, z-½

## 6. Azidopyridine-cyanate-complexes

### 6.1 [Ni(4-azidopyridine)<sub>4</sub>(OCN)<sub>2</sub>] (10)

#### Synthesis

Nickel(II)chloride hexahydrate (0.237g; 1.0 mmol) and 4-azidopyridine (0.240g; 2.0 mmol) were dissolved in 10mL of dist. H<sub>2</sub>O. A slightly cloudy green solution developed, as in the synthesis of complex **(6)**. The solution was then heated up to 85°C for approximately 20 minutes before being filtered. Solid KOCN (0,406g; 5.0 mmol) was then added with additional stirring and heating (at 85°C for about 10 minutes). The solution turned a greyish-blue colour. After another filtration the solution was placed in a compartment dryer (50°C) over night. After cooling to room temperature the solution was allowed to stand. Then the solution was stored in a fridge (4°C). After two to three days green-greyish needles start crystallizing. The needles were obtained in an approx. 65 % yield.

#### C H N –Analytics found(theor.) in %

C: 41,7 (42,4) H: 2,5 (2,6) N: 39,8 (40,4)

#### IR-values (spectrum on p.115)

$\nu$  (cm<sup>-1</sup>): 2417w, 2265w, 2132 sh, 2100 sh  $\nu_{as}$  (OCN<sup>-</sup>, N<sub>3</sub><sup>-</sup>); 1595 s, 1560 s, 1496 s, 1424 m, 1131 m, 1011 s, 816 vs (pyridine moiety); 1352 sh, 1281 vs, 1207 s,  $\nu_{sym}$  (OCN<sup>-</sup>, N<sub>3</sub>); 520s  $\delta$  (OCN<sup>-</sup>, N<sub>3</sub><sup>-</sup>); 2265 w, 2197 vs, 1595 vs, 1560 s (probably OCN moiety and interference with N<sub>3</sub><sup>-</sup> moiety)

#### Discussion of the structure

[Ni(4-Azidopyridine)<sub>4</sub>(OCN)<sub>2</sub>] (shortened **(10)**) crystallized in the triclinic space group P-1. The complex of **(10)** has one special feature. The molecules in its unit cell occupy so-called general positions. General positions mean that they are left invariant only for *one* symmetry operation, the identity (*E*). The environment of the metal centre of **(10)** is similar to the SCN<sup>-</sup> analogues. The unit cell contains 4 formula units of **(10)**. In this complex also the values for the second independent polyhedra are similar to that from the first polyhedra, so only one will be discussed. The octahedral geometry, with four 4-azidopyridines and two cyanate ligands

show at the metal centre the following lengths: Ni(1)-N(11) 2.114(3) Å, Ni(1)-N(1) 2.133(4) Å, Ni(1)-N(15) 2.148(4) Å and Ni(1)-N(5) 2.143(4) Å. For the OCN<sup>-</sup> moiety it is Ni(1)-N(51) 2.049(3) Å, Ni(1)-N(52) 2.050(4) Å. As can be seen, the bond to OCN<sup>-</sup> group is slightly shorter than the one to the pyridine is. Therefore the molecule has a slightly distorted octahedral geometry. The bond angles for the six ligands are: N(11)-Ni(1)-N(1) 176.64(13)°, N(52)-Ni(1)-N(51) 178.12(14)° and N(15)-Ni(1)-N(5) 176.23(12)°. The terminal ligated OCN<sup>-</sup> group shows intrinsic asymmetry. The bond lengths are N(51)-C(51) 1.159(5) Å and C(51)-O(51) 1.217(5) Å with an angle of 177.7(5)° for N(51)-C(51)-O(51). As usual, the terminal N<sub>3</sub><sup>-</sup> group of 4-azidopyridine shows asymmetric geometry, with  $\Delta d(\text{N-N})$  0.106(7) Å, 0.130(5) Å, 0.138(6) Å and 0.142(18) Å. The corresponding bond angles are: for N(2)-N(3)-N(4) 174.2(5)°, N(6)-N(7)-N(8) 171.7(4)°, N(12)-N(13)-N(14) 173.9(5)° and for N(16)-N(17)-N(18) 174.4(4)°, respectively.

In Tab. 6.1.1 all crystallographic data and processing parameters are listed. Tab. 6.1.2 displays all the relevant bond angles and lengths for **(10)**. The structure of **(10)** is illustrated in Fig. 6.1.1, The packing plot is detailed in Fig.6.1.2.

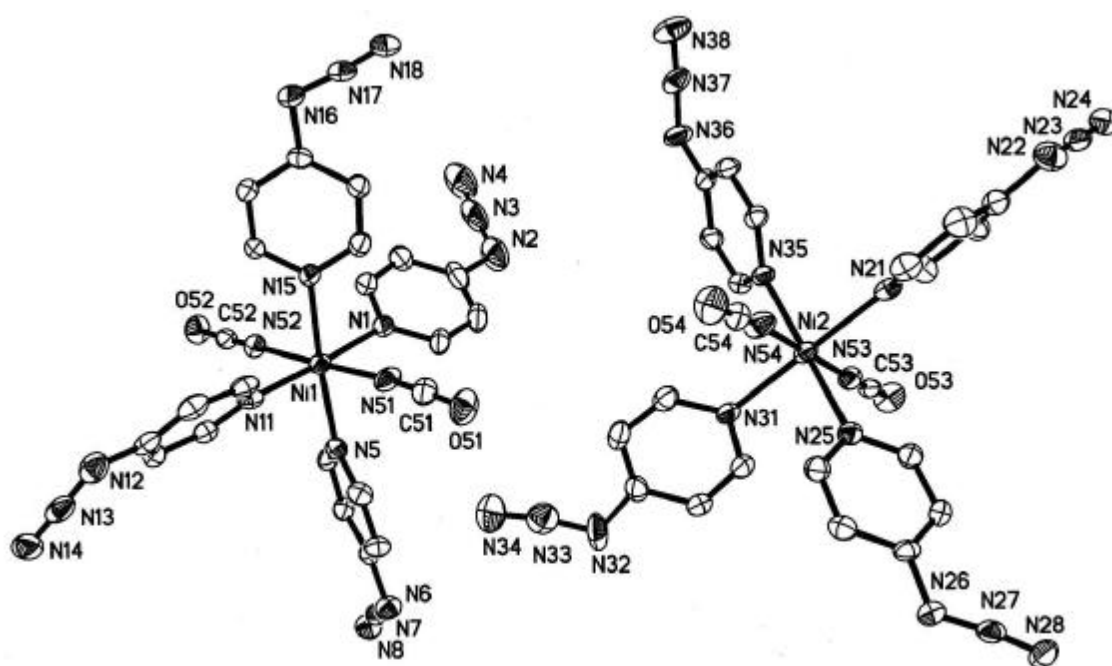


Fig.6.1.1: Structure of  $[\text{Ni}(\text{4-Azidopyridine})_4(\text{OCN})_2]$

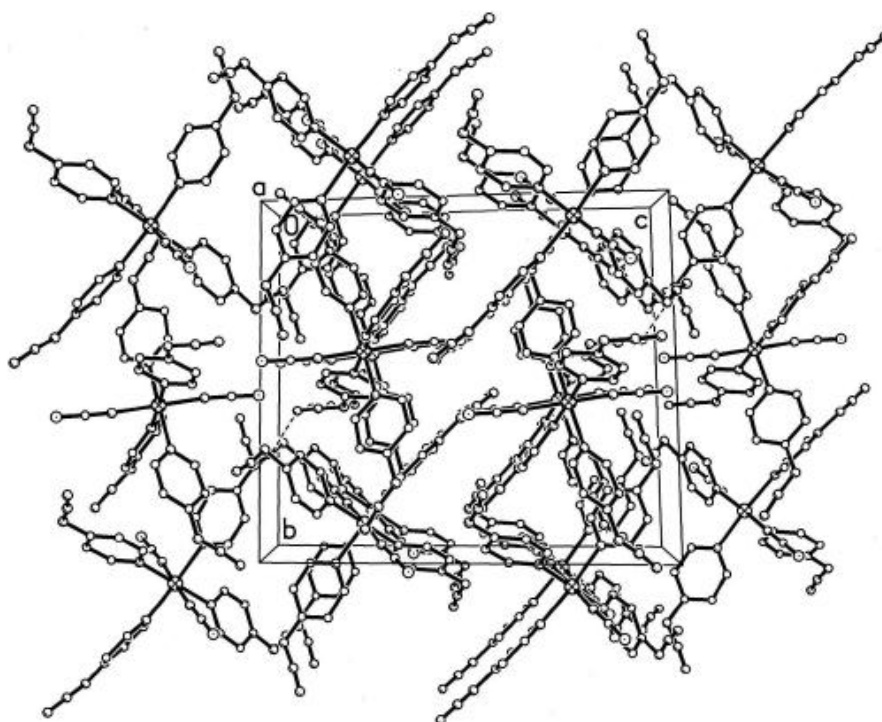


Fig.6.1.2: Packing view of  $[\text{Ni}(\text{4-Azidopyridine})_4(\text{OCN})_2]$

Tab. 6.1.1: Crystallographic data and processing parameter

---

Identification-code	J909BF2
Empirical formula	C <sub>22</sub> H <sub>16</sub> NiN <sub>18</sub> O <sub>2</sub>
Formula mass	623.22
System	Triclinic
Space group	P-1
a (Å)	10.0060(13)
b (Å)	15.870(2)
c (Å)	17.819(2)
α (°)	87.22(2)
β (°)	78.48(2)
γ (°)	76.98(2)
V(Å <sup>3</sup> )	2701.3(6)
Z	4
F (0 0 0)	1272
T (K)	100(2)
μ (MoK <sub>α</sub> )(mm <sup>-1</sup> )	0.778
D <sub>calc</sub> (Mg/m <sup>3</sup> )	1.532
Crystal size (mm)	0.35 x 0.15 x 0.08
Θ range (°)	1.20-26.00
Reflections collected	20815
Independent refl./ R <sub>int</sub>	10468/0.0513
Parameters	775
Goodness-of-Fit on F <sup>2</sup>	1.118
R1/wR2 (all data)	0.0668/0.1517
Residual extrema (e/ Å <sup>3</sup> )	0.851/-0.430

---

Tab. 6.1.2: Selected bond lengths (Å) and angles (°) for (10)

Ni(1)-N(1)	2.133(4)	Ni(2)-N(21)	2.168(4)
Ni(1)-N(51)	2.049(3)	Ni(2)-N(54)	2.054(4)
Ni(1)-N(52)	2.050(4)	Ni(2)-N(53)	2.067(4)
Ni(1)-N(11)	2.114(3)	Ni(2)-N(35)	2.127(3)
Ni(1)-N(15)	2.148(4)	Ni(2)-N(25)	2.141(3)
Ni(1)-N(5)	2.143(4)	Ni(2)-N(31)	2.159(4)
N(51)-C(51)	1.159(5)	N(53)-C(53)	1.173(5)
C(51)-O(51)	1.217(5)	C(53)-O(53)	1.214(5)
N(52)-C(52)	1.161(5)	N(54)-C(54)	1.155(5)
C(52)-O(52)	1.209(5)	C(54)-O(54)	1.223(5)
N(2)-N(3)	1.252(7)	N(22)-N(23)	1.259(6)
N(3)-N(4)	1.146(7)	N(23)-N(24)	1.129(6)
N(6)-N(7)	1.257(5)	N(26)-N(27)	1.262(5)
N(7)-N(8)	1.127(5)	N(27)-N(28)	1.119(5)
N(12)-N(13)	1.266(6)	N(32)-N(33)	1.223(5)
N(13)-N(14)	1.128(6)	N(33)-N(34)	1.149(6)
N(16)-N(17)	1.259(5)	N(36)-N(37)	1.268(5)
N(17)-N(18)	1.117(5)	N(37)-N(38)	1.121(5)
N(51)-Ni(1)-N(52)	178.12(14)	N(54)-Ni(2)-N(53)	179.44(15)
N(11)-Ni(1)-N(1)	176.64(13)	N(54)-Ni(2)-N(35)	90.36(13)
N(15)-Ni(1)-N(5)	176.23(12)	N(53)-Ni(2)-N(35)	89.79(13)
N(51)-Ni(1)-N(11)	92.10(14)	N(54)-Ni(2)-N(25)	89.64(13)
N(52)-Ni(1)-N(11)	87.84(13)	N(53)-Ni(2)-N(25)	90.02(13)
N(51)-Ni(1)-N(1)	90.39(14)	N(35)-Ni(2)-N(25)	179.53(13)
N(52)-Ni(1)-N(1)	89.60(13)	N(54)-Ni(2)-N(31)	93.13(15)
N(51)-Ni(1)-N(5)	89.97(13)	N(53)-Ni(2)-N(31)	87.41(13)
N(52)-Ni(1)-N(5)	91.91(13)	N(35)-Ni(2)-N(31)	90.67(12)
N(11)-Ni(1)-N(5)	91.92(13)	N(25)-Ni(2)-N(31)	88.86(13)
N(1)-Ni(1)-N(5)	90.33(13)	N(54)-Ni(2)-N(21)	90.77(15)
N(51)-Ni(1)-N(15)	87.22(14)	N(53)-Ni(2)-N(21)	88.20(13)
N(52)-Ni(1)-N(15)	90.90(14)	N(35)-Ni(2)-N(21)	87.65(12)
N(11)-Ni(1)-N(15)	90.69(13)	N(25)-Ni(2)-N(21)	92.82(12)
N(1)-Ni(1)-N(15)	87.19(13)	N(31)-Ni(2)-N(21)	175.77(13)
Ni(1)-N(51)-C(51)	175.4(4)	Ni(2)-N(53)-C(53)	173.1(3)
N(51)-C(51)-O(51)	177.7(5)	N(53)-C(53)-O(53)	178.8(4)
Ni(1)-N(52)-C(52)	168.8(3)	Ni(2)-N(54)-C(54)	170.4(3)
N(52)-C(52)-O(52)	177.8(5)	N(54)-C(54)-O(54)	178.2(5)
C(3)-N(2)-N(3)	113.8(4)	C(23)-N(22)-N(23)	114.5(4)
N(2)-N(3)-N(4)	174.2(5)	N(22)-N(23)-N(24)	173.5(5)
C(8)-N(6)-N(7)	115.3(3)	C(28)-N(26)-N(27)	115.9(3)
N(6)-N(7)-N(8)	171.7(4)	N(26)-N(27)-N(28)	171.6(4)
C(13)-N(12)-N(13)	113.5(4)	C(33)-N(32)-N(33)	115.9(5)
N(12)-N(13)-N(14)	173.9(5)	N(32)-N(33)-N(44)	169.9(6)

## Azidopyridine-complexes

---

C(18)-N(16)-N(17)	113.4(3)	C(38)-N(36)-N(37)	115.0(4)
N(16)-N(17)-N(18)	174.4(4)	N(36)-N(37)-N(38)	171.9(4)
C(4)-C(3)-N(2)-N(3)	(-) 176.4(5)	C(24)-C(23)-N(22)-N(23)	(-) 178.4(4)
C(2)-C(3)-N(2)-N(3)	4.6(7)	C(22)-C(23)-N(22)-N(23)	0.7(6)
C(9)-C(8)-N(6)-N(7)	173.9(4)	C(29)-C(28)-N(26)-N(27)	(-) 176.4(4)
C(7)-C(8)-N(6)-N(7)	(-) 6.7(6)	C(27)-C(28)-N(26)-N(27)	5.1(6)
C(14)-C(13)-N(12)-N(13)	(-) 168.8(4)	C(32)-C(33)-N(32)-N(33)	3.5(7)
C(12)-C(13)-N(12)-N(13)	9.6(6)	C(34)-C(33)-N(32)-N(33)	(-)177.1(4)
C(17)-C(18)-N(16)-N(17)	(-) 6.1(6)	C(39)-C(38)-N(36)-N(37)	(-)175.1(4)
C(19)-C(18)-N(16)-N(17)	173.9(4)	C(37)-C(38)-N(36)-N(37)	3.4(6)

**6.2 [Co(4-azidopyridine)<sub>2</sub>(OCN)<sub>2</sub>]****(11)****Synthesis**

CoCl<sub>2</sub> × 6H<sub>2</sub>O (0.237g; 1.0 mmol) and 4-azidopyridine (0.301g; 2.5 mmol) were dissolved in 5mL of dist. H<sub>2</sub>O. The solution turned a red-to-pink hue. The solution was heated to 40°C for approximately 20 minutes in order to dissolve all the remaining salt and ligand, while being dilute further with another 5 mL of dist. H<sub>2</sub>O. Filtration was then necessary. Next solid KOCN (0,406 g; 5.0 mmol) was added. Stirring and heating continued (at 50°C for about 5 minutes). The solution then turned from pink to a dark blue colour with a blue precipitate. After another filtration the solution was placed a compartment dryer (50°C) for one day where the solution turned pink again. After another day in the compartment dryer, two different kinds of crystals were found in the solution. One was made up of small clear blue crystals similar in colour to cobalt blue. This is the form which the described crystal structure belongs to. The other form, made of pink thin plates, was useless for analysis. These were not investigated in more detail due to a lack of time and problems during the crystallization of each separate phase- The blue phase crystals were obtained in about a 68 % yield.

**C H N –Analytics** found(theor.) in %

C: 30,7 (37,6) H: 1,8 (2,1) N: 30,8 (39,5)

**IR-values** (spectrum on p.116)

$\nu$  (cm<sup>-1</sup>): 2420w, 2267 sh, 2132 sh, 2100 s, 2070 sh  $\nu_{as}$  (OCN<sup>-</sup>, N<sub>3</sub><sup>-</sup>); 1603 s, 1560 s, 1498 s, 1430 m, 1132 m, 1025 s, 816 vs (pyridine moiety); 1351 m, 1288 vs, 1210 s,  $\nu_{sym}$  (OCN<sup>-</sup>; N<sub>3</sub>); 520s  $\delta$  (OCN<sup>-</sup>, N<sub>3</sub><sup>-</sup>); 2265 w, 2196 vs, 1603 vs, 1560 s (probably OCN moiety and interference with N<sub>3</sub><sup>-</sup> - moiety)

**Discussion of the structure**

The beautiful blue crystals of [Co(4-Azidopyridine)<sub>2</sub>(OCN)<sub>2</sub>] (abbreviated **(11)**) crystallized in the triclinic space group P-1 and are the first of this work with the coordination number four. It therefore reveals a tetrahedric geometry. The unit cell of **(11)** contains 2 formula units. The tetrahedral geometry of **(11)** is simply determined by two 4-azidopyridine and two cyanate ligands. The ligands show the following parameters around the metal centre: Co(1)-N(1)

2.021(6) Å, Co(1)-N(5) 2.031(6) Å, Co(1)-N(11) 1.931(6) Å and Co(1)-N(12) 1.939(6) Å. The enclosed angles are: N(5)-Co(1)-N(1) 107.1(2)° and N(12)-Co(1)-N(11) 120.4(3)°. The OCN<sup>-</sup> group shows N(11)-C(11) 1.174(10) Å and C(11)-O(11) 1.187(10) Å with an angle of N(11)-C(11)-O(11) 178.6(8)° and therefore can be seen as linear. The second OCN<sup>-</sup> group shows similar values (see Tab.6.1.2). Both N<sub>3</sub><sup>-</sup> moieties (from 4-azidopyridine) show obvious asymmetric geometry; the  $\Delta d(\text{N-N})$  values would be: 0.136(9) Å and 0.136(9) Å the corresponding bond angles are: for N(2)-N(3)-N(4) 172.8(8)°, and for N(6)-N(7)-N(8) 173.8(7)°, respectively. Tab. 6.2.1 summarizes the relevant crystallographic data, Tab. 6.2.2 displays the relevant bond angles and lengths. The structure of **(11)** is pictured in Fig. 6.2.1. The Packing view can be seen in Fig.6.2.2.

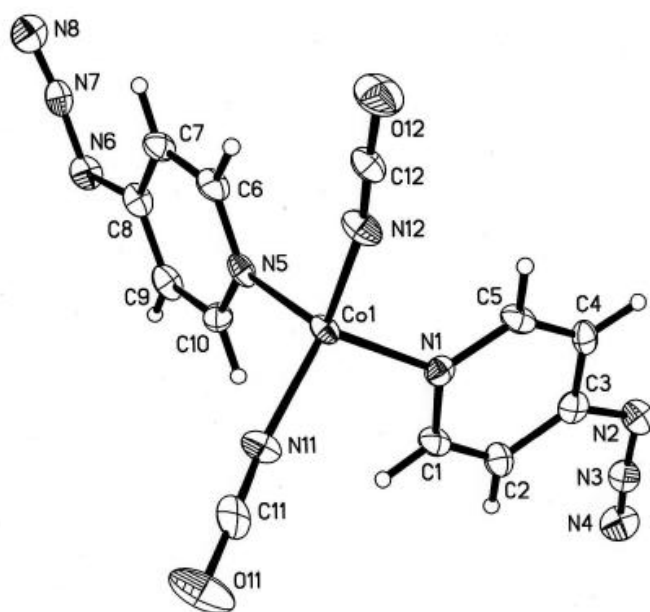


Fig.6.2.1: Structure of [Co(4-Azidopyridine)<sub>2</sub>(OCN)<sub>2</sub>]

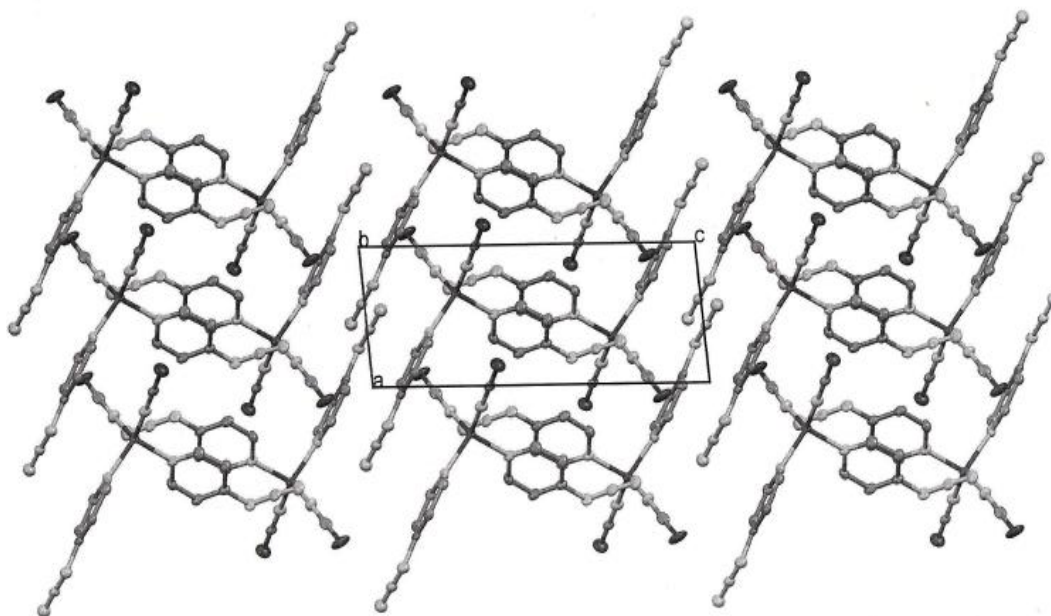


Fig.6.2.2: Packing view of [Co(4-Azidopyridine)<sub>2</sub>(OCN)<sub>2</sub>]

Tab. 6.2.1: Crystallographic data and processing parameter

---

Identification-code	J920CF1
Empirical formula	C <sub>12</sub> H <sub>8</sub> CoN <sub>10</sub> O <sub>2</sub>
Formula mass	383.21
System	Triclinic
Space group	P-1
a (Å)	5.5331(6)
b (Å)	9.6117(9)
c (Å)	15.5430(15)
α (°)	74.56(2)
β (°)	81.08(2)
γ (°)	78.15(2)
V(Å <sup>3</sup> )	775.38(16)
Z	2
F (0 0 0)	386
T (K)	100(2)
μ (MoK <sub>α</sub> )(mm <sup>-1</sup> )	1.139
D <sub>calc</sub> (Mg/m <sup>3</sup> )	1.641
Crystal size (mm)	0.38 x 0.25 x 0.08
Θ range (°)	1.37-26.00
Reflections collected	5907
Independent refl./ R <sub>int</sub>	2998/0..447
Parameters	226
Goodness-of-Fit on F <sup>2</sup>	1.285
R1/wR2 (all data)	0.0972/0.2091
Residual extrema (e/ Å <sup>3</sup> )	1.384/-1.293

---

Tab. 6.2.2: Selected bond lengths (Å) and angles (°) for **(11)**

Co(1)-N(11)	1.931(6)	N(11)-Co(1)-N(12)	120.4(3)
Co(1)-N(12)	1.939(6)	N(11)-Co(1)-N(1)	106.0(3)
Co(1)-N(1)	2.021(6)	N(12)-Co(1)-N(1)	108.5(3)
Co(1)-N(5)	2.031(6)	N(11)-Co(1)-N(5)	107.0(3)
N(11)-C(11)	1.174(10)	N(12)-Co(1)-N(5)	107.2(3)
C(11)-O(11)	1.187(10)	N(1)-Co(1)-N(5)	107.1(2)
N(12)-C(12)	1.145(9)	C(11)-N(11)-Co(1)	162.8(6)
C(12)-O(12)	1.206(9)	N(11)-C(11)-O(11)	178.6(8)
		C(12)-N(12)-Co(1)	167.8(6)
N(2)-N(3)	1.262(9)	N(12)-C(12)-O(12)	177.7(9)
N(3)-N(4)	1.126(9)	N(3)-N(2)-C(3)	114.6(6)
N(6)-N(7)	1.250(9)	N(4)-N(3)-N(2)	172.8(8)
N(7)-N(8)	1.114(9)	N(8)-N(7)-N(6)	173.8(7)
		N(7)-N(6)-C(8)	115.9(6)
C(4)-C(3)-N(2)-N(3)	(-) 179.4 (6)		
C(2)-C(3)-N(2)-N(3)	0.2(10)		
C(9)-C(8)-N(6)-N(7)	179.2(7)		
C(7)-C(8)-N(6)-N(7)	0.7 (11)		

**6.3 [Zn(4-azidopyridine)<sub>2</sub>(OCN)<sub>2</sub>]****(12)****Synthesis**

Zinc(II)chloride (0.136g; 1.0 mmol) and 4-Azidopyridine (0.240g; 2.0 mmol) were dissolved in 10mL of dest.H<sub>2</sub>O. The resulting white cloudy solution was heated to 70°C for approximately 20 minutes in order to dissolve all the remaining salt and ligand, while being diluted with another 5 mL of dist. H<sub>2</sub>O. Then filtration was applied twice (to form a fine precipitate). Next solid KOCN (0,406g; 5.0 mmol) was added. A white precipitate again was formed. Further stirring and heating was carried out (at 75°C for about 35 minutes) while adding another 5 mL of dist. (DISTILLED?) H<sub>2</sub>O. The solution was finally filtered and placed in a compartment dryer (50°C) for three days. Colourless slightly cloudy crystals were obtained in an approx. 73% yield.

**CHN –Analytics** found(theor.) in %

C: 36,5 (36,9) H: 2,0 (2,6) N: 35,1 (35,9)

**IR-values** (spectrum on p.116)

$\nu$  (cm<sup>-1</sup>): 2420w, 2267 sh, 2138 sh, 2110 s, 2070 sh  $\nu_{as}$  (OCN<sup>-</sup>, N<sub>3</sub><sup>-</sup>); 1604 s, 1560 s, 1499 s, 1432 m, 1132 m, 1024 s, 818 vs (pyridine moiety); 1355 m, 1290 vs, 1210 s,  $\nu_{sym}$  (OCN<sup>-</sup>, N<sub>3</sub><sup>-</sup>); 522s  $\delta$  (OCN<sup>-</sup>, N<sub>3</sub><sup>-</sup>); 2267 w, 2213 vs, 1604 vs, 1560 s (probably OCN moiety and interference with N<sub>3</sub><sup>-</sup> - moiety)

**Discussion of the structure**

The last OCN<sup>-</sup> complex [Zn(4-Azidopyridine)<sub>2</sub>(OCN)<sub>2</sub>] (shortened **(12)**) crystallized in the triclinic space group P-1, like **(11)** and **(10)**. **(12)** was only four times coordinated (CN 4), so it formed a tetrahedral geometry. In the unit cell of **(12)** two formula units can be found. Its tetrahedral geometry contains two 4-azidopyridine and two cyanate ligands. The parameters of the ligands around the metal centre are: Zn(1)-N(1) 2.036(4)Å, Zn(1)-N(5) 2.036(4)Å, Zn(1)-N(11) 1.863(5)Å and Zn(1)-N(12) 1.860(5)Å. The according angles around Zn<sup>2+</sup>: N(5)-Zn(1)-N(1) with 105.22(17)° and N(12)-Zn(1)-N(11) with 119.7(2)°. The OCN<sup>-</sup> group show N(11)-C(11) 1.063(7) Å and C(11)-O(11) 1.206(8)Å as lengths and with an angle of N(11)-C(11)-O(11) 177.7(7)°. The values for the second OCN<sup>-</sup> group are very similar (see Tab.6.2.2). N<sub>3</sub><sup>-</sup> at 4-

azidopyridin tends, as usual, to be asymmetric, with  $\Delta d(\text{N-N})$  0.141(7) Å and 0.106(7) Å. The bond angles are: for N(2)-N(3)-N(4) 173.2(5)° and for N(6)-N(7)-N(8) 172.3(6)°, respectively. Tab. 6.3.1 summarizes relevant crystallographic data, Tab. 6.3.2 all relevant bond angles and lengths. The structure of **(12)** is pictured in Fig. 6.3.1. The packing plot can be seen in Fig.6.3.2.

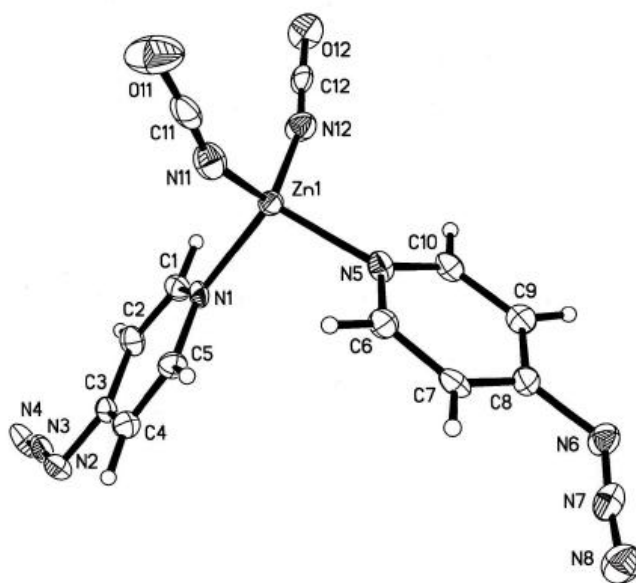


Fig.6.3.1: Structure of [Zn(4-Azidopyridine)<sub>2</sub>(OCN)<sub>2</sub>]

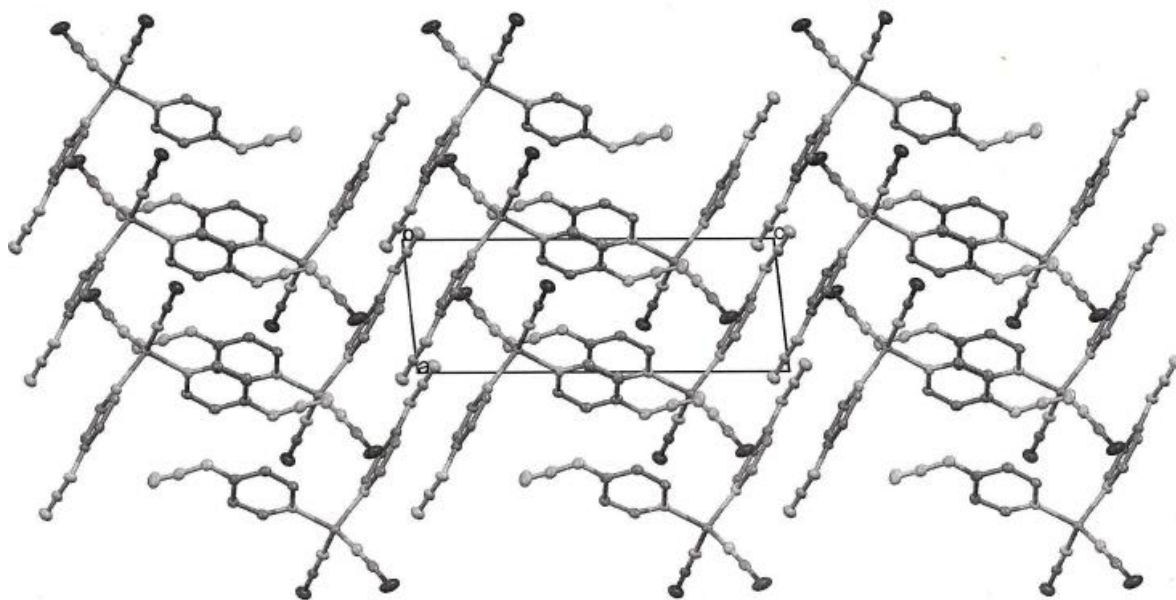


Fig.6.3.2: Packing view of [Zn(4-Azidopyridine)<sub>2</sub>(OCN)<sub>2</sub>]

Tab. 6.3.1: Crystallographic data and processing parameter

Identification-code	J919BF2
Empirical formula	C <sub>12</sub> H <sub>8</sub> N <sub>10</sub> O <sub>2</sub> Zn
Formula mass	389.67
System	Triclinic
Space group	P-1
a (Å)	5.5546(11)
b (Å)	9.0633(18)
c (Å)	15.527(3)
α (°)	74.72(2)
β (°)	80.86(2)
γ (°)	78.21(2)
V(Å <sup>3</sup> )	733.6(3)
Z	2
F (0 0 0)	392
T (K)	100(2)
μ (MoK <sub>α</sub> )(mm <sup>-1</sup> )	1.708
D <sub>calc</sub> (Mg/m <sup>3</sup> )	1.764
Crystal size (mm)	0.40 x 0.12 x 0.08
Θ range (°)	1.40-25.50
Reflections collected	5450
Independent refl./ R <sub>int</sub>	2675/0.0404
Parameters	226
Goodness-of-Fit on F <sup>2</sup>	1.200
R1/wR2 (all data)	0.0639/0.1337
Residual extrema (e/ Å <sup>3</sup> )	0.826/-1.197

Tab. 6.3.2: Selected bond lengths (Å) and angles (°) for **(12)**

Zn(1)-N(11)	1.863(5)	N(11)-Zn(1)-N(12)	119.7(2)
Zn(1)-N(12)	1.860(5)	N(11)-Zn(1)-N(5)	104.63(19)
Zn(1)-N(1)	2.036(4)	N(12)-Zn(1)-N(5)	110.47(19)
Zn(1)-N(5)	2.036(4)	N(11)-Zn(1)-N(1)	108.61(19)
N(11)-C(11)	1.063(7)	N(12)-Zn(1)-N(1)	107.37(19)
C(11)-O(11)	1.206(8)	N(1)-Zn(1)-N(5)	105.22(17)
N(12)-C(12)	1.117(7)	C(11)-N(11)-Zn(1)	158.7(5)
C(12)-O(12)	1.174(7)	N(11)-C(11)-O(11)	177.7(7)
N(7)-N(8)	1.128(7)	C(12)-N(12)-Co(1)	166.2(4)
N(2)-N(3)	1.254(7)	N(12)-C(12)-O(12)	177.6(6)
N(3)-N(4)	1.113(7)	N(3)-N(2)-C(3)	116.0(5)
N(6)-N(7)	1.234(6)	N(4)-N(3)-N(2)	173.2(5)
		N(7)-N(6)-C(8)	117.5(4)
		N(8)-N(7)-N(6)	172.3(6)
C(4)-C(3)-N(2)-N(3)	177.8 (5)		
C(2)-C(3)-N(2)-N(3)	0.5(8)		
C(9)-C(8)-N(6)-N(7)	(-)-179.5(5)		
C(7)-C(8)-N(6)-N(7)	0.2 (8)		

## 7. Azidopyridine-nitrite-complex

### 7.1 [Zn(4-azidopyridine)<sub>2</sub>(NO<sub>2</sub>)<sub>2</sub>] (13)

#### Synthesis

Waterfree ZnCl<sub>2</sub> (0,1376g; 1.0 mmol) and 4-Azidopyridine (0.240g; 2.0 mmol) were dissolved in 10mL of dist.H<sub>2</sub>O. The solution became a yellowish- white precipitate. The solution was heated to 75°C for approximately 20 minutes in order to dissolve the rest of the salt and ligand. To the resulting nearly clear solution was added solid NaNO<sub>2</sub> (0,344g; 5.0 mmol). After filtering once, stirring and heating was continued (at 70°C for about 2-3 minutes). The solution became completely clear. It was placed into a fridge (4°C) and after two days yellow to white needles started crystallizing. Yield: about 90%

**C H N –Analytics:** found(theor.) in %

C: 23,4 (30,2) H: 3,4 (4,5) N: 27,1 (35,2)

**IR-values** (spectrum on p.117)

$\nu$  (cm<sup>-1</sup>): 2420 w, 2264 m, 2138 sh, 2100 vs,  $\nu_{as}$  (N<sub>3</sub><sup>-</sup>); 1602 vs, 1558 s, 1499 s, 1432 s, 1132 m, 1010 s, 819 vs (pyridine moiety); 1293 vs, 1213 s,  $\nu_{sym}$  (N<sub>3</sub>); 521s  $\delta$  N<sub>3</sub><sup>-</sup>; 1241 m (probably NO<sub>2</sub><sup>-</sup> - moiety)

#### Discussion of the structure

The [Zn(4-Azidopyridine)<sub>2</sub>(NO<sub>2</sub>)<sub>2</sub>] complex (shortened **(13)**) crystallized in the monoclinic space group P21/c and is six times coordinated (CN 6). It has an octohedric geometry with two NO<sub>2</sub><sup>-</sup> groups (bidentate ligand) and two 4-azidopyridine arranged around the zinc centre. Z is determined with four formula units per unit cell. The characteristic lengths and angles for **(13)** concerning the Zn<sup>2+</sup> core are: Zn(1)-N(1) 2.052(2) Å, Zn(1)-N(5) 2.063(2) Å, Zn(1)-O(1) 2.132(2) Å, Zn(1)-O(2) 2.263(2)Å, Zn(1)-O(3) 2.083(2) Å and Zn(1)-O(4) 2.354(2) Å. The corresponding angles for the Zn<sup>2+</sup> centre are: N(5)-Zn(1)-N(1) 102.76(8)° and O(1)-Zn(1)-O(2) 55.87(8)° and O(3)-Zn(1)-O(4) 55.19(8)°. The bidentate NO<sub>2</sub><sup>-</sup> group shows slightly asymmetric geometry, with  $\Delta$ N-O (difference of N-O bond lengths within the nitrite group): 0.018(3) Å and 0.044(3)Å and an angle of O(3)-N(10)-O(4) 120.1(3)° and O(1)-N(9)-O(2) 115.7(2)°. Free NO<sub>2</sub><sup>-</sup>

has an angle of about  $115^\circ$ . The 4-azido group (from 4-azidopyridine) is strongly asymmetric. The  $\Delta d(\text{N-N})$  values are  $0.142(3) \text{ \AA}$  and  $0.136(3) \text{ \AA}$  and the corresponding bond angles are: for N(2)-N(3)-N(4)  $171.8(3)^\circ$ , N(6)-N(7)-N(8)  $172.3(3)^\circ$ , respectively. All relevant bond angles and lengths are listed in Tab. 7.1.2. The processing parameter and crystal data can be taken from Tab.7.1.1. The structure plot of **(13)** is pictured in Fig.7.1.1 and its packing mode in Fig.7.1.2.

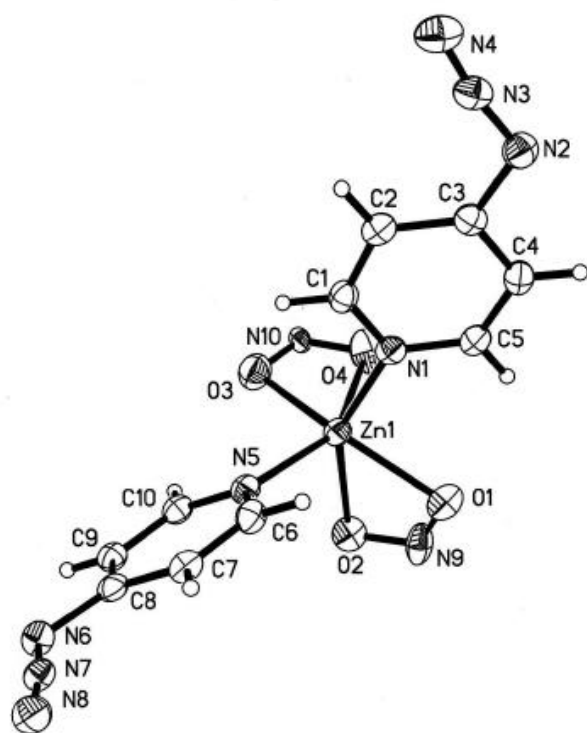


Fig.7.1.1: Structure of [Zn(4-Azidopyridine)<sub>2</sub>(NO<sub>2</sub>)<sub>2</sub>]

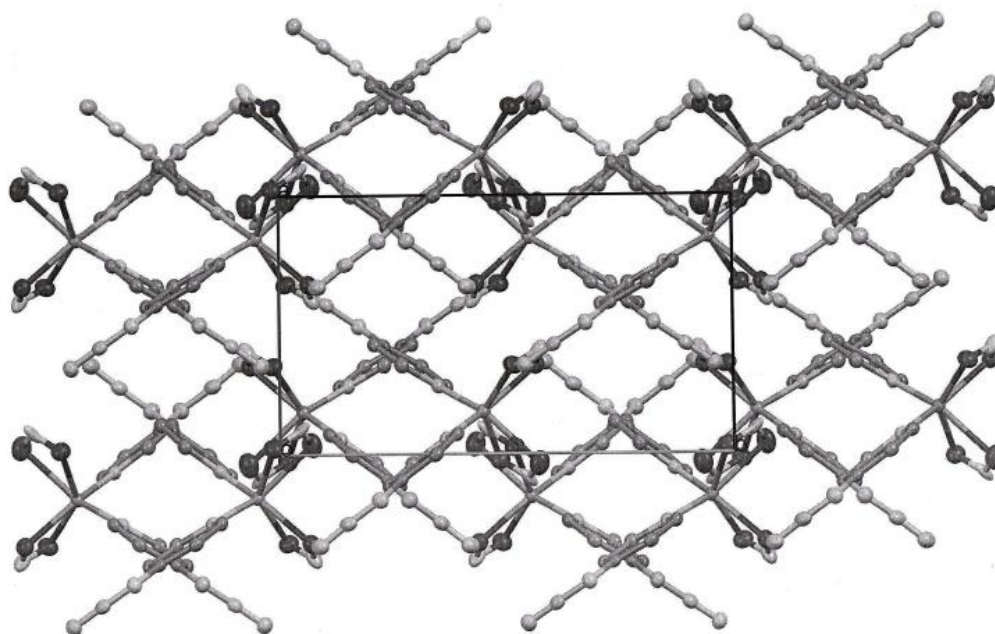


Fig.7.1.2: Packing view of [Zn(4-Azidopyridine)<sub>2</sub>(NO<sub>2</sub>)<sub>2</sub>]

Tab. 7.1.1: Crystallographic data and processing parameter

---

Identification-code	J919BF2
Empirical formula	C <sub>10</sub> H <sub>8</sub> N <sub>10</sub> O <sub>4</sub> Zn
Formula mass	397.65
System	Monoclinic
Space group	P 21/c
a (Å)	8.0600(12)
b (Å)	14.0316(18)
c (Å)	13.4153(17)
α (°)	90.00
β (°)	97.456(16)
γ (°)	90.00
V(Å <sup>3</sup> )	1504.4(4)
Z	4
F (0 0 0)	800
T (K)	100(2)
μ (MoK <sub>α</sub> )(mm <sup>-1</sup> )	1.677
D <sub>calc</sub> (Mg/m <sup>3</sup> )	1.756
Crystal size (mm)	0.35 x 0.28 x 0.18
Θ range (°)	2.15-26.38
Reflections collected	11669
Independent refl./ R <sub>int</sub>	3074/0.0266
Parameters	226
Goodness-of-Fit on F <sup>2</sup>	1.052
R1/wR2 (all data)	0.0349/0.0918
Residual extrema (e/ Å <sup>3</sup> )	0.887/-0.413

---

Tab. 7.1.2: Selected bond lengths (Å) and angles (°) for **(13)**

Zn(1)-N(5)	2.063(2)	N(1)-Zn(1)-N(5)	102.76(8)
Zn(1)-N(1)	2.052(2)	N(5)-Zn(1)-O(3)	92.00(8)
Zn(1)-O(3)	2.083(2)	N(1)-Zn(1)-O(1)	94.55(8)
Zn(1)-O(4)	2.354(2)	O(3)-Zn(1)-O(1)	140.21(9)
Zn(1)-O(1)	2.132(2)	N(1)-Zn(1)-O(2)	150.24(8)
Zn(1)-O(2)	2.263(2)	O(3)-Zn(1)-O(2)	95.19(8)
O(1)-N(9)	1.196(3)	O(1)-Zn(1)-O(2)	55.87(8)
O(2)-N(9)	1.240(3)	N(1)-Zn(1)-O(4)	92.08(8)
O(3)-N(10)	1.203(3)	O(3)-Zn(1)-O(4)	55.19(8)
O(4)-N(10)	1.185(3)	O(1)-Zn(1)-O(4)	93.19(8)
N(2)-N(3)	1.262(3)	O(4)-N(10)-O(3)	120.1(3)
N(3)-N(4)	1.120(3)	O(1)-N(9)-O(2)	115.7(2)
N(6)-N(7)	1.259(3)	C(3)-N(2)-N(3)	115.2(2)
N(7)-N(8)	1.123(3)	N(2)-N(3)-N(4)	171.8(3)
		C(8)-N(6)-N(7)	115.6(2)
Zn(1)-O(4)-N(10)-O(3)	(-) 3.4 (2)	N(6)-N(7)-N(8)	172.3(3)
Zn(1)-O(1)-N(9)-O(2)	(-) 2.7(2)		
C(2)-C(3)-N(2)-N(3)	(-) 0.9(3)		
N(3)-N(2)-C(3)-C(4)	179.3(2)		
C(7)-C(8)-N(6)-N(7)	(-) 4.7(3)		
C(9)-C(8)-N(6)-N(7)	175.7 (2)		

## 8. Azidopyridine-chloro-complex

### 8.1 [Zn(4-azidopyridine)<sub>2</sub>(Cl)<sub>2</sub>] (14)

#### Synthesis

Zinc(II)chloride (0,1376g; 1.0 mmol) and 4-azidopyridine (0.240g; 2.0 mmol) were dissolved in 10mL of dist. H<sub>2</sub>O. The solution turned a yellowish color with a white precipitate. It was then heated to 75°C for approximately 20 minutes to dissolve all the remaining salt and ligand. At the same time, 2,5mL of dist. H<sub>2</sub>O was added in order to obtain a solution. The solution was stored in a compartment dryer (50°C) for three days. After cooling, it was stored at room temperature and yellowish to white crystals were obtained in about a 62 % yield.

**C H N –Analytics** found(theor.) in %

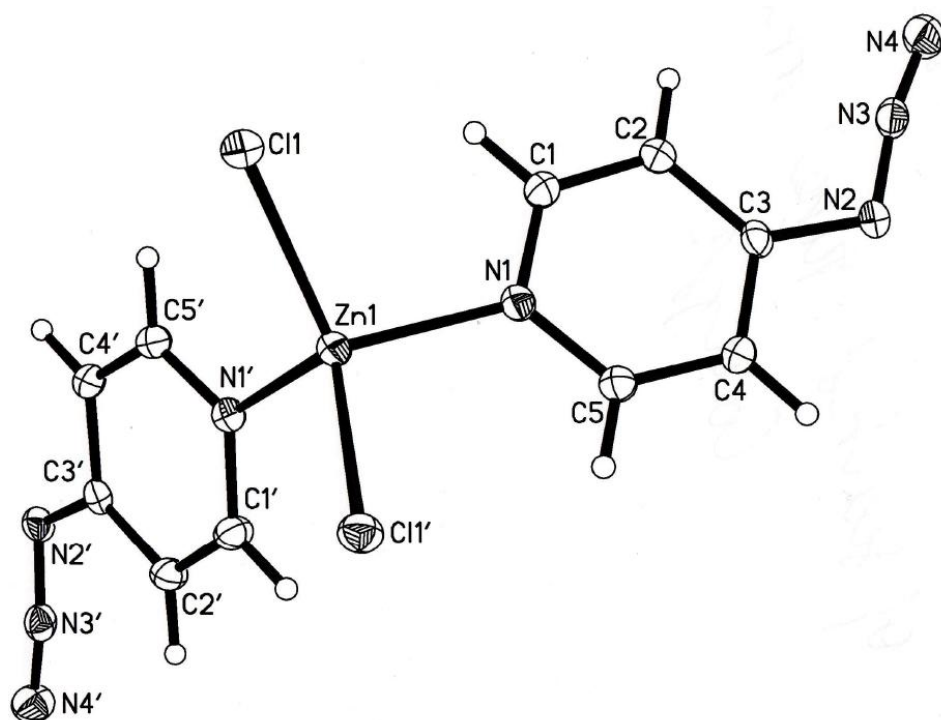
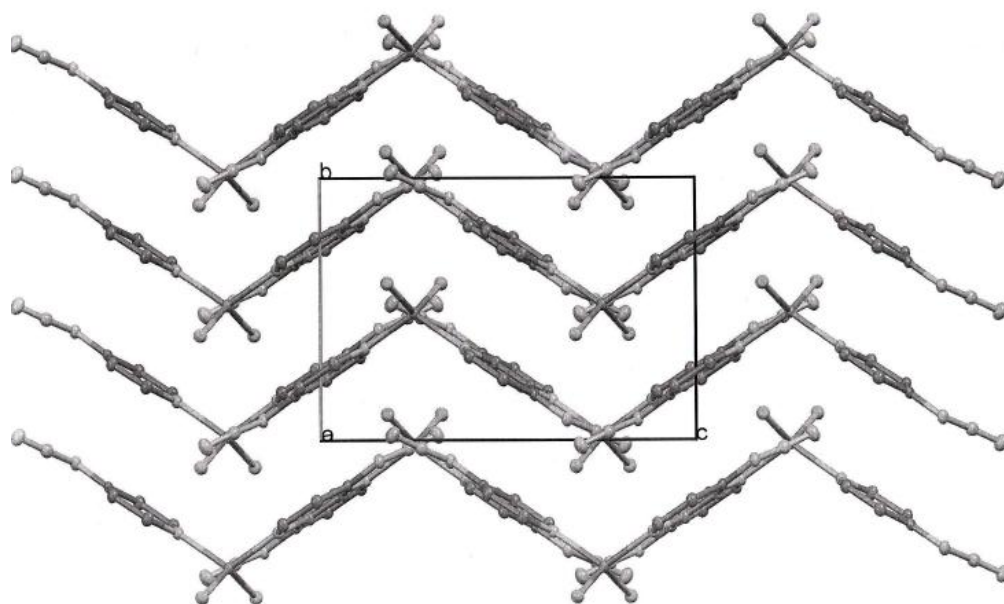
C: 32,2 (31,9) H: 2,0 (2,1) N: 30,4 (29,8)

**IR-values** (spectrum on p.117)

$\nu$  (cm<sup>-1</sup>): 2420 w, 2264 m, 2138 sh, 2100 vs, 2069 sh  $\nu_{as}$  (N<sub>3</sub><sup>-</sup>); 1606 vs, 1558 s, 1499 s, 1432 s, 1132 m, 1010 s, 819 vs (pyridine moiety); 1293 vs, 1211 s,  $\nu_{sym}$  (N<sub>3</sub>); 521s  $\delta$  N<sub>3</sub><sup>-</sup>;

#### Discussion of the structure

The simplest complex in this master thesis is [Zn(4-Azidopyridine)<sub>2</sub>(Cl)<sub>2</sub>] (abbreviated **(14)**). It crystallized in the monoclinic space group C2/c and has a coordination number four. Due to this, a tetrahedral geometry was obtained. The unit cell of **(14)** contains 2 formula units. The tetrahedral geometry of **(14)** consists of two 4-azidopyridine as well as two chloride ligands. The metal centre is located at the centre of inversion. The metal centre show the following characteristics: Zn(1)-N(1) 2.0558(11) and Zn(1)-Cl(1) 2.2419(3)Å. The corresponding bond angles are Cl(1)-Zn(1)-Cl(1A) 103.52(3)° and N(1)-Zn(1)-N(1A) 114.05(6)°. The terminal N<sub>3</sub><sup>-</sup> group (from 4-azidopyridine) usually has an asymmetric geometry of  $\Delta d(N-N)$  0.1225(17) Å and a corresponding bond angle of N(2)-N(3)-N(4) 170.00(14)°, respectively. In Tab. 8.1.1 crystallographic data are summarized, Tab. 8.1.2 show all relevant bond angles and lengths. The structure of **(14)** is pictured in Fig.8.1.1. The packing arrangement can be seen in Fig.8.1.2.

Fig.8.1.1: Structure of [Zn(4-Azidopyridine)<sub>2</sub>(Cl)<sub>2</sub>]Fig.8.1.2: Packing view of [Zn(4-Azidopyridine)<sub>2</sub>(Cl)<sub>2</sub>]

Tab. 8.1.1: Crystallographic data and processing parameter

---

Identification-code	AT2
Empirical formula	C <sub>20</sub> H <sub>16</sub> Cl <sub>4</sub> N <sub>16</sub> Zn <sub>2</sub>
Formula mass	753.03
System	Monoclinic
Space group	C 2/c
a (Å)	14.5730(7)
b (Å)	8.2325(4)
c (Å)	13.4106(10)
α (°)	90.00
β (°)	118.4550(10)
γ (°)	90.00
V(Å <sup>3</sup> )	1414.53(14)
Z	2
F (0 0 0)	752
T (K)	100(2)
μ (MoK <sub>α</sub> )(mm <sup>-1</sup> )	2.119
D <sub>calc</sub> (Mg/m <sup>3</sup> )	1.768
Crystal size	0.45 x 0.35 x 0.25
Θ range (°)	2.94-29.58
Reflections collected	30164
Independent refl./ R <sub>int</sub>	2721/0.0246
Parameters	96
Goodness-of-Fit on F <sup>2</sup>	1.013
R1/wR2 (all data)	0.0198/0.0569
Residual extrema (e/ Å <sup>3</sup> )	0.442/-0.275

---

**Tab. 8.1.2: Selected bond lengths (Å) and angles (°) for (14)**

Zn(1)-N(1)	2.0558(11)	N(1)-Zn(1)-N(1 <sup>a</sup> )	114.05(6)
Zn(1)-Cl(1)	2.2419(3)	N(1)-Zn(1)-Cl(1)	103.52(3)
N(2)-N(3)	1.2463(16)	Cl(1)-Zn(1)-Cl(1 <sup>a</sup> )	130.358(19)
N(3)-N(4)	1.1239(18)	C(3)-N(2)-N(3)	117.16(11)
		N(2)-N(3)-N(4)	170.00(14)
C(2)-C(3)-N(2)-N(3)	5.20(19)		
C(4)-C(3)-N(2)-N(3)	-176.18(11)		

Symmetry codes: (a)  $x, y, z$  (b)  $-x, y, -z+1/2$  (c)  $x+1/2, y+1/2, z$  (d)  $-x+1/2, y+1/2, -z+1/2$  (e)  $-x, -y, -z$  (f)  $x, -y, z-1/2$  (g)  $-x+1/2, -y+1/2, -z$  (h)  $x+1/2, -y+1/2, z-1/2$

## 9. Racah parameter und Dq

During the investigation of the synthesized complexes the decision was taken to calculate the Racah parameter and Dq for some of the complexes from the experimental data. In the attachment please find the recorded UV-VIS spectra (p.118). Six coloured complexes of Ni<sup>2+</sup> and Co<sup>2+</sup> were chosen: **(2)**, **(3)**, **(6)**, **(9)**, **(10)** and **(11)**. The calculation of Dq and B was based on an already printed article<sup>70</sup>.

Some transitions of metal centres can be viewed in the UV-VIS range. So according to the article, which is dedicated to Ni<sup>2+</sup> and Co<sup>2+</sup> complexes, the visible bands are:  $\nu_2$  (transition:  ${}^3A_{2g} - {}^3T_{1g}(F)$ ) and  $\nu_3$  (transition  ${}^3A_{2g} - {}^3T_{1g}(P)$ ). These transitions are only valid for Ni<sup>2+</sup> in octahedral complexes. Co<sup>2+</sup> in tetrahedral complexes reveals  $\nu_2$  (transition:  ${}^4A_{2g} - {}^4T_{1g}(F)$ ) and  $\nu_3$  (transition  ${}^4A_{2g} - {}^4T_{1g}(P)$ ); similar to Ni<sup>2+</sup>. For Co<sup>2+</sup> in octahedral environments the transitions are  $\nu_2$  ( ${}^4T_{1g}(F) - {}^4A_{2g}$ ) and  $\nu_3$  ( ${}^4T_{1g}(F) - {}^4T_{1g}(P)$ ). In Tab. 9.1 the data from the recorded spectra are summarized.

Tab.9.1: Data for Dq and B

	coordination	$\nu_3$ (cm <sup>-1</sup> )	$\nu_2$ (cm <sup>-1</sup> )
<b>Ni<sup>2+</sup> (d<sup>8</sup>)</b>			
N <sub>3</sub> <sup>-</sup> <b>(3)</b>	octahedral	9487	15576
SCN <sup>-</sup> <b>(6)</b>	octahedral	11161	17123
OCN <sup>-</sup> <b>(10)</b>	octahedral	9416	15244
<b>Co<sup>2+</sup> (d<sup>7</sup>)</b>			
N <sub>3</sub> <sup>-</sup> <b>(2)</b>	octahedral	18898	8192
SCN <sup>-</sup> <b>(9)</b>	octahedral	21130	9435
OCN <sup>-</sup> <b>(11)</b>	tetrahedral	7966	18588

These values can be used to find Dq according the following equation:

$$340Dq^2 - 18(\nu_2 + \nu_3)Dq + \nu_2\nu_3 = 0 \quad (9.1)$$

From this equation two values for Dq are derived. To find B equation 9.2 is used:

$$B = \frac{\nu_3 + \nu_2 - 30Dq}{15} \quad (9.2)$$

These equations can only be applied to  $d^8$  ions in octahedral environment and to  $d^7$  ions in tetrahedral complexes. For  $d^7$  ions with octahedral geometry the equations must be modified as follows:

$$340Dq^2 + 18(v_3 - 2v_2)Dq + v_2^2 - v_2v_3 = 0 \quad (9.3)$$

$$B = \frac{v_3 - 2v_2 + 30Dq}{15} \quad (9.4)$$

In most cases it is obvious which values are correct for both Dq and B. Tab.9.2 lists the results.

Tab.9.2: Results for Dq und B

	coordination	Dq (cm <sup>-1</sup> )	B (cm <sup>-1</sup> )
<b>Ni<sup>2+</sup> (d<sup>8</sup>)</b>			
N <sub>3</sub> <sup>-</sup> <b>(3)</b>	octahedral	589	492
SCN <sup>-</sup> <b>(6)</b>	octahedral	_*	-
OCN <sup>-</sup> <b>(10)</b>	octahedral	590	463
<b>Co<sup>2+</sup> (d<sup>7</sup>)</b>			
N <sub>3</sub> <sup>-</sup> <b>(2)</b>	octahedral	445	1058**
SCN <sup>-</sup> <b>(9)</b>	octahedral	512	1174**
OCN <sup>-</sup> <b>(11)</b>	tetrahedral	460	848

\*: determinant negative

\*\* : these values seem to be mathematical correct but do not make sense in chemical context.

From these values the following conclusions can be drawn. First, if the simplification and the formulas are correct, the Ni<sup>2+</sup> complexes show a very strong tendency to form covalent bonds. In contrast to this value, Ni<sup>2+</sup> (as free ion) has a B value of about 1055 cm<sup>-1</sup>. Second, due to the fact that the complexes do not show perfect octahedral geometry (which is a requirement for such calculations) the observed bands and calculated values could be either wrong or roughly shifted. The value for the Co<sup>2+</sup>/OCN<sup>-</sup> complex is in good agreement with the value of Co<sup>2+</sup> as a free ion (about 971cm<sup>-1</sup>) and shows a slight rate of covalent bonds. The two B values of complexes **(2)** and **(9)** are completely useless. Probably the application of eq. 9.3 and 9.4 is not designed for such complexes and the simplification, which is mentioned in the cited article above, renders it inaccurate. Also classical trends, known out of the spectrochemical series of ligands, do not agree with this evaluation.

In general, the above formulas are a simple possibility for calculating  $Dq$  und  $B$ , but the application appears to be very limited. This evaluation is a good example for illustrating that the functionality of such simplifications do not always work perfectly.

## 10. Discussion

### 10.1 Comparison of the 4-azidopyridine-azide complexes

Only one structure,  $[\text{Mn}(\text{4-Azidopyridine})_2(\text{N}_3)_2]_n$  in two different modifications, was known before. The Ni, Cd, Co and Zn structures are new. All crystal structures of complexes **(1)** to **(5)** show the known characteristic  $\text{N}_3^-$  EE- and EO bridges and form a 1D structure (chain). All metal centres are coordinated six times and show distorted octahedral geometry. They crystallize, without exception, in triclinic space group P-1. The two 4-azidopyridine ligands coordinate in trans-position to each other and to the metal centre.

### 10.2 Comparison of the 4-azidopyridine-thiocyanate complexes

The synthesis of the thiocyanate complexes **(6)**-**(9)** was successful with Mn, Co, Zn and Ni. The first complex **(6)**, crystallizes as Ni-dimer (with double  $\text{SCN}^-$  bridge) in monoclinic space group P21/c. The dimer of complex **(6)** has three pyridines and two  $\text{SCN}^-$  groups at each coordinated  $\text{Ni}^{2+}$  centre. All other representatives of this class exhibit the same space group but crystallize as monomers. They are all six times coordinated, with four 4-azidopyridines (in one plane) and two  $\text{SCN}^-$  ligands. The  $\text{SCN}^-$  group is N-ligated without exception. The  $\text{SCN}^-$  moiety exhibits nearly linear geometry in all complexes (also in double bridge of complex **(6)**). All complexes of this class are centrosymmetric regarding the metal centre (except Ni-dimer) and show distorted octahedral geometry.

### 10.3 Comparison of the 4-azidopyridine-cyanate complexes

The cyanate complexes of Ni, Co, and Zn are similar to the thiocyanate complexes. Two different coordination numbers are available. Compound **(10)**, the nickel cyanate complex, is six times coordinated (four 4-azidopyridines and two cyanate groups), **(11)** and **(12)** are four times coordinated (two 4-azidopyridines and two cyanates). The  $\text{OCN}^-$  moiety is strictly N-ligated and exhibits an almost linear geometry. The molecules of the Ni compound are the only ones that occupy general positions in the unit cell. All structures crystallize in triclinic space group P-1 with distorted octahedral and tetrahedral geometry.

#### 10.4 4-azidopyridine-nitrite complex

This complex can be obtained as a monomer in monoclinic space group P21/c. The compound has distorted octahedral geometry and is six times coordinated (two 4-azidopyridines and two bidentate  $\text{NO}_2^-$  groups). The nitrite ion bonds through its two oxygen atoms.

#### 10.5 4-azidopyridine complex

The monomeric 4-azidopyridine complex with  $\text{ZnCl}_2$  has tetrahedral geometry and crystallizes in monoclinic space group C2/c. It has two pyridine and two chloride ligands.

#### 10.6 General comparison

A comparison of all complexes can be done using torsion angles of the 4-azidopyridine. The 14 complexes show different characteristics, structure types and coordination numbers. One feature is characteristic to all of them: the torsion angle of the terminal azido group at the pyridine ring (in para position). In the table for each compound the angles are listed. The torsion angles are defined along two carbon atoms and two nitrogen atoms (which define the two planes). These angles range from  $170.0^\circ$  to  $179.5^\circ$ . This indicates that this moiety, because of its single bond to the carbon atom, can rotate best in these structures. In complexes with CN 6, the pyridine ring seems to be hindered by the stereochemistry of the complex itself. Therefore no complete rotation seems to be possible. The  $\text{N}_3^-$  group can rotate, also promoted through disorders in the crystal lattice.

Another important feature, which is common to all compounds in this work, is that 4-azidopyridine always coordinates first to the metal centre. Afterwards the bridging ligands (like  $\text{N}_3^-$ ) or  $\text{SCN}^-$  and  $\text{OCN}^-$  coordinate to the centre. This is best exhibited by the 4-azidopyridine-chloro-complex with  $\text{ZnCl}_2$ .

The  $Dq$  values and the Racah parameter  $B$  were calculated for the six coloured complexes of  $\text{Ni}^{2+}$  and  $\text{Co}^{2+}$  ((2), (3), (6), (9), (10) and (11)) for spectroscopic reasons.

## 11. Summary

The aim of this master thesis was to synthesize and characterize complexes with 4-azidopyridine and pseudohalogenides as ligands. As a result 14 complexes (and therefore 13 new ones) of the metals Cobalt, Nickel, Zinc, Cadmium and Manganese were produced from this work.

All structures with the five metals exhibited the known alternate EO- and EE-bridges and formed a 1D chain using  $N_3^-$ .

Four new complexes of Ni, Co, Zn and Mn were synthesized with  $SCN^-$ . The Nickel complex was obtained as dimer. All other complexes were monomers.

The three synthesized cyanate complexes of Ni, Co and Zn showed different coordination number: Nickel CN 6, Co and Zn CN4. All were monomers.

A monomeric bidentate nitrite-complex was obtained with CN 6.

The monomeric tetrahedral 4-azidopyridine-chloro-complex with CN 6 was synthesized.

CN 5 or others were not obtained during this work. No complex showed perfect octahedral or tetrahedral geometry. Measurements such as IR and CHN analytics were taken to confirm crystal data.

## 12. References

- 1) Jobelius H., Scharff H., "Hydrazoic Acid and Azides", Ullmann's Encyclopedia of Industrial Chemistry, 2005, Wiley-VCH, Weinheim.
- 2) Müller U., Struct. Bonding, 1973, 14, p.141
- 3) Dori Z., Ziolo R., Chem.Rev., 1973, 73, p.247
- 4) E.M. Arnett et al., Commission on Physical Sciences, Mathematics, and Applications, Prudent Practices in the Laboratory: Handling and Disposal of Chemicals, National Academic Press, 1995, p. 165
- 5) Huisgen, R., "Centenary Lecture - 1,3-Dipolar Cycloadditions". *Proceedings of the Chemical Society of London*, 1961, october issue, p.357-396
- 6) Fair H.D., Walker R.F, Energetic Materials, , Technology of the Inorganic Azides, Plenum Press, New York, 1977, Vol.2
- 7) Tornieporth-Oetting I.C., Klapötke T.M., Covalent Inorganic Non-Metal azides, Combustion Efficiency and Air Quality, (Hargittai I., Vidoczy T., Eds.) Plenum Press, New York,1995, 51
- 8) Rokosch U., Airbags und Gurtstraffer, Vogel Buchverlag, Würzburg, 2002
- 9) Devi A., Sussek H., Pritzkow H., Winer M., Fische R.A., Eur. J. Inorg. Chem., 1999, 2127
- 10) Sulkes M., Baldwin L.C., Fink M.J., Chem.Phys.Lett., 2000, 318, p.448
- 11) Yamane H., Kinno D., Shimada M., Sekiguchi T., Disalvo F.J., J.Matt.Sci., 2000, 35, 801
- 12) Acosta E.P., Page L.M., Fletcher C., Clin. Pharmacokin., 1996, 30, p.251
- 13) Yan M., Wybourne M.N., Kena J.F.W., React. Funkt. Polym., 2000, 43, p.221
- 14) Barnes R.J., Sinha A., Amitabha D.P.J, Lambert H.M., J. Chem. Phys., 1999, 111,p. 151
- 15) Scriven E.F.V., "Azides and Nitrenes-Reactivity and Uility", Academic Press, Orlando, 1984
- 16) Cenini S., Gallo E., Caselli A., Ragaini F., Fantauzzi S., Piangiolino C., Coord. Chem. Rev., 2006, 250, p.1234-1253
- 17) Bräse S., Gil C., Knepper K., Zimmermann V., Angew. Chem., Int. Ed., 2005, 44, p 5188-5240
- 18) Mautner F., Egger A., Sodin B., Goher M.A.S., Abu-Youssef M.A.M., Moussad A., Escuer A.and Vicente R., Journ. Mol. Struct., 2010, 969, p.192
- 19) Escuer A.,Mautner F.A, Goher M.A.S., Abu-Youssef M.A.M. and Vicente R., Chem.Comm., 2005, p.605-607
- 20) Kahn O., Molecular Magnetism, VCH Publishers, Weinheim, 1993
- 21) Willet R.D., Gatteschi D., Kahn O. (Eds.), Magneto-structural Correlations in Exchange Couplet Systems, NATO ASI Series, Reidel, Dordrecht, 1985
- 22) Cortes R., Lezama L., Mautner F.A. und Rojo T., in Molecule-Based Magnetic Materials. Theory, Techniques and Applications; Turnbull M.M., Sugimoto T., Thompson L.K. (Eds.), ACS Symposium Series, , ACS Washington, 1996, no. 644,
- 23) Ribas J., Escuer A., Monfort M., Vicente R., Cortes R., Letama L.und Rojo T., Coord.Chem.Rev., 1999, 1027, p.193-195

- 24) Commarmond J., Plimere P., Lehn J.M., Agnus Y., Weiss R., Kahn O. and Morgenstern-Badarau I., *J.Am.Chem.Soc.*, 1982, 104,p. 6330
- 25) Escuer A., Mautner F.A., Goher M.A.S., Abu-Youssef M.A.M. and Vicente R., *Chem.Commun.*, 2005, p.605-607
- 26) Massa W., *Kristallstrukturbestimmung*, Teubner, 5<sup>th</sup> edition, 2007
- 27) [http://www.ctcms.nist.gov/wulffman/docs\\_1.2/](http://www.ctcms.nist.gov/wulffman/docs_1.2/), requested : 11.10.2012, 13.38 pm
- 28) Bravais M.A., *J. de lécole Polyt*, 1859,Cahier XIX, 1
- 29) <http://www.seas.upenn.edu/~chem101/sschem/solidstatechem.html>, requested: 13.10.2012 9.21 am
- 30) Hermann G., *Z. Kristallogr.*, 1928, 68 p.257 / Mauguin G., *Z. Kristallogr.* 1931, 76, p.542
- 31) Schönflies A., *Kristallsysteme und Kristallstruktur*, Leipzig ,1891
- 32) Massa W., *Kristallstrukturbestimmung*, Teubner, 2007 5<sup>th</sup> edition, p.37
- 33) Massa W., *Kristallstrukturbestimmung*, Teubner, 2007 5<sup>th</sup> edition, p.30,
- 34) [http://www-structmed.cimr.cam.ac.uk/Course/Basic\\_diffraction/Diffraction.html](http://www-structmed.cimr.cam.ac.uk/Course/Basic_diffraction/Diffraction.html), requested 13.10.2012 11.49 am
- 35) <http://pd.chem.ucl.ac.uk/pdnn/diff1/scaten.htm>, requested: 13.10.2012 14.22 pm
- 36) Massa W., *Kristallstrukturbestimmung*, Teubner, 2007,5<sup>th</sup> edition p.55
- 37) Massa W., *Kristallstrukturbestimmung*, Teubner, 2007, 5<sup>th</sup> edition p.46
- 38) Patterson A.L, *Phys.Rev.*, (1934), 46, p.372/ Harker D., *J.Chem. Phys.*, 1936, 4, p.381
- 39) Massa W., *Kristallstrukturbestimmung*, Teubner, 2007, 5<sup>th</sup> edition,, p..133
- 40) Harker D., Kasper J.S., *Acta Cris.*, 1948, 1, p.70
- 41) Sayre D., *Acta Cryst.*, 1952, 5, p.60
- 42) Gillespie R.J., „Molecular geometry“, Van Nostrand Reinhold, Lodon, 1972
- 43) Hollemann A., Wiberg E., *Lehrbuch der Anorganischen Chemie*, Walter de Gruyter (New York), 1995,101st. edition., p.1226
- 44) Pauling L., *Die Natur der chemischen Bindung*, Verlag Chemie, Weinheim. 1976
- 45) Crabtree, R., *The organometallic chemistry of transition metals*, Wiley, New Jersey, 5<sup>th</sup> edition, 2009
- 46) Pearson R., *Inorg. Chim. Acta.* 1995, Vol. 240, No.1/2
- 47) van Vleck J.H., *Phys. Rev.*, 1932, 41, p.208-215
- 48) <http://amrita.vlab.co.in/?sub=2&brch=193&sim=610&cnt=1>, requested 20.10.2012 15.15 pm
- 49) Coulson C., *Valence*. Oxford at the Clarendon Press, 1952
- 50) Elschenbroich C., *Organometallchemie*, Teubner Verlag, 6. Auflage, 2008, S.258
- 51) [http://www.ccdc.cam.ac.uk/free\\_services/teaching/modules/backbonding/backbonding.1.8.html](http://www.ccdc.cam.ac.uk/free_services/teaching/modules/backbonding/backbonding.1.8.html), requested 22.10.2012 9.45 am
- 52) Hollemann A., Wiberg E., *Lehrbuch der Anorganischen Chemie*, Walter de Gruyter (New York), 1995, 101st ed., p.1264
- 53) Tanabe, Y., Sugano, S. "On the absorption spectra of complex ions I". *Journal of the Physical Society of Japan* 1954, 9, p.753–766.

- 54) <http://wwwchem.uwimona.edu.jm/courses/Tanabe-Sugano/TSHelp.html> , abgefragt am 12.10.2012, 13.42 Uhr.
- 55) Racah G.: *Theory of Complex Spectra II*. In: *Physical Review*, 1942, 62, S. 438
- 56) Lábbe G., Beenaerts L., *Tetrahedron* 1989, Vol. 45, No.3, p. 749
- 57) Dobramysl W., Fritzer H.P., *Inorg. Chem. Letters*, 1978,14, p.269
- 58) Egger A., Diploma thesis „Structure determination and Characterisation of azido complexes with ions of manganese and rare earths“ , TU Graz, 2005
- 59) APEX and SAINT, Area Detector Software package and AXS Area Detector Integration program, Bruker Analytical X-ray, Madison, WI, 1997
- 60) SADABS, AXS Area Detector Absorption program, Bruker Analytical X-ray, Madison, WI, 1997
- 61) Sheldrick G., *Acta Cryst., Sect.A*.2008, 64, p.112
- 62) PLATON, A.L. Spek (2005), A Multipurpose Crystallographic tool, Utrecht University, Utrecht, Netherlands
- 63) XPert-Highscore PLUS Software package; PANAnalytical, 2009
- 64) OPUS-software, Vers. 5., Bruker Optics, Billerica, MA, US
- 65) UVWin Lab software, Vers.5.1; Perkin Elmer LAS, Rodgau - Germany, 2005
- 66) MestReNova LITE software, Vers. 5.2.5-5780 (2008), Mestrelab research, Tangelwood-California – US
- 67) Mautner F., Egger A., Sodin B., Goher M.A.S., Abu-Youssef M.A.M., Moussad A., Escuer A.and Vicente R., *Journ. Mol. Struct.*, 2010, 969, p. 192
- 68) Escuer A., Mautner F.A., Goher M.A.S., Abu-Youssef M.A.M. and Vicente R., *Chem.Comm.*, 2005, 605-607
- 69) Escuer A., Vicente R., Goher M.A.S., Mautner F.A., *Inorg. Chem.* 1998, 37, p.782
- 70) Underhill A., Billing D., *Nature*, 1966, Vol.210, p.834

Attachement

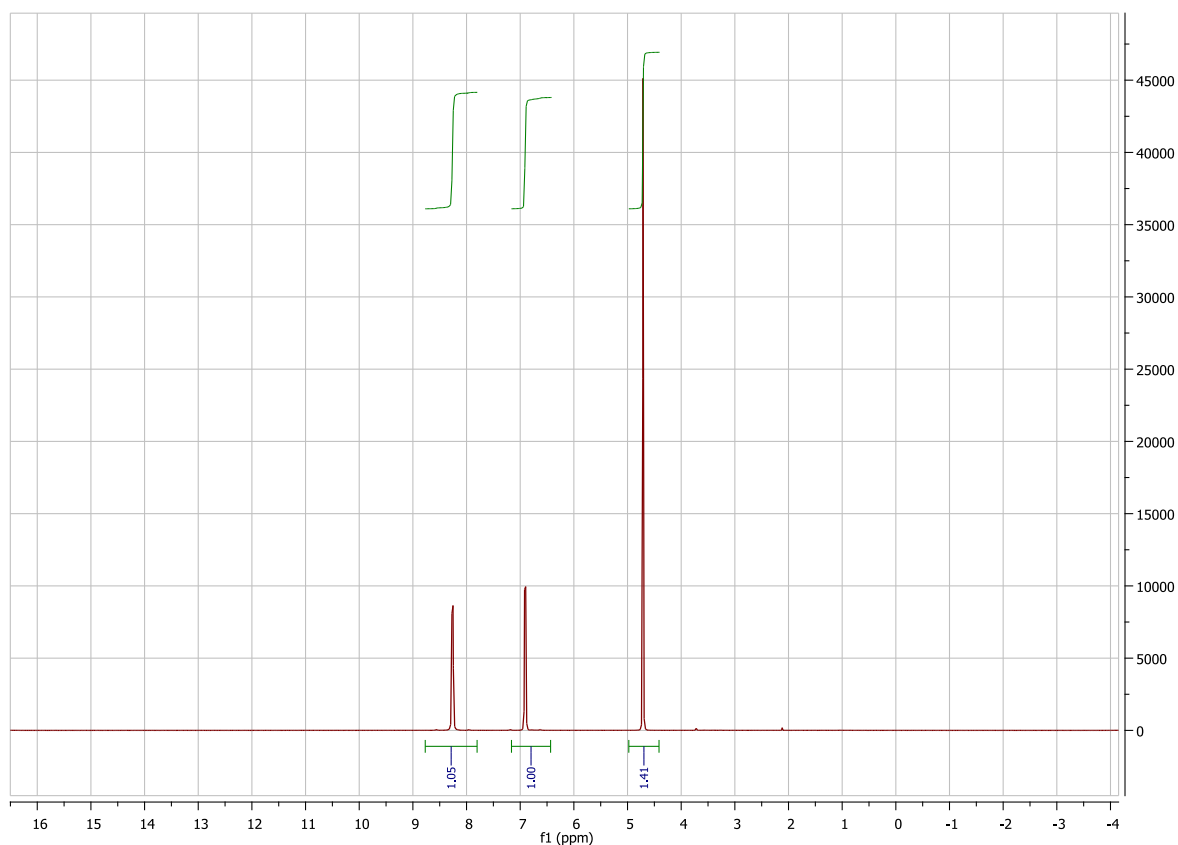
---

Attachement:

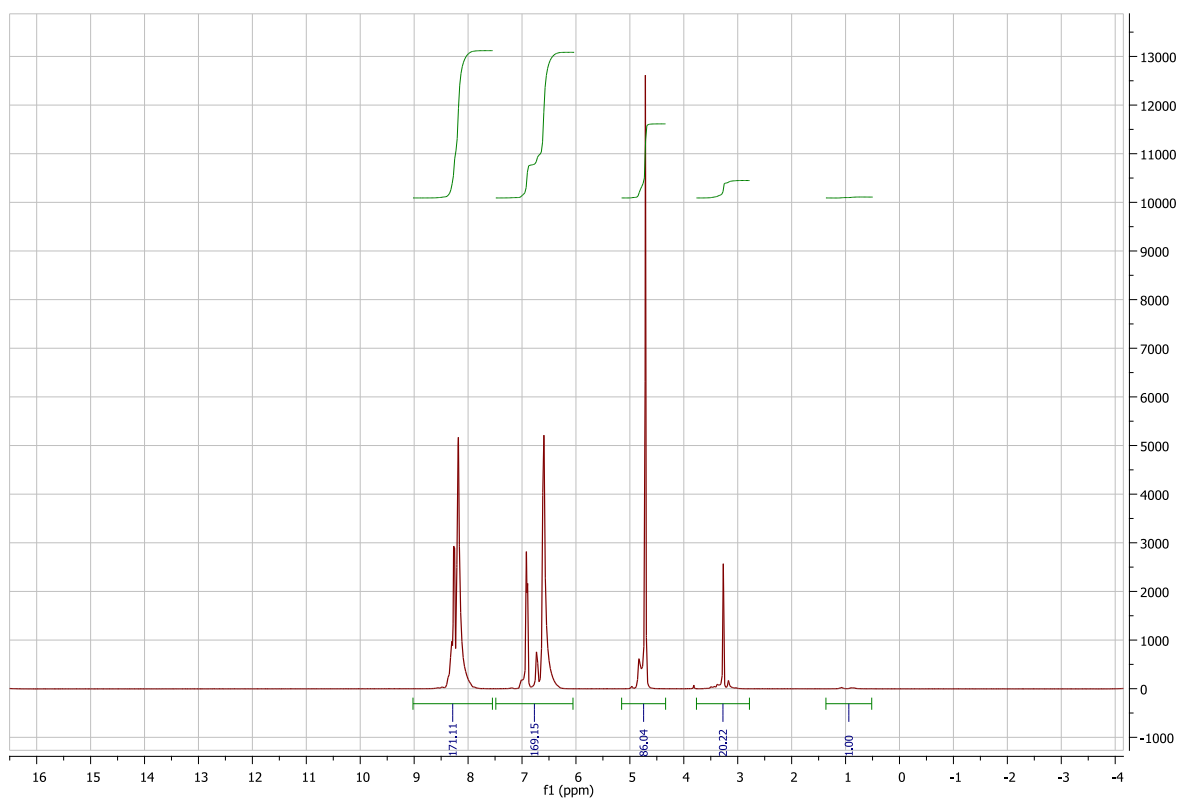
NMR-spectra

IR-spectra (characterisation)

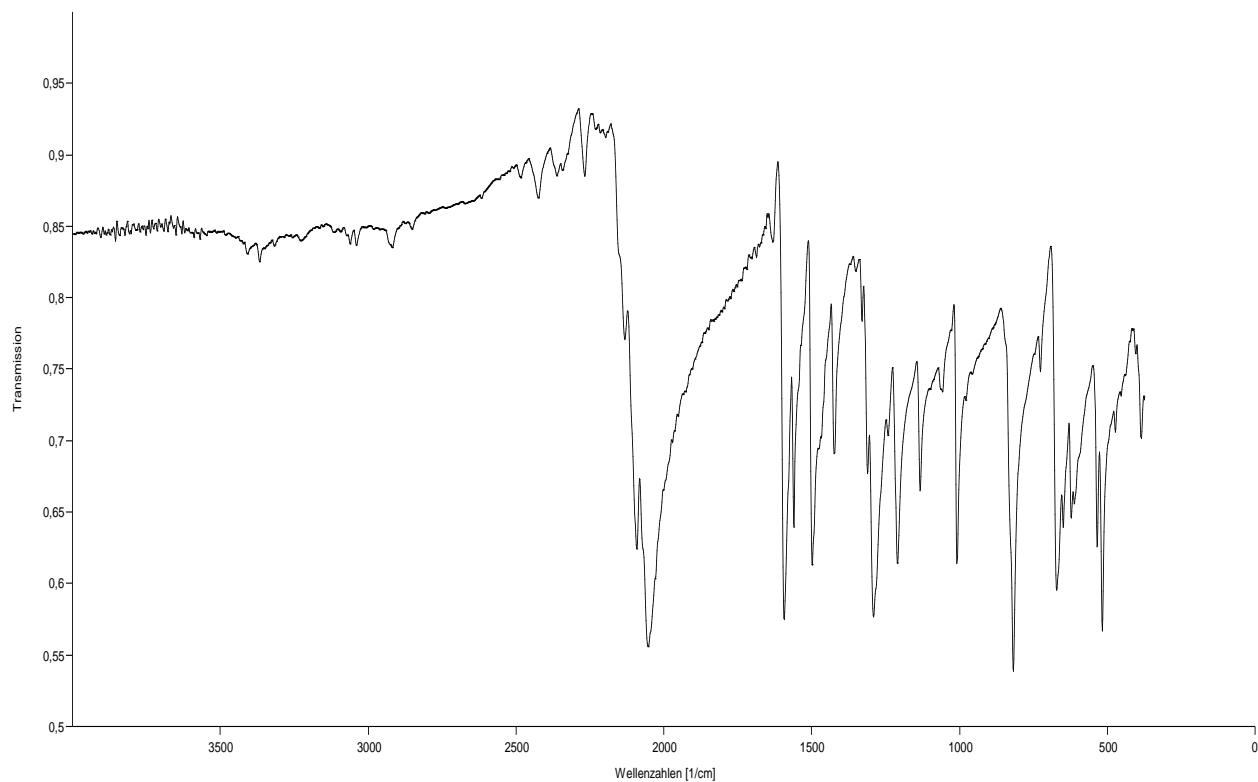
UV-VIS spectra (crystal field analysis)



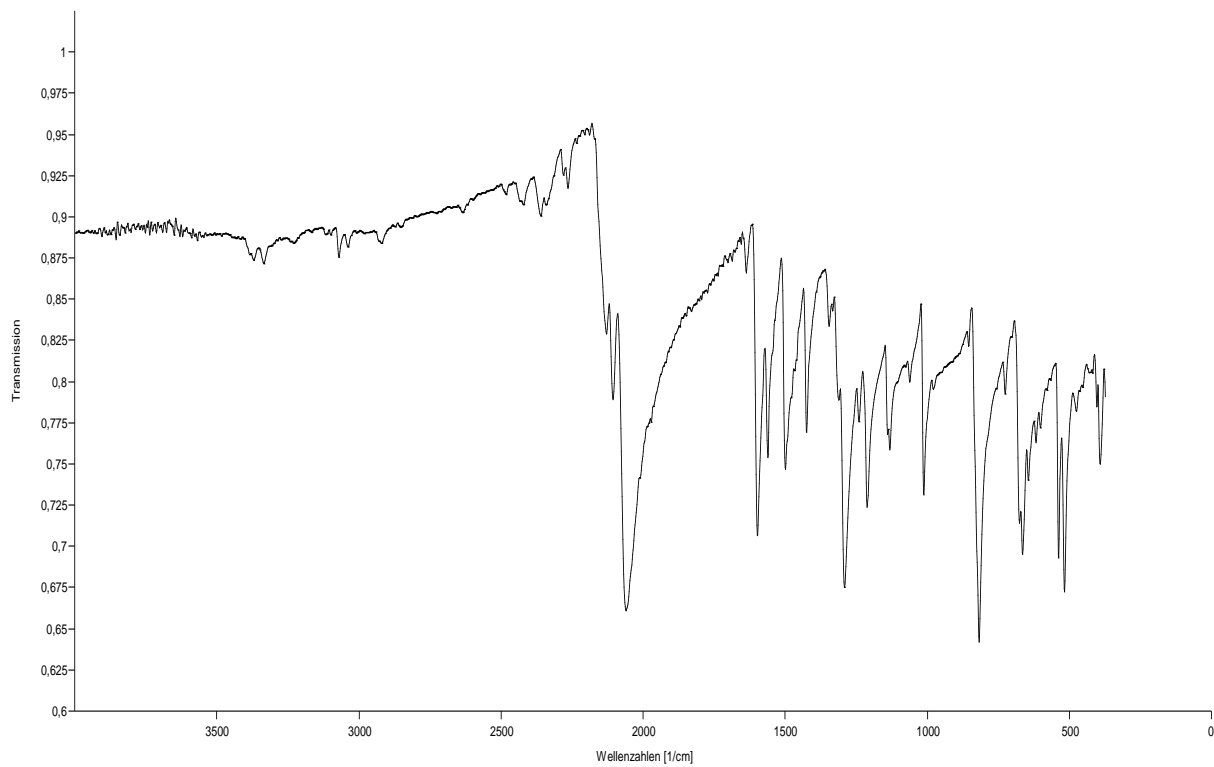
1H-NMR- spectrum of 4-azidopyridine (prepared with fresh distilled absolute diethylether)



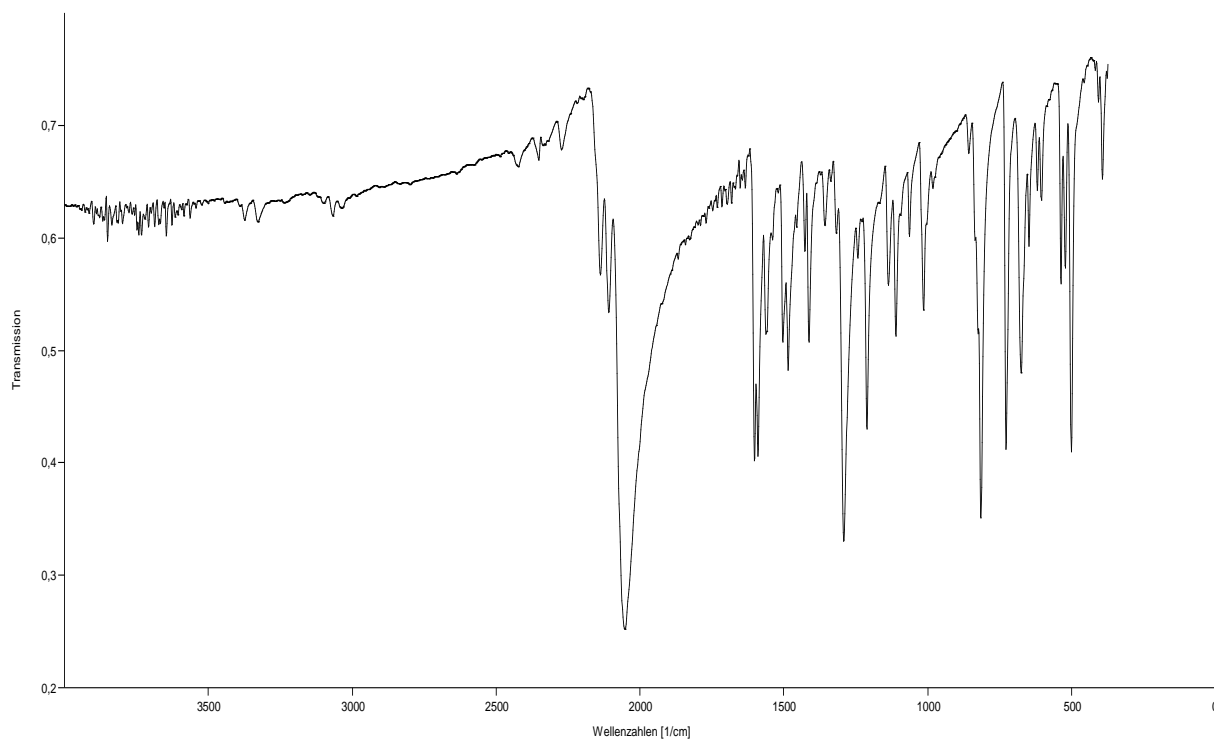
1H-NMR- spectrum of 4-azidopyridine (prepared with commercial diethylether)



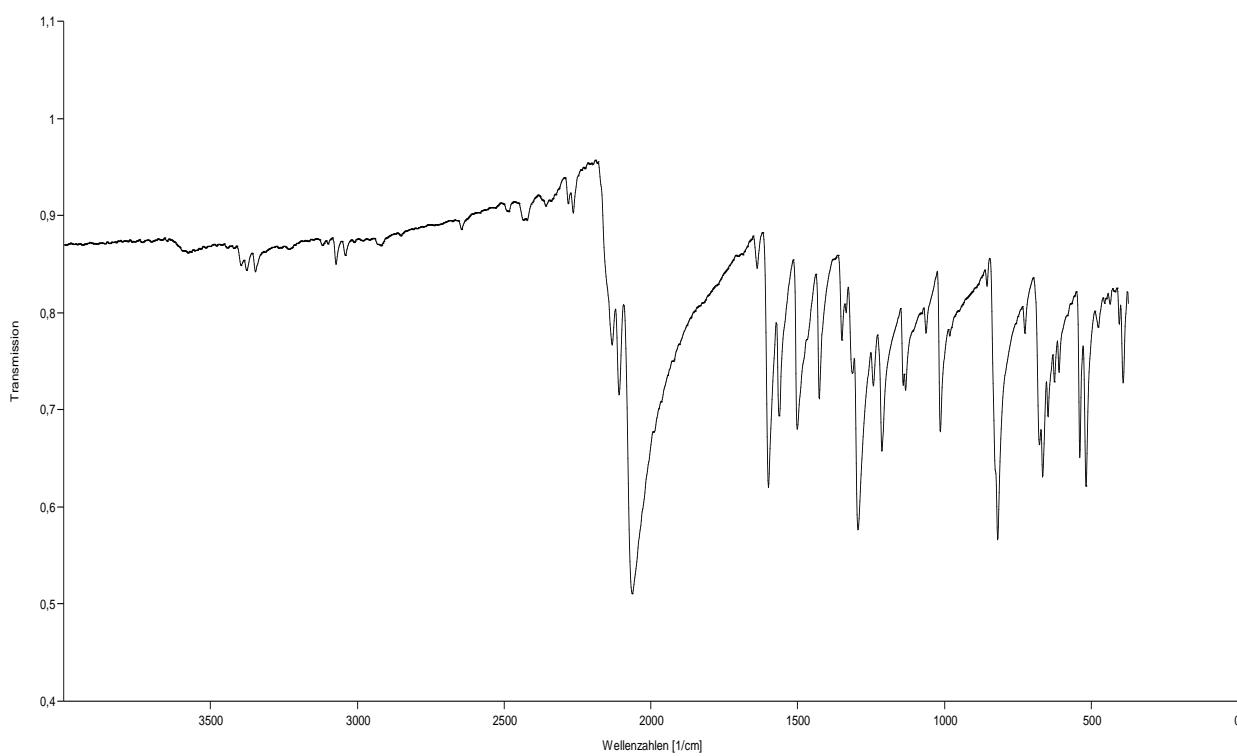
IR-spectrum of  $[\text{Mn}(\text{4-Azidopyridine})_2(\text{N}_3)_2]_n$  (1)



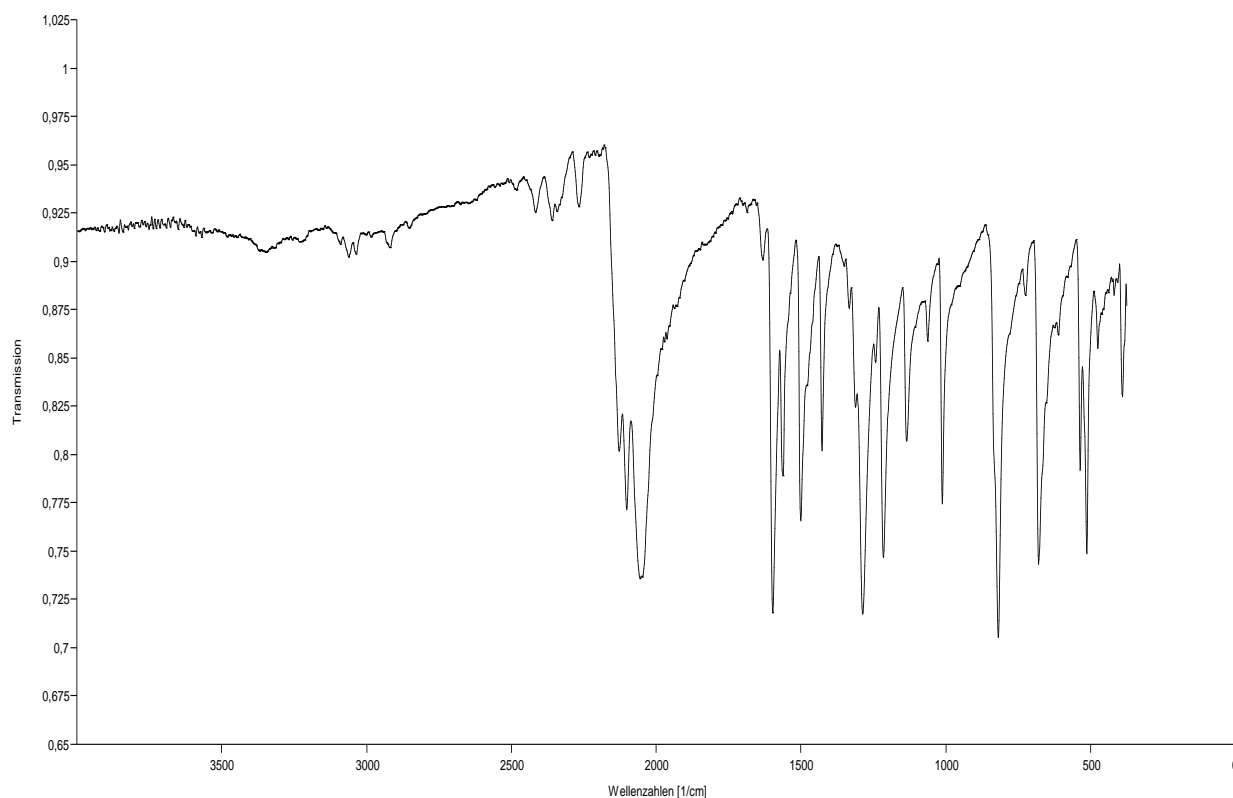
IR Spectrum of  $[\text{Co}(\text{4-Azidopyridine})_2(\text{N}_3)_2]_n$  (2)



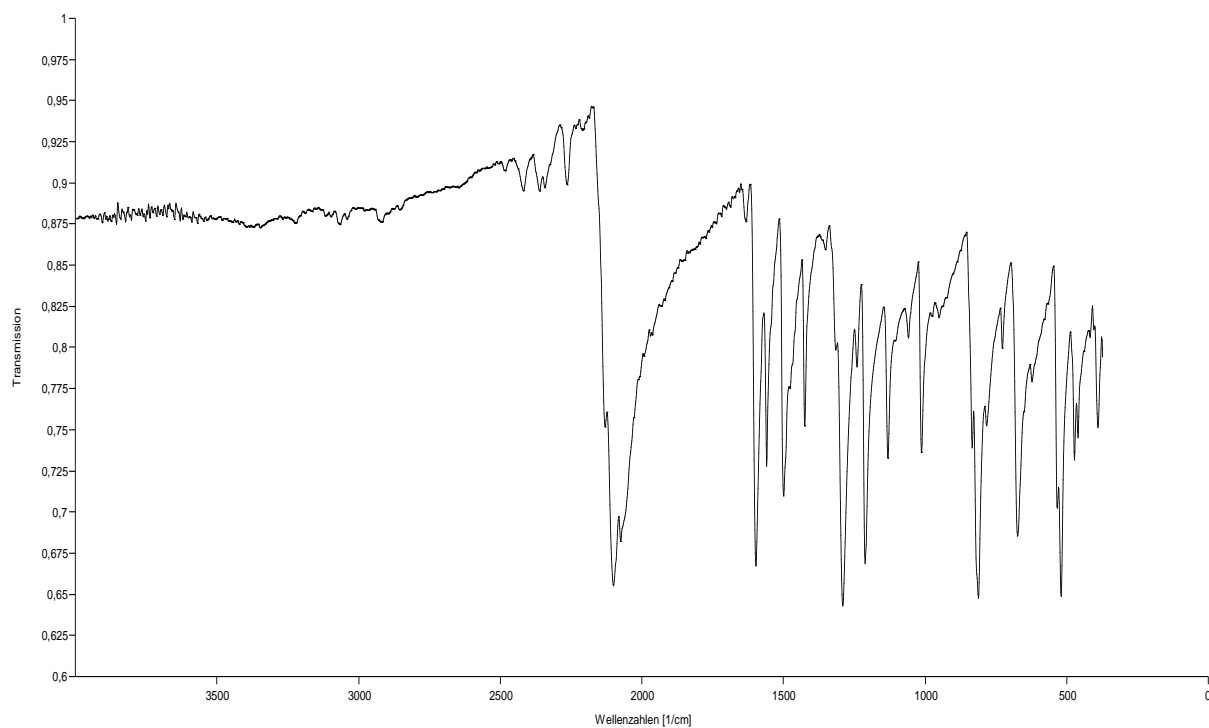
IR-Spectrum of  $[\text{Ni}(4\text{-Azidopyridine})_2(\text{N}_3)_2]_n$  (3)



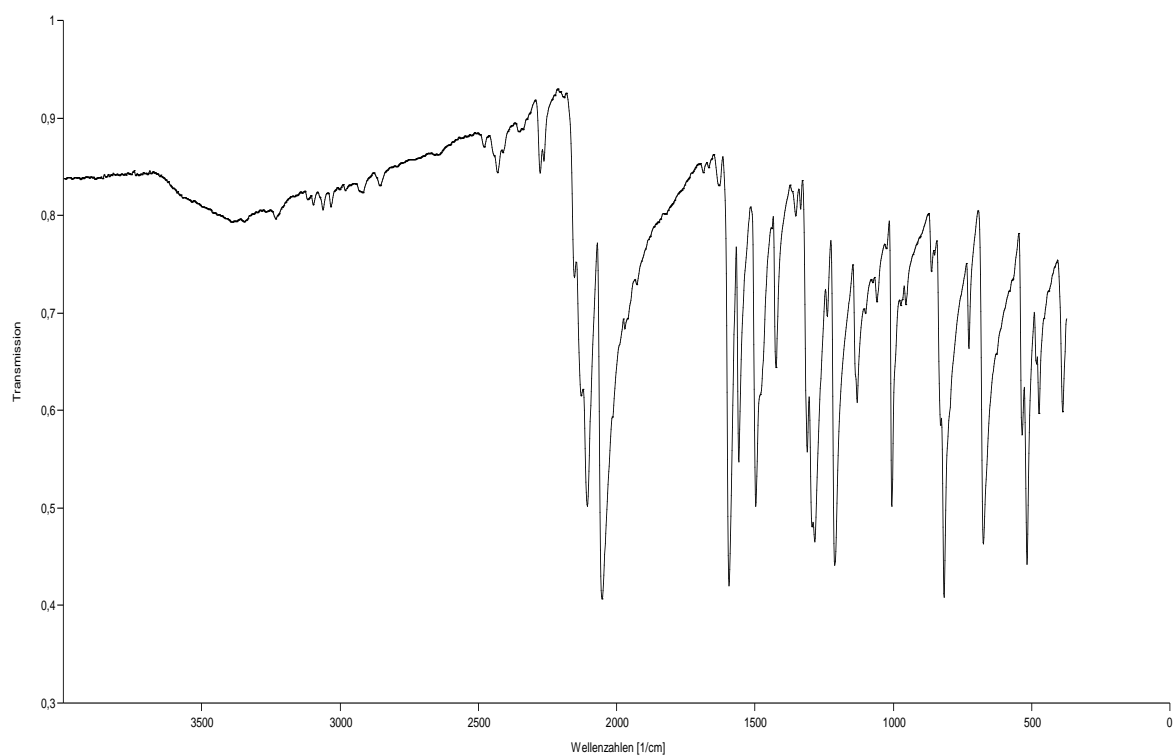
IR-Spectrum of  $[\text{Zn}(4\text{-Azidopyridine})_2(\text{N}_3)_2]_n$  (4)



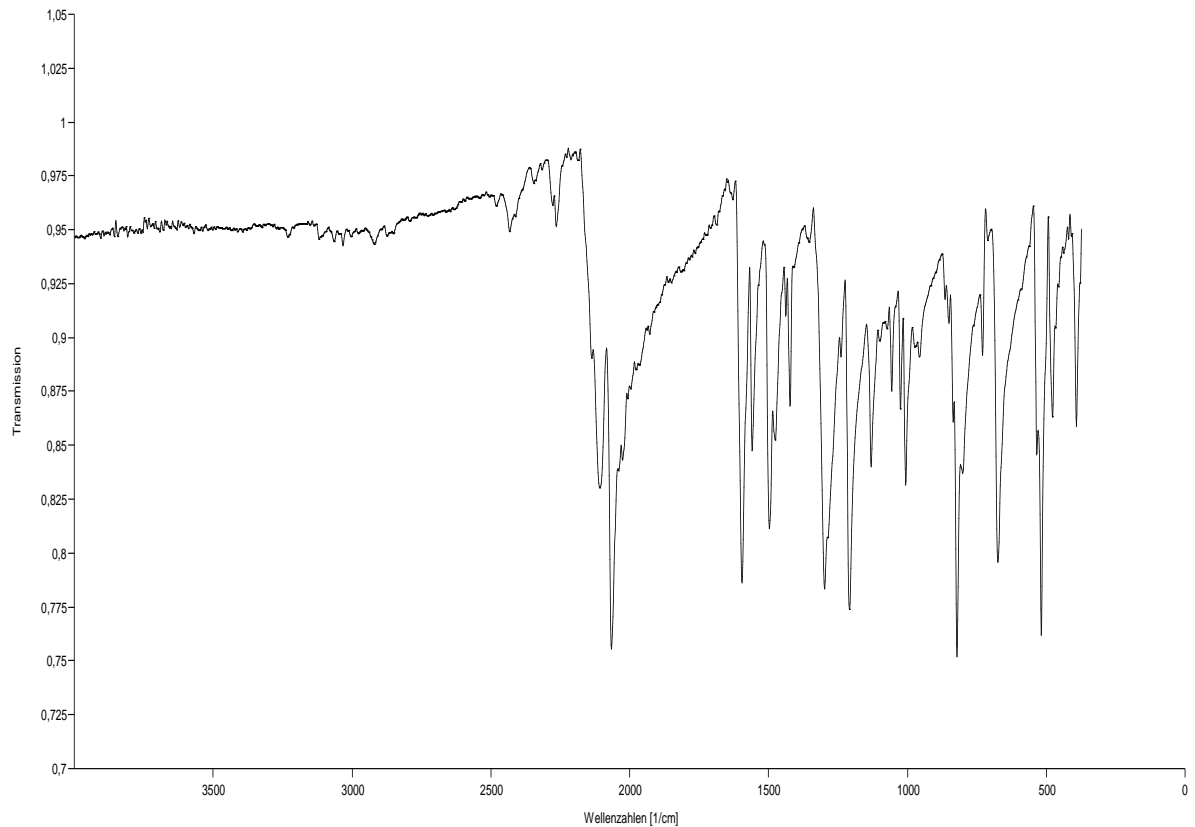
IR-Spectrum of  $[\text{Cd}(\text{4-Azidopyridine})_2(\text{N}_3)_2]_n$  (5)



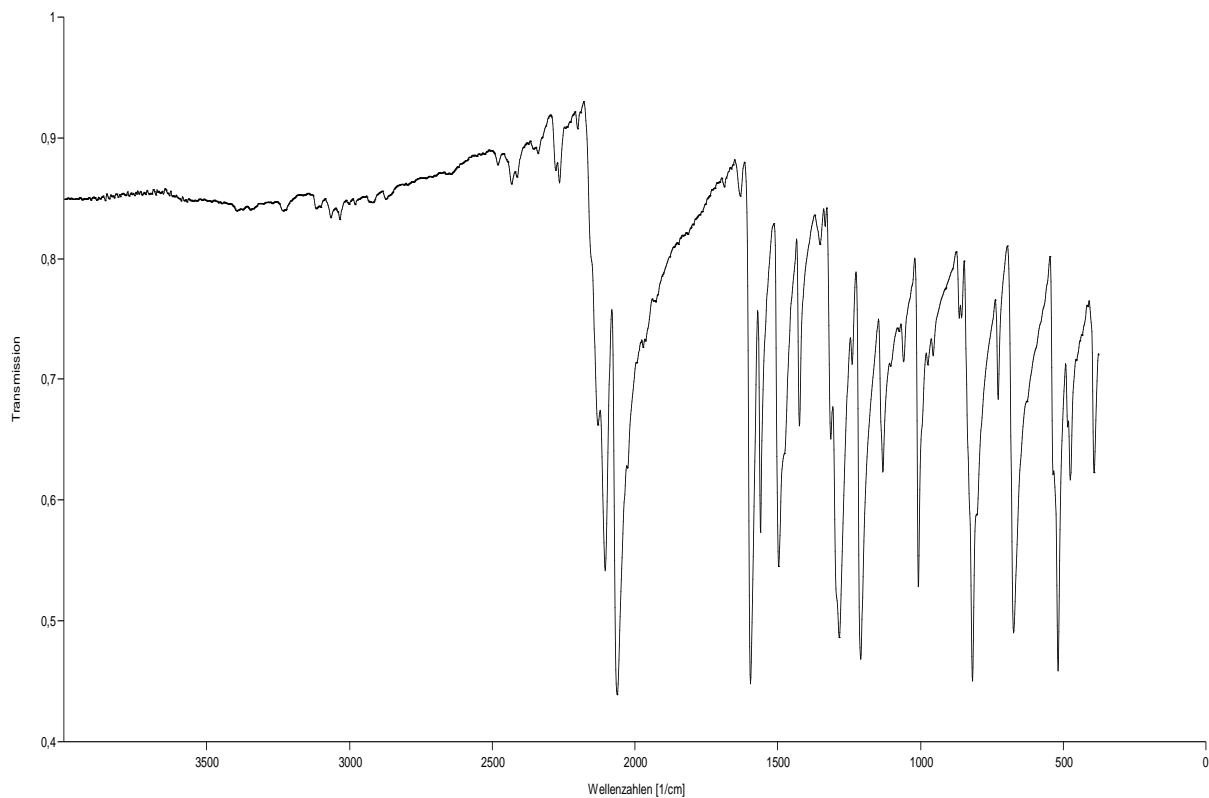
IR-Spectrum of  $[\text{Ni}_2(\text{4-Azidopyridine})_6(\text{SCN})_4]$  (6)



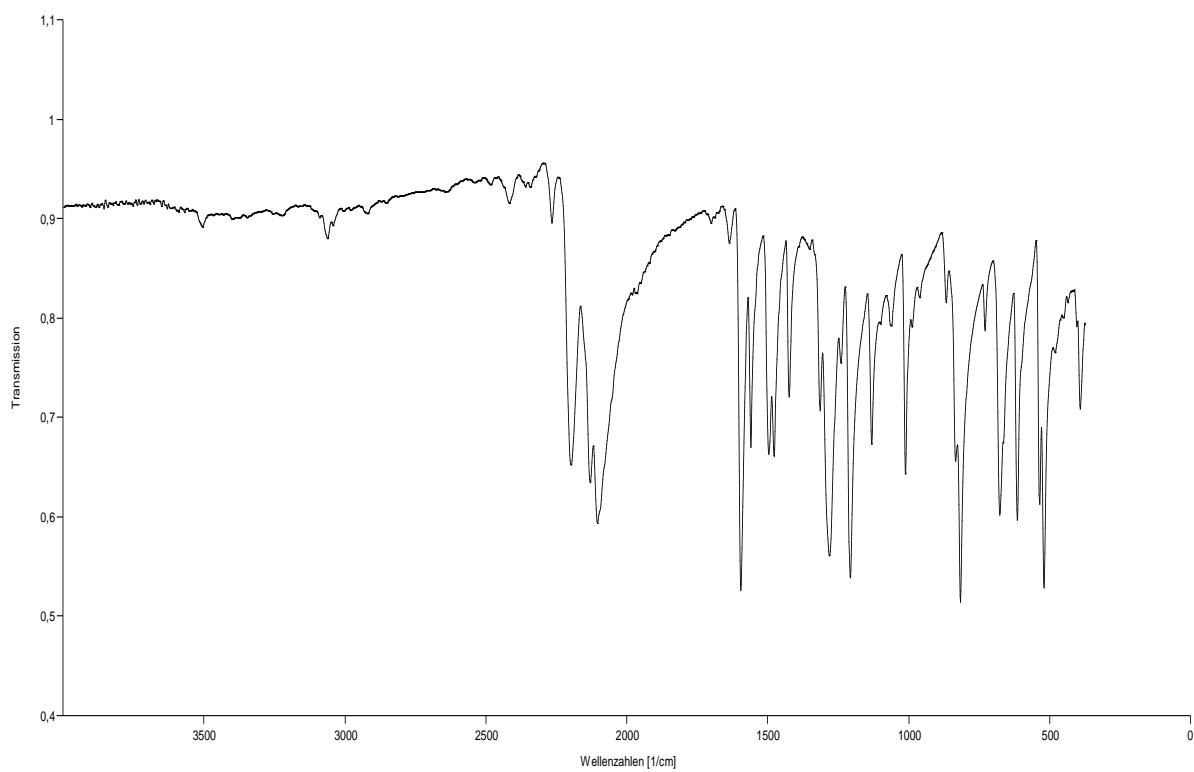
IR-Spectrum of  $[\text{Mn}(4\text{-Azidopyridine})_4(\text{SCN})_2]$  (7)



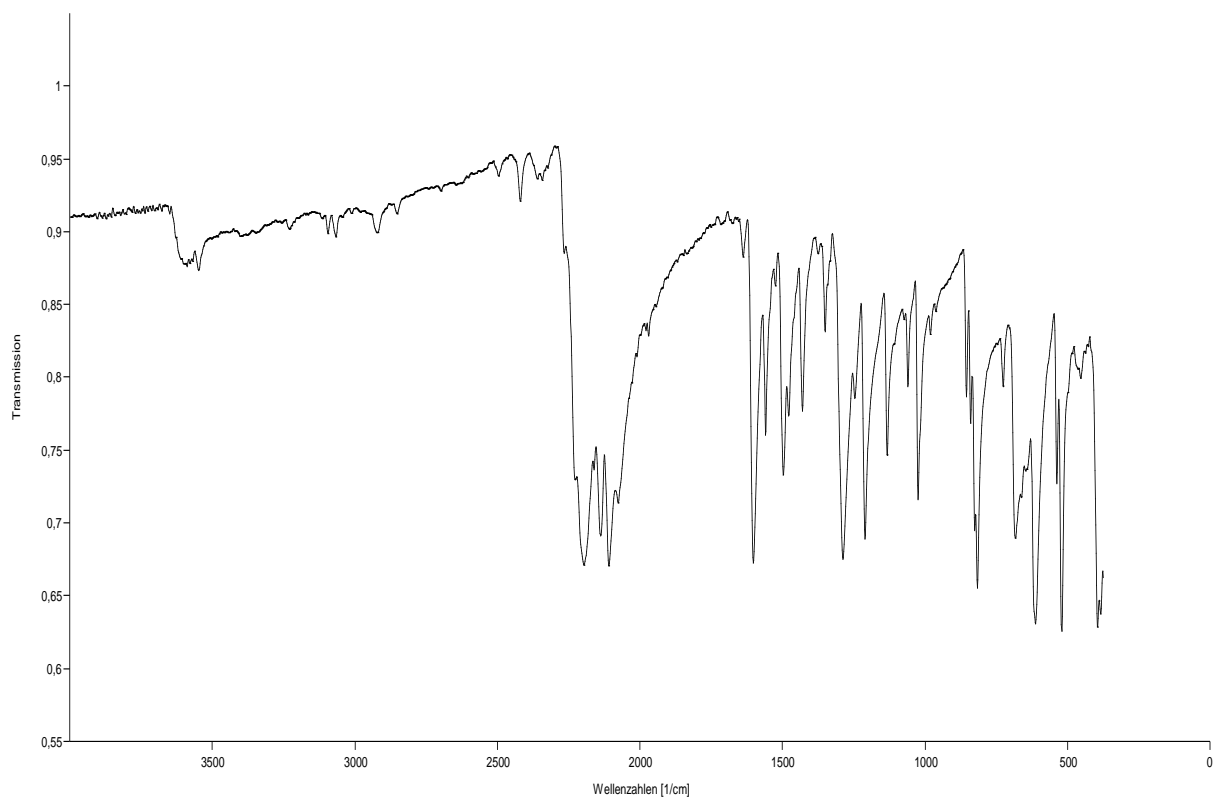
IR-Spectrum of  $[\text{Zn}(4\text{-Azidopyridine})_4(\text{SCN})_2]$  (8)



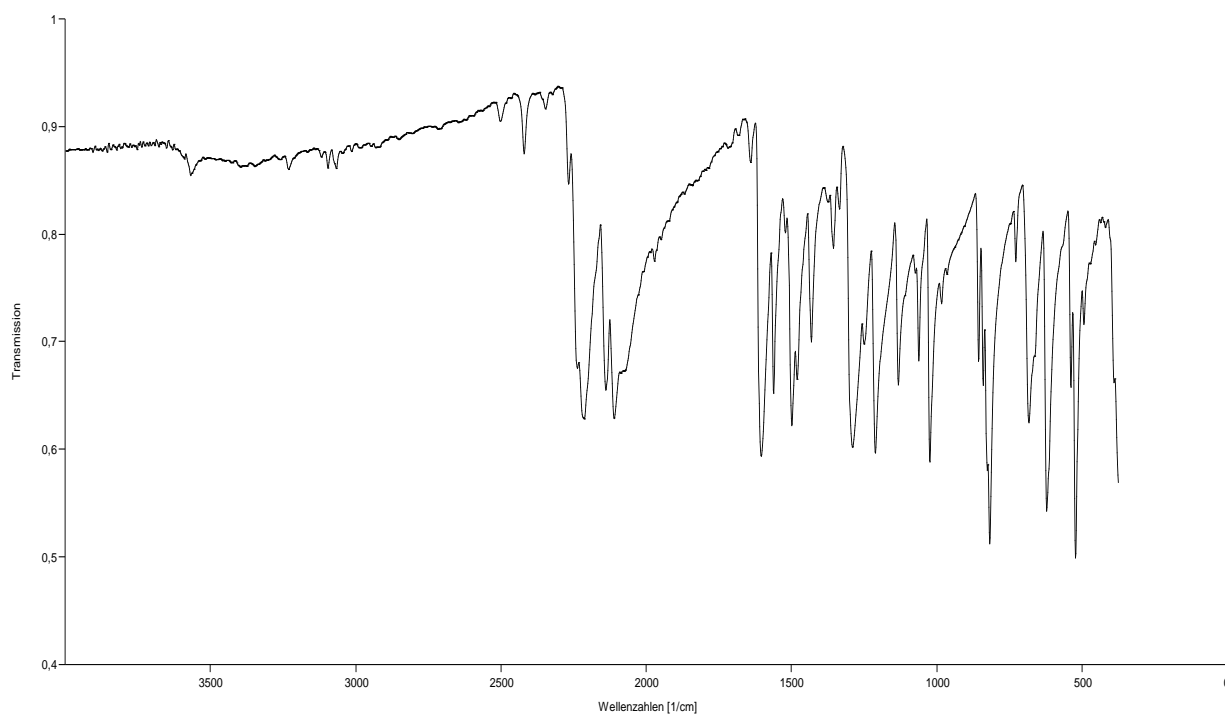
IR-Spectrum of  $[\text{Co}(\text{4-Azidopyridine})_4(\text{SCN})_2]$  (9)



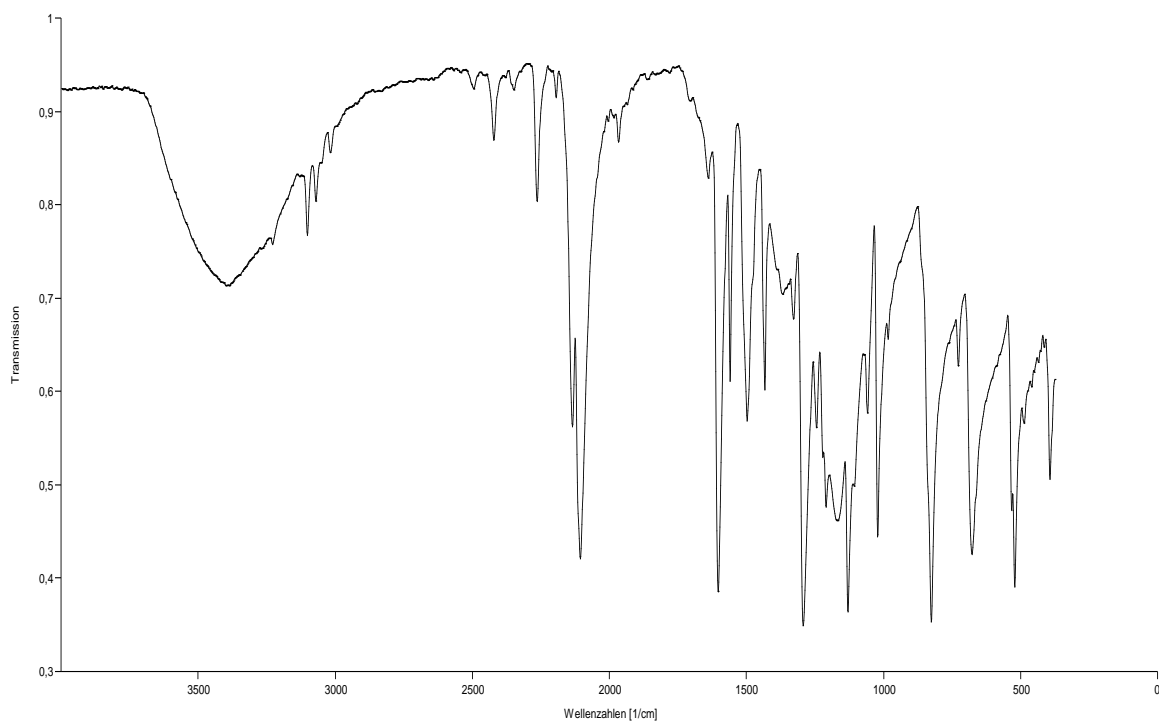
IR-Spectrum of  $[\text{Ni}(\text{4-Azidopyridine})_4(\text{OCN})_2]$  (10)



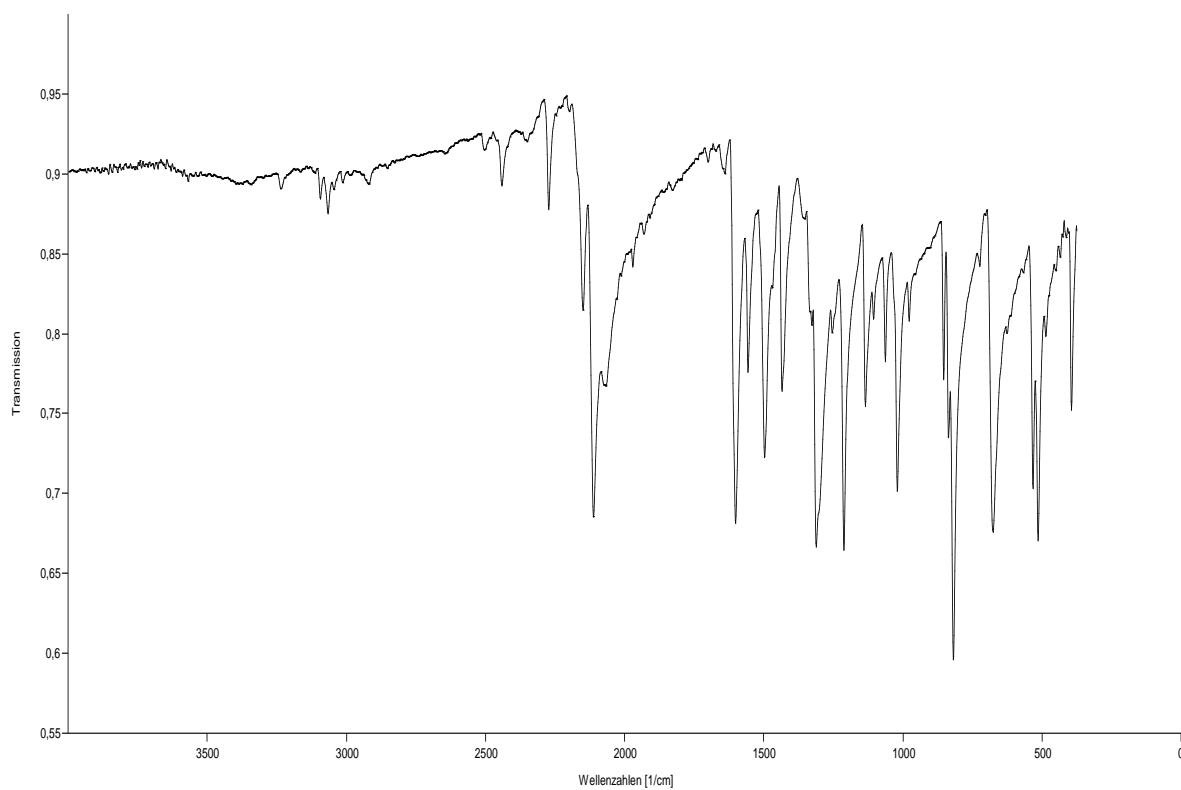
IR-Spectrum of [Co(4-Azidopyridine)<sub>2</sub>(OCN)<sub>2</sub>] (11)



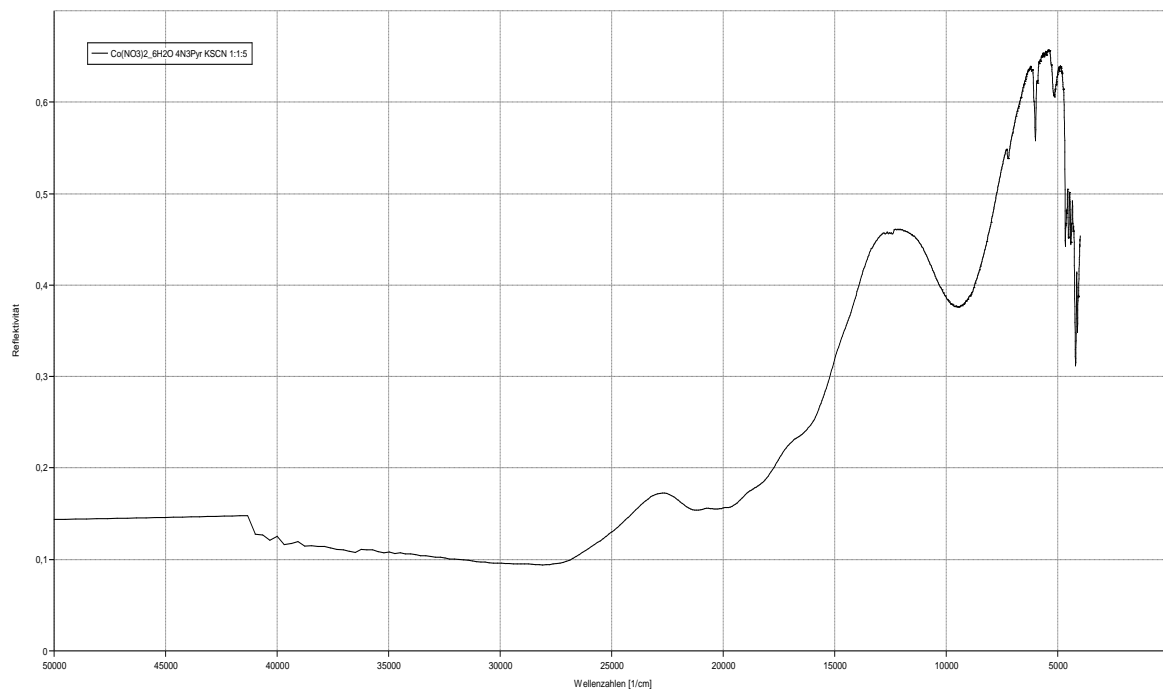
IR-Spectrum of [Zn(4-Azidopyridine)<sub>2</sub>(OCN)<sub>2</sub>] (12)



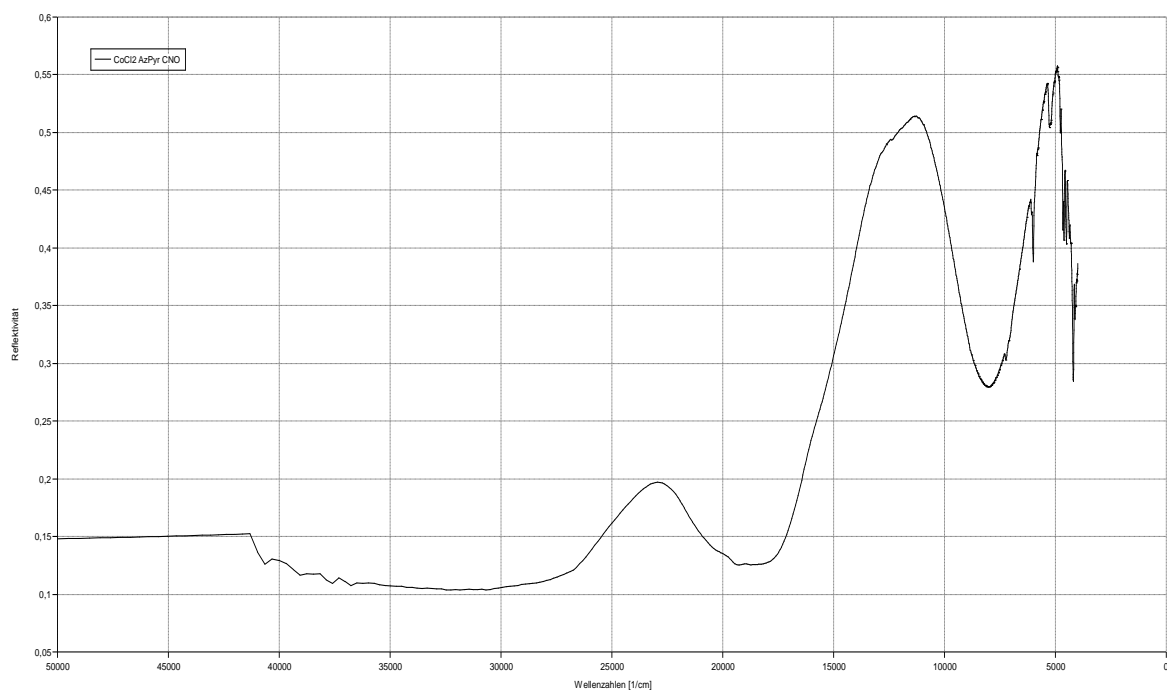
IR-Spectrum of  $[\text{Zn}(\text{4-Azidopyridine})_2(\text{NO}_2)_2]$  (13)



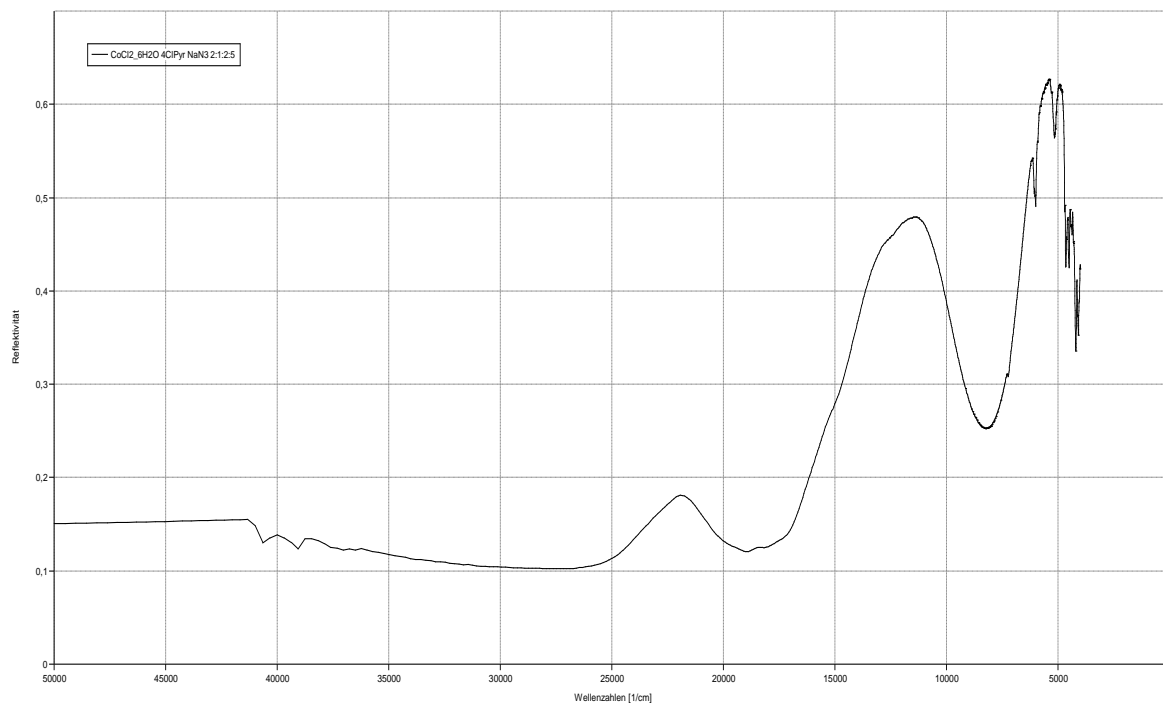
IR-Spectrum of  $[\text{Zn}(\text{4-Azidopyridine})_2(\text{Cl})_2]$  (14)



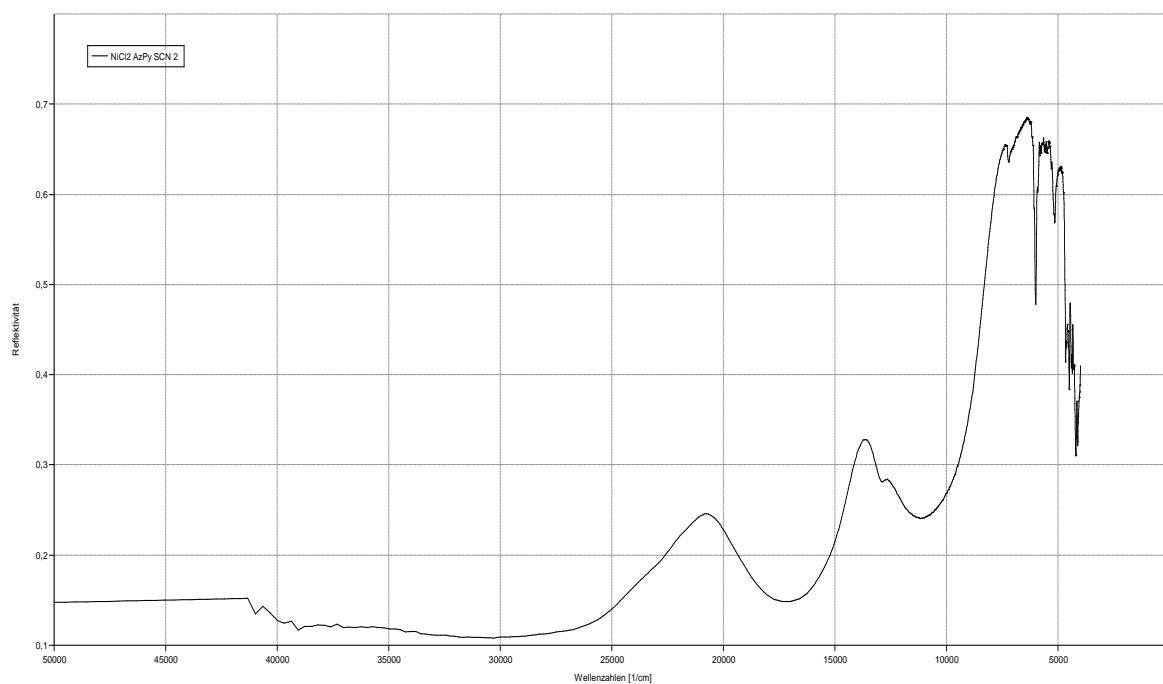
UV VIS spectrum of  $[\text{Co}(4\text{-azidopyridine})_4(\text{SCN})_2]$  (9)



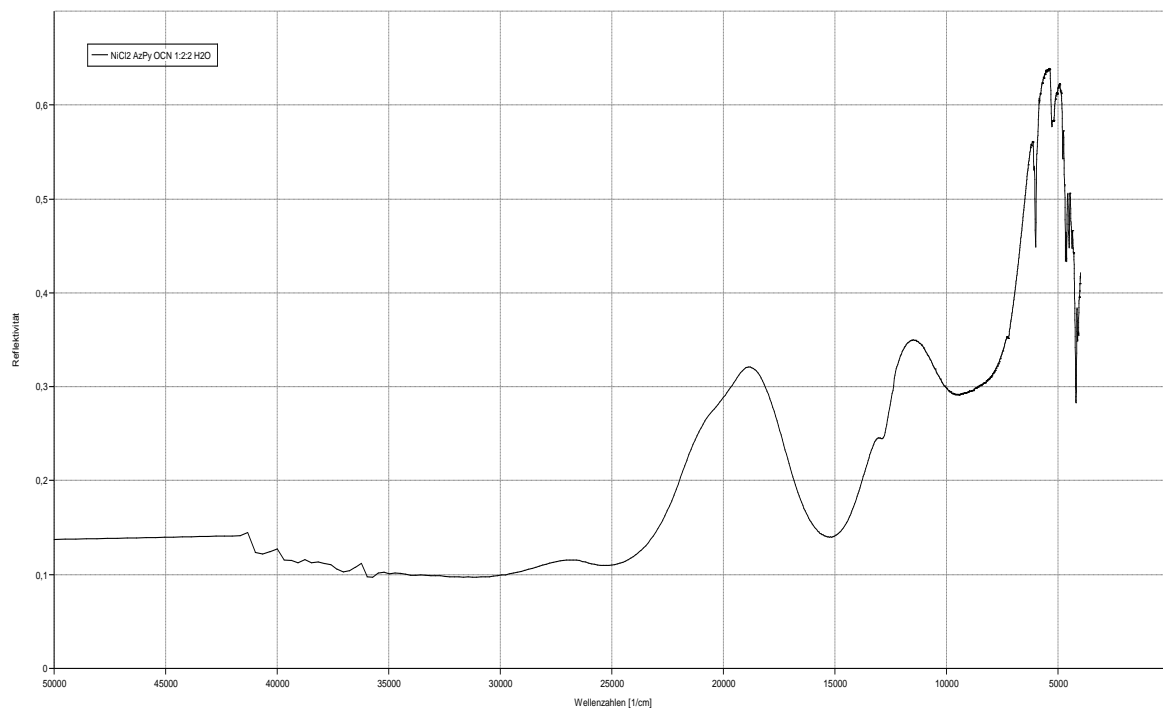
UV VIS spectrum of  $[\text{Co}(4\text{-azidopyridine})_2(\text{OCN})_2]$  (11)



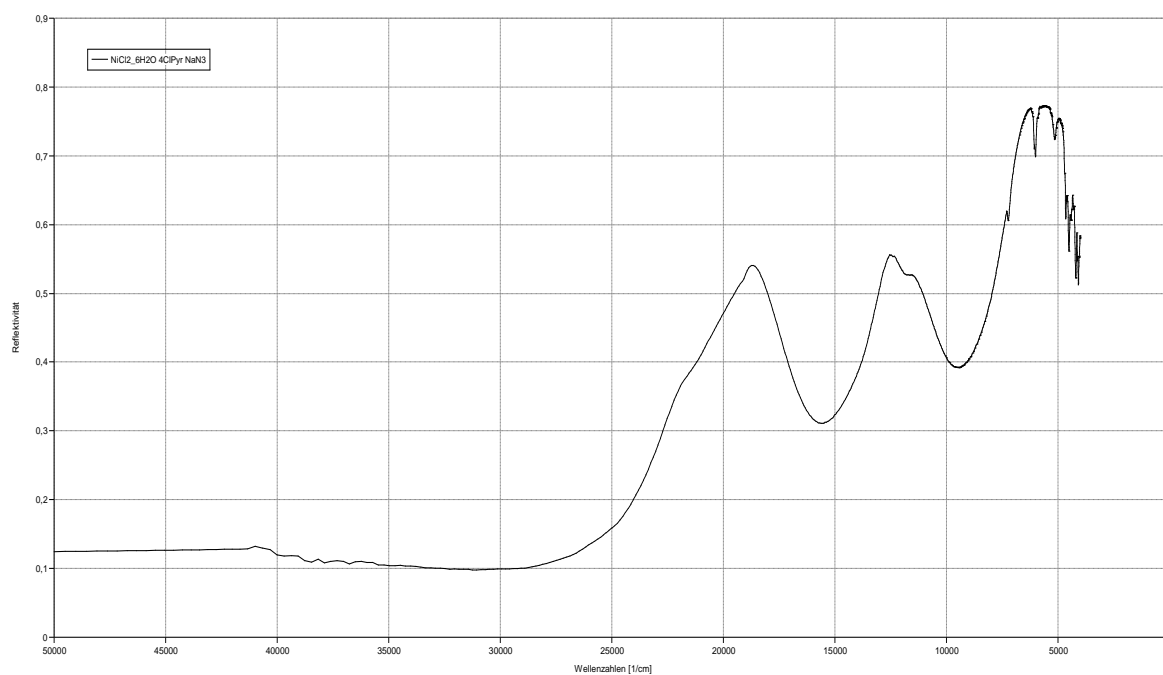
UV VIS spectrum of  $[\text{Co}(\text{4-azidopyridine})_2(\text{N}_3)_2]_n$  (2)



UV VIS spectrum of  $[\text{Ni}(\text{4-azidopyridine})_6(\text{SCN})_4]$  (6)



UV VIS spectrum of  $[\text{Ni}(\text{4-azidopyridine})_2(\text{OCN})_2]$  (10)



UV VIS spectrum of  $[\text{Ni}(\text{4-azidopyridine})_2(\text{N}_3)_2]_n$  (3)

---

## STATUTORY DECLARATION

I declare that I have authored this thesis independently, that I have not used other than the declared sources / resources, and that I have explicitly marked all material which has been quoted either literally or by content from the used sources.

.....  
date

.....  
(signature)